

Optimization-Based Biomechanical Evaluation
of Isometric Exertions on a Brake Wheel

by

Christian Axel Johnson

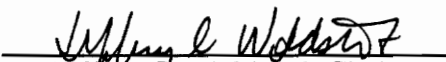
Thesis Submitted to the Faculty of
Virginia Polytechnic Institute and State University
in Partial Fulfillment of the Requirements for the Degree of

Masters of Science

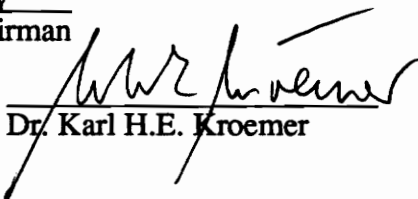
in

Industrial and Systems Engineering

APPROVED:


Dr. Jeffrey C. Woldstad, Chairman


Dr. Dennis L. Price


Dr. Karl H.E. Kroemer

Blacksburg, Virginia

July, 1992

LD
5655
V855
1992
J635
c.2

Optimization-Based Biomechanical Evaluation
of Isometric Exertions on a Brake Wheel

by

Christian Axel Johnson

Committee Chairman: Dr. Jeffrey C. Woldstad

Industrial and Systems Engineering

(ABSTRACT)

Low-back pain and injury claims account for a large number of occupational illnesses each year. In the railroad industry, many maintenance and operation activities require a high degree of manual labor, often resulting in increased stress on the low-back. One of the most common functions of railroad yardmen is the setting and releasing of railcar hand brakes. A static three-dimensional low-back biomechanical model was developed to estimate the levels of compressive force on the L3/L4 spinal joint that existed in subjects during an experiment that simulated the hand brake setting task. We recorded three-dimensional body posture and resultant forces at the hands for analysis by the model. The model resolved the external forces acting on the body to a resultant moment about L3/L4 and then employed an optimization algorithm to estimate the internal lumbar muscle forces generated to resist the external forces. The muscle forces and external forces were added to arrive at a prediction of compressive force at L3/L4.

The experiment investigated the effects of general body posture, left hand grip, subject anthropometry, and hand brake torque level upon predicted compressive force at L3/L4. An analysis of variance revealed that compressive force was significantly affected by each of the experimental variables. Additional analyses at subjects' maximum voluntary torque levels indicated that compressive force would exceed NIOSH guidelines for low-back compressive force, especially in males. Predicted L3/L4 compressive force at maximum torque ranged from an average of 2350N in small females to an average of

7485N for large males. We then used regression analysis to predict brake torque levels that would cause compressive force to exceed the NIOSH (1981) recommended maximum of 3400N. Based on the prediction methods used, hand brake torques of 40 to 80 Nm would be likely to cause compressive force to exceed this maximum.

ACKNOWLEDGMENTS

This work would not have been possible without the advice and support of many people. First, I would like to thank Dr. Jeff Woldstad, who first gave me the idea for this project and saw it through to its completion. He has not only been an observant and knowledgeable advisor, but a friend. I would like to thank Dr. Price for his inspirations and teachings both inside and outside the classroom. He also provided me with a fellowship for 18 months from the National Institute for Occupational Safety and Health for which I am grateful. Dr. Kroemer provided me with helpful insights into low-back compression and anthropometry issues. Randy Waldron in the research machine shop constructed a number of items for the experimental apparatus. His prompt and quality craftsmanship did not go unnoticed.

My colleagues in the Industrial Ergonomics lab also deserve mention. Marc Dysart spent many long hours programming segments of the experimental software and I am grateful for his help. Chris Rockwell was instrumental in providing advice on equipment concerns and programming problems. Thanks to Mark McMulkin for his help in the data analysis phase of the project. I can also thank my other labmates Greg Stewart, Carolyn Bussi, Jerry Purswell, and Marianne Jedrziewski for putting up with me and the project for the past year.

My family deserves special mention for supporting me with their thoughts and love throughout my graduate career. Their care and advice made the going a little easier through the tough times.

I would finally like to thank the Association of American Railroads, who supported this project under research contract 4-36242.

TABLE OF CONTENTS

Section	Page
ABSTRACT.....	ii
ACKNOWLEDGMENTS	iv
LIST OF TABLES	vii
LIST OF FIGURES	viii
LIST OF APPENDICES	xi
1. INTRODUCTION	1
1.1 Rationale	1
1.2 Objectives.....	2
2. LITERATURE REVIEW	3
2.1 Overview	3
2.2 Low-Back Biomechanical Models.....	3
2.2 Resolution of External Forces.....	5
2.2.1 Link Lengths	5
2.2.2 Body Segment Mass and Centers-of-Mass	7
2.2.3 Determination of the Net Reaction Due to External Forces	8
2.3 Resolution of Internal Forces	9
2.3.1 Low-back Anatomy and Muscle Geometry	10
2.3.2 Spinal Disc Compressive Force	13
2.3.3 Intraabdominal Pressure.....	15
2.3.4 Estimation of Internal Forces by Electromyographic Analysis.....	16
2.3.5 Optimization-based Biomechanical Models	20
2.3.5.1 Linear and Nonlinear Programming	22
2.3.5.2 Minimization of Disc Compressive Force	25
2.3.5.3 Double Linear Programming	27
3. MODEL FORMULATION	34
3.1 External Force Model Formulation.....	34
3.2 Transformation to Body Reference Frame.....	39
3.3 Optimization Model Formulation	44

Section	Page
4. METHOD.....	49
4.1 Subjects	49
4.2 Apparatus	49
4.2.1 Whole-body Static Strength Measuring System	50
4.2.2 Hand Brake Mockup	50
4.2.3 Force Measurement Apparatus	50
4.2.4 Posture Measurement System	53
4.2.5 Calibration Procedures	55
4.3 Experimental Design.....	58
4.3.1 Independent Variables.....	59
4.3.2 Counterbalancing of Independent Variables	60
4.3.3 Dependent Variables	66
4.4 Experimental Task	67
4.5 Experimental Protocol.....	67
5. RESULTS	75
5.1 Data Reduction.....	75
5.2 Predicted Compressive Force at L3/L4.....	77
5.3 Analysis of Maximum Torque Levels	88
5.4 Torque levels at the NIOSH AL and MPL	95
6. DISCUSSION	103
6.1 Estimated Compressive Force at L3/L4	103
6.2 Maximum Torque and Resulting Compressive Force at L3/L4	104
6.3 Comparison of Predicted Compressive Force with Recommended Limits.....	105
6.4 Prediction of Torque from Compressive Force Limits	106
6.5 Weaknesses in Models, Methods, and Equipment.....	107
6.6 Future Research.....	109
6.7 Summary and Conclusions.....	110
7. REFERENCES.....	111

LIST OF TABLES

Table	Page
3.1 Variables used in external force model.	37
3.2 Data used in optimization model	45
4.1 Four levels of the independent variable Anthropometry	59
4.2 Treatment combinations of the independent variables Ladder Rung and Posture.	60
4.3 Random Latin Squares generated for the experiment.....	65
4.4 Example treatment order of the independent variable Torque Level.	66
4.5 Anthropometric measurements taken during Session One.	70
4.6 Summary anthropometric measurements of subject population.....	71
4.7 Summary mean whole-body lift strengths (N) for each subject group.....	73
5.1 ANOVA summary table for predicted compressive force at the L3/L4 joint.	80
5.2 Orthogonal Polynomial Contrast analysis on main effect Torque Level.	80
5.3 ANOVA summary table for maximum torque about the hand brake wheel	89
5.4 ANOVA summary table for predicted compressive force at L3/L4 at maximum hand brake torque	89
5.5 Mean torque at maximum level of Torque Level and corresponding predicted compressive force at L3/L4 for each level of Anthropometry, Ladder Rung, and Posture.....	95
5.6 ANOVA summary table for analysis of predicted hand brake torque at the NIOSH Action Limit for low-back compressive force.....	97
5.7 ANOVA summary table for analysis of predicted hand brake torque at the NIOSH Maximum Permissible Limit for low-back compressive force.	98
5.8 Mean predicted hand brake torque levels (Nm) at the NIOSH AL and MPL compressive force limits.	98
C.1 Summary table of subject anthropometry	121
D.1 Names and uses of different data analysis programs.....	123
E.1 Coefficients, R ² values, and model significance levels for linear regressions for each treatment cell and each subject	126

LIST OF FIGURES

Figure	Page
2.1 Human linkage system.....	6
2.2 Lumbar vertebra and intervertebral disc.....	11
2.3 Average muscle force, over all subjects, of each of the ten muscles as a function of trunk symmetry and externally generated torque.....	21
2.4 Average muscle EMG for three elbow muscles and predicted muscle forces under three optimization constraint conditions.....	24
2.5 Typical muscular endurance function.....	26
2.6 Predicted compression forces on the spine as a function of intradiscal pressure.....	30
3.1 Orientation of the room coordinate system.....	36
3.2 Three-dimensional coordinate system used in the model.....	40
3.3 The axes of the body coordinate system as defined by the vectors β , δ , and γ_1 (X, Y, and Z - axes respectively).	43
3.4 The 5 lumbar muscle pairs used in the model.....	46
4.1 Schematic of whole-body static strength measurement system.....	51
4.2 Schematic of custom rig built for the handbrake study.....	52
4.3 Force measurement apparatus configuration.	54
4.4 Top view of arrangement of experimental apparatus.....	56
4.5 Posterior view of placement of WATSMART position markers on subject.	57
4.6 'Face the wall' posture with upper rung grip.....	61
4.7 'Face the wall' posture with lower rung grip.....	62
4.8 'Face the wheel' posture with upper rung grip.....	63
4.9 'Face the wheel' posture with lower rung grip.....	64

Figure	Page
4.10 Photograph of handbrake rig showing feedback monitor	68
4.11 Example of visual feedback to subject during submaximal trial	69
4.12 Three postures used for whole-body static strength testing	72
5.1 Flow diagram showing steps in data reduction.	76
5.2 Main effect of Anthropometry plotted against predicted compressive force at L3/L4.....	78
5.3 Ladder Rung main effect plotted against predicted compressive force at L3/L4.....	81
5.4 Torque Level main effect plotted against predicted compressive force at L3/L4.....	82
5.5 Posture main effect plotted against predicted compressive force at L3/L4.	83
5.6 Torque Level x Anthropometry interaction plot against predicted compressive force at L3/L4.....	84
5.7 Posture x Ladder Rung interaction plotted against predicted compressive force at L3/L4.....	85
5.8 Torque Level x Ladder Rung interaction plotted against predicted compressive force at L3/L4.....	86
5.9 Posture x Ladder Rung x Anthropometry interaction plotted against predicted compressive force at L3/L4.....	87
5.10 Anthropometry main effect at maximum torque plotted against torque	90
5.11 Ladder Rung main effect at maximum torque plotted against torque.....	91
5.12 Anthropometry main effect at maximum torque plotted against predicted compressive force at L3/L4.....	92
5.13 Posture main effect at maximum torque plotted against predicted compressive force at L3/L4.....	93
5.14 Ladder Rung main effect at maximum torque plotted against predicted compressive force at L3/L4.....	94

Figure	Page
5.15 Main effect of Ladder Rung plotted against predicted torque at NIOSH Action Limit for compressive force	99
5.16 Interaction effect of Posture x Ladder Rung x Anthropometry plotted against predicted torque at NIOSH Action Limit for compressive force	100
5.17 Main effect of Anthropometry plotted against predicted torque at NIOSH Maximum Permissible Limit for compressive force.....	101
5.18 Main effect of Ladder Rung plotted against predicted torque at NIOSH Maximum Permissible Limit for compressive force.....	102

LIST OF APPENDICES

	Page
APPENDIX A: Informed Consent Form for Experiment	115
APPENDIX B: Subject Physical Fitness Questionnaire	118
APPENDIX C: Individual Anthropometry of Subject Population.....	120
APPENDIX D: Summary Table of Data Analysis Software	122
APPENDIX E: Summary of Regression Analyses of Wheel Torque on Compression at L3/L4	125
VITA	128

1. INTRODUCTION

1.1 Rationale

Low-back pain and low-back injuries account for a large number of occupational injuries each year. Webster and Snook (1990) estimated the total compensable cost for all low-back pain in the United States to be about \$11.1 billion in 1986. In the railroad industry, many maintenance and operation activities are manual in nature and strenuous, which often results in increased stress on the low-back. One of the most common functions of railroad brakemen is the setting and releasing of railcar hand brakes. The hand brake, usually circular in shape, is mounted on the back of the railcar along with a ladder. Tightening or setting of the brake wheel secures the brake mechanism on the car and prevents it from rolling. This operation occurs in the railyard when cars are set off from trains or picked up for train make-up. Hand brake operations are a major safety concern for the railroads and can pose an elevated risk to low-back injury. About 1.5 percent of all railroad employee lost-time injuries and 6 percent of yardmen lost-time injuries are associated with the operation of hand brakes.

Therefore, there clearly exists a need to develop a method for evaluating the possible high levels of low-back stress associated with this occupational task. This research describes a biomechanical model developed for this purpose. The model predicts levels of compressive force in the low-back region that result from stresses placed on the body by both external and internal forces. The model is sensitive to variations in these stresses and changes in work posture. The compressive force values can then be compared to established limits for low-back stress and evaluated in terms of relative injury risk.

In addition to the specific needs mentioned above, there is an issue of broader concern. A gap exists in ergonomic research between biomechanical models of human physical performance and application of those models to practical situations. This research

provides an example of how the existing knowledge about biomechanical models can be integrated and applied to a real world work task. It is hoped that this research will help motivate others to address practicality in future occupational biomechanics problems.

1.2 Objectives

The primary experimental objectives of this study are as follows:

- Objective 1:** To develop and implement a comprehensive three-dimensional biomechanical model that can be used to reasonably predict levels of low-back compressive force given inputs of body posture, anthropometry, and resultant forces at the limbs.
- Objective 2 :** To investigate the effects of work posture on predicted low-back compressive force during the hand brake setting task.
- Objective 3 :** To predict brake wheel torque levels that could cause low-back compressive force to reach unsafe levels.

2. LITERATURE REVIEW

2.1 Overview

The literature review is presented in three major sections. First, introductory material related to biomechanical modeling is covered. Second, literature relevant to the resolution of external forces acting on the body is presented, including brief discussions of the link system of the body, centers-of-mass of the joints, and the computation of externally produced net reactions. The third major section of the literature review addresses the various principles driving the resolution of internal forces in the body. Low-back anatomy and trunk muscle geometry are covered, the issue of spinal disc compressive force is discussed, followed by electromyographic (EMG) analysis of trunk loading, and finally optimization modeling approaches to spinal loading.

2.2 Low-Back Biomechanical Models

The immense cost of low-back pain (LBP) has justified the need for an effective means by which LBP can be studied and by which practical solutions can be developed. Biomechanical modeling is one approach to the investigation of low-back stress. A biomechanical model is a mechanical representation of the operation of the musculoskeletal system of the body. This representation involves the application of engineering concepts and the laws of physics to describe forces and motions acting on various body parts (Chaffin and Andersson, 1991).

The development of a low-back biomechanical model encompasses the resolution of external forces acting on the body and the resolution of internal forces acting within the body that counteract the external stresses. In a static three-dimensional analysis, such as that of the proposed research, the external and internal forces counteract to satisfy the six equations of static equilibrium:

$$\begin{aligned} \sum M_x = 0, \quad \sum M_y = 0, \quad \sum M_z = 0 \\ \sum F_x = 0, \quad \sum F_y = 0, \quad \sum F_z = 0 \end{aligned} \quad (2.1),$$

which state that all forces in each dimension must sum to zero and all moments in each direction must sum to zero. If these equations are not satisfied, the system is not static.

External forces are divided into two categories. The first category includes externally applied loads, such as a load at the hands caused by the weight of a box being held. The second category of external forces are segmental loads which are caused by the force of gravity acting upon a body segment or link. Internal forces in the body are generated by the musculoskeletal structures to resist the external forces and moments created by these forces. The muscles of the low-back contract to resist external loads and the structure of the spinal column acts to passively resist a portion of the load. Inherent to the biomechanical research of these external and internal forces is a body of anthropometric data, including body segment lengths and locations of segment centers-of-mass. Muscle lines of action, moment arms, and muscle cross-sectional areas are necessary for internal force estimation. Spinal disc load resistance data are also necessary for the prediction of injury risk or safety.

Chaffin (1988) points out that the need for low-back biomechanical models is motivated by three distinct interests. First, these models are needed to help understand the large amount of complex data that is available from today's advanced bioinstrumentation. Second, biomechanical low-back models are necessary because investigators cannot purposely induce injury to humans and living human tissue. Some means must be available to assess the possible risks inherent to certain tasks. Third, practicality drives the need for low-back biomechanical modeling. It is sometimes not possible to measure the effects of certain types of manual work. A distinct advantage of biomechanical modeling is the ability to assess the possible risk of a proposed new task or job before it is actually

performed. Therefore, the overall goal of low-back biomechanical modeling is to accurately predict the risk involved with performing an activity for a certain individual when provided with an adequate amount of data describing the task of interest.

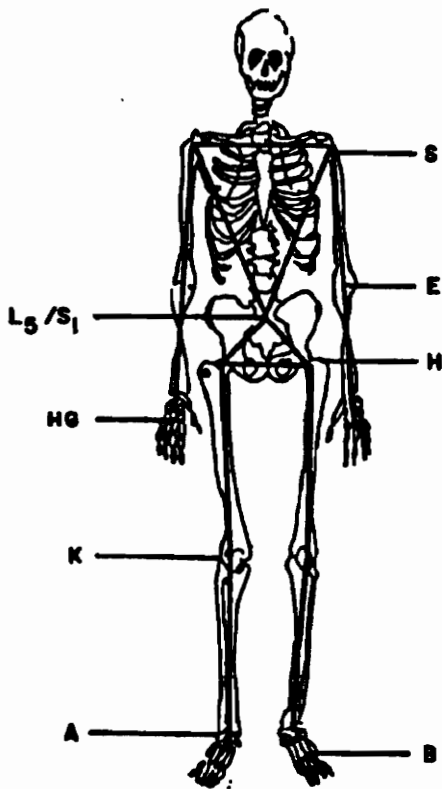
2.2 Resolution of External Forces

External forces in biomechanics result from two primary sources, forces due to the effect of gravity on body segments and forces resulting from externally applied loads. These forces can be resolved into net reactions about joints of interest throughout the body such as the lumbar vertebrae in low-back biomechanical models. This process involves treating the body as a system of links or levers and then integrating anthropometric data and force values with the principles of mechanics to compute moments and forces. A typical human linkage system is shown in Figure 2.1. Static analyses, such as in this research, require knowledge of link length values, segment masses, and segment center-of-mass locations for the resolution of external forces. Dynamic analyses are more complex, requiring kinematics and kinetics to define segment motion. Kinematics describe motion without regard for the role of the forces causing the motion. Kinetics consider the relationship of the forces to the kinematic variables in describing system motion (Ginsberg and Genin, 1984).

The next three sections cover relevant literature and information regarding the resolution of external forces acting on the body. The types of data needed for these analyses, such as link lengths and segment mass characteristics are discussed. A general procedure by which external forces can be resolved to a joint of interest is also presented.

2.2.1 Link Lengths

The measurement of link lengths relies on the assumption that body segments are connected at easily identifiable joints. Associated with each joint is a joint center-of-rotation, which can be estimated in two ways. The center of rotation of the simple hinge



NOTATION:

- HG**—CENTER OF GRIP OF THE HAND
- E** — ELBOW JOINT CENTERS
- S** — SHOULDER JOINT CENTERS
- L₅/S₁**— L₅/S₁ VERTEBRAL DISC CENTER
- H** — HIP JOINT CENTERS
- K** — KNEE JOINT CENTERS
- A** — ANKLE JOINT CENTERS
- B** — BALL OF FOOT

Figure 2.1 Human linkage system. Taken from Chaffin and Andersson (1991).

joints of the limbs can be approximated by the intersection of two perpendicular lines drawn from lines parallel to the long axis center-line of the segments while they are moved through a range of motion. Centers-of-rotation for the more complex joints have been estimated from cadaver dissections (Chaffin and Andersson, 1991). Link lengths are the distances between the centers-of-rotation of a joint. Link lengths have been correlated with the distance between palpable bony landmarks for ease of identification (Webb Associates, 1978). Link length data are discussed in more detail in the next chapter which covers the specifics of the development of the low-back biomechanical model to be used in this research.

2.2.2 Body Segment Mass and Centers-of-Mass

In addition to link lengths, the knowledge of segment masses and the location of the center- of-mass of each segment is needed to calculate the contribution of the effects of gravity on body segments to the overall net reaction. Body segment density and volume are used to calculate the mass of a segment. Segment densities have been determined from cadaver studies (Dempster, 1955) and segment volumes can be estimated by immersion techniques. Body segment masses (or weights) can be predicted from total body weight using regression equations (Webb Associates, 1978). The center-of-mass or center-of-gravity of a limb represents the equilibrium point of a supported body where all its weight is concentrated (Chaffin and Andersson, 1991). Center-of-mass locations for body segments have been measured on cadavers by suspending frozen limb sections (Dempster, 1955, Clauser, McConville, and Young, 1969). Segment centers-of-mass can be estimated on living beings using the sequential immersion method or the moment subtraction technique. Both of these methods are summarized in Chaffin and Andersson (1991). Segment center-of-mass data are reported either as percentages of link length or as distances from joint centers-of-rotation.

2.2.3 Determination of the Net Reaction Due to External Forces

A net reaction is the set of forces and moments acting at a given point. As mentioned before, the location of this net reaction can vary, but usually the only locations of interest in biomechanics are joint centers such as the elbow, shoulder, or low-back region. Body segment lengths, weights, center-of-mass locations, and external force magnitudes all must be known before the externally caused net reaction about a point can be determined.

To compute the net moment about a given joint, the analysis starts at the joint endpoint closest to the externally applied force. Once the moment about the initial joint has been found, additional joints are evaluated in succession until the moment is resolved to the joint of interest. The force vector acting at the joint of interest is simply the vector sum of all the forces acting on links included in the analysis. Thus, the net reaction is composed of both a moment and a force vector.

In three-dimensional static biomechanical analyses, forces and moment arms are expressed as three-component vector quantities. The vector moment about a point can be expressed as the cross product of two vectors:

$$\mathbf{M} = \mathbf{r} \times \mathbf{F} \quad (2.2),$$

where \mathbf{r} is the three-dimensional vector representing the moment arm or the distance from the point about which the moment rotates to the point of application of the force and \mathbf{F} is the three-dimensional vector representing the force applied to the moment arm. The moment about the initial joint of study is the sum of two moments, expressed as:

$$\mathbf{M}_{\text{initial joint}} = \mathbf{M}_{\text{ext force}} + \mathbf{M}_{\text{seg wt}} \quad (2.3),$$

where $\mathbf{M}_{\text{ext force}}$ is the moment due to the externally applied force such as that of holding a weight in the hands and $\mathbf{M}_{\text{seg wt}}$ is the moment due to the weight of the appropriate body segment such as the forearm. The moment arm for the body segment weight is the distance

from the joint center-of-rotation to the location of the joint center-of-mass. The moment about successive joints of study can be expressed as:

$$\mathbf{M}_{\text{successive joint}} = \mathbf{M}_{\text{seg wt}} + \mathbf{M}_{\text{ext force}} + \mathbf{M}_{\text{prev joint}} \quad (2.4),$$

where $\mathbf{M}_{\text{seg wt}}$ is the moment due to the weight of the next segment of study, $\mathbf{M}_{\text{ext force}}$ is the moment created by the sum of the external force and weights of previous joints which acts at the end of the joint of interest, and $\mathbf{M}_{\text{prev joint}}$ is the moment computed for the immediately preceding joint.

As an example, consider the problem of determining the moment about the shoulder when a load is applied at the hand. The first step in the analysis is to determine the moment about the elbow. The elbow can be considered the initial joint in this problem and thus the moment about the elbow is the sum of the moment due to the force applied to the hands and the moment due to the weight of the forearm body segment acting at the forearm center-of-mass. The moment about the shoulder is then computed by summing the moment due to the weight of the upper arm, the moment due to the externally applied force and forearm weight acting at the elbow (end of the upper arm), and the moment about the elbow. The force vector acting at the shoulder is simply the vector sum of the externally applied force, the weight of the lower arm, and the weight of the upper arm. The shoulder problem is a simple example of the process of resolving external forces to an externally caused net reaction. The resolution of external forces of the low-back, especially in three dimensions, is much more involved and will be discussed in more detail in the next chapter.

2.3 Resolution of Internal Forces

The resolution of external forces in a biomechanical analysis has already been discussed. To satisfy the six equations of static equilibrium, the body must generate internal forces to withstand these external forces. The only internal forces considered in this research are muscle forces, but internal forces can also result from passive tissue

restraint. For most joints, the number of internal forces exceeds the number of equations of equilibrium, resulting in a statically indeterminate system. This makes biomechanical analysis difficult. Direct measurement of internal forces is usually not feasible due to safety issues. Therefore, a great deal of research has focused on the development of estimation techniques. In the following sections, low-back anatomy, muscular geometry, the role of intraabdominal pressure, and spinal disc compressive force limits are discussed. These topics each play an important role in the development and evaluation of low-back biomechanical models. Two major techniques used to estimate low-back stress are also covered. EMG-based methods represent one approach to solving the indeterminate problem. They rely on the relationship between EMG activity and muscle force to predict muscle activity. Optimization-based techniques predict an optimal system of internal activity based on the minimization of some objective function subject to a set of constraints.

2.3.1 Low-back Anatomy and Muscle Geometry

The lumbar vertebrae are the main skeletal structures present in the low-back. They are characterized by thick bodies, flat spinous processes and the lack of ribs attached to them, as opposed to the vertebrae of the thoracic region (Wilson and Wilson, 1983). An intervertebral disc lies in-between each set of vertebrae and is composed of a nucleus surrounded by the annulus fibrosis. The nucleus is a mass of incompressible watery gel. The annulus fibrosis is made up of concentric layers of fibrocartilage material. These discs are in effect joints and allow the movements of flexion, extension, and rotation. The spinal column is further stabilized by a network of spinous and longitudinal ligaments. A lumbar vertebra and intervertebral disc are shown in Figure 2.2.

The muscular system that mobilizes and supports the low-back is extensive, but only five major sets of muscles are most often included in biomechanical models. In the posterior region, the latissimus dorsi is a broad and large muscle that originates at the lower

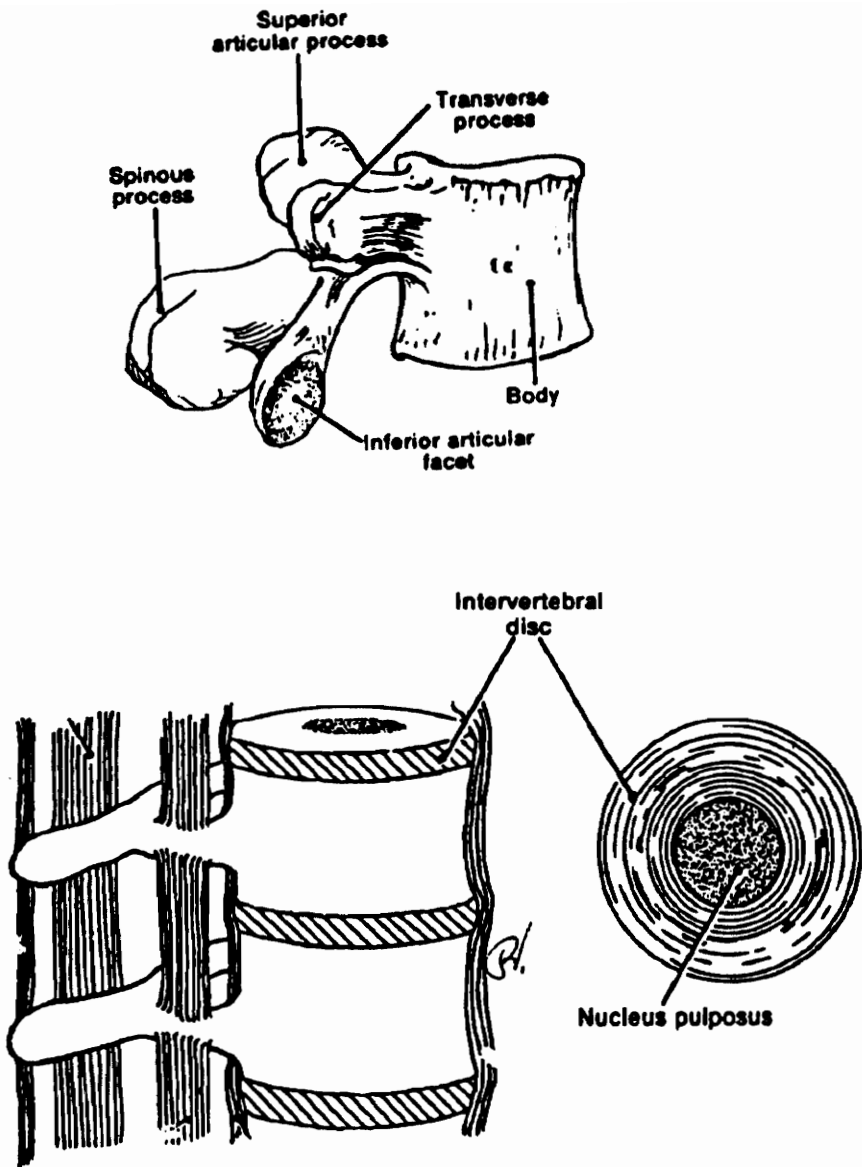


Figure 2.2 Lumbar vertebra and intervertebral disc. Taken from Wilson and Wilson (1983).

thoracic vertebrae, thoracolumbar fascia, ilium, and lower ribs and extends to the humerus. Deeper in the posterior are the erector spinae muscles which extend from the sacrum upward along the back and neck to the base of the skull. They attach at different levels along the spine and are arranged in bundles. The erector spinae muscles serve to maintain the erect position of the trunk. On the anterior side of the body cavity, the external obliques originate at the lower eight ribs and reach medially downward. The internal obliques start at the iliac crest (below the hip) and pass upward and medially around the trunk to the lower ribs. The rectus abdominus also lies on the anterior side and reaches from the pubic crest upward to the xiphoid process of the sternum. The rectus abdominus when contracted causes flexion at the hips (Wilson and Wilson, 1983).

Nemeth and Ohlsen (1985) estimated the moment arm lengths of the erector spinae, psoas, oblique abdominal, and rectus abdominus muscles to the lumbosacral joint. They relied on the computed tomography (CT) scans of 11 males and 10 females for their estimations. The moment arms for the muscles were reported relative to the bilateral motion axis about which flexion and extension occur and to the anteroposterior motion axis about which lateral bending occurs. Reid and Costigan (1985) reported estimates of volume and cross sectional area for the rectus abdominus and erector spinae muscles. These values were based on the CT scans of 16 males and 12 females. McGill, Patt, and Norman (1988) also used CT scans to estimate the muscle cross sectional areas and moment arms of 13 men in the L4/L5 region. They also presented a method for fiber orientation correction to account for the fact that some of the muscles did not run perpendicular to the scan slice.

Tracy, Gibson, Szypryt, Rutherford, and Corlett (1988) conducted a detailed analysis of the geometry of the lumbar spinal musculature. They reported the cross sectional area and the distance from muscle center-of-mass to center of spinal disc for the L2/L3 to L5/S1 sections of the lumbar spine. The data were based on the scans of 26

males using Magnetic Resonance Imaging, a technique that does not use ionizing radiation and also produces good soft tissue contrast in the images. The results showed that areas and lever arms varied strongly between levels. The data reported in this study will be used in the biomechanical model presented in this research.

Earlier low-back models integrated muscle moment arms into the computational algorithms used to estimate muscle forces, but assumed that the forces acted perpendicularly to the transverse plane. Muscle lines of action help to reduce the error inherent in the earlier models by defining the general orientation of the fibers of the low-back musculature. Dumas, Poulin, Gagnon, and Jovanovic (1988) used a three dimensional digitization system incorporating precision potentiometers to establish muscle lines of action for one embalmed cadaver. They reported the results graphically, and also presented unit force vectors and unit moment vectors for nine muscle groups about the L3/L4 and L4/L5 discs. The unit force vectors provide a simple and very useful quantification of muscle orientation for use in low-back biomechanical modeling. The data from this study are discussed in greater detail in the next chapter, as they are used in the model developed for this research.

2.3.2 Spinal Disc Compressive Force

The notion that externally applied forces and internal forces load the spine is well accepted. The cumulative effects of spinal loading can cause microfractures in the fibrocartilage structure of the spinal discs as well as other problems. A weakened disc is more susceptible to possible rupture or dislocation. The objective of most low-back biomechanical models is to predict spinal loads. It is therefore important for researchers and safety specialists to have some idea of the levels of disc compressive force that would result in an increased risk of back injury. Cadaver studies have been conducted to examine the behavior of spinal motion segments under different loading configurations. Part of the

motivation for these investigations was a need for the development of reasonable safety limits for spinal loading. These values could then form the basis for safety standards intended for use in the analysis of manual tasks.

The cadaver studies of Evans and Lissner (1959) disclosed that large variations exist in the ability of spinal discs to resist large pressures. Data from the Evans and Lissner (1959) study generally showed that spinal discs of persons less than 40 years of age resist loads of 1500 pounds before beginning to show signs of microfractures. Jäger and Luttman (1989) summarized the disc compressive force data from 16 comparable cadaver studies. They reported the mean ultimate compressive strength of a spinal disc based on the testing of 307 lumbar segments to be 4400N with a standard deviation of 1900N.

Other studies have examined the behavior of cadaver spine segments under varied loadings. Adams and Hutton (1981) found that a slightly flexed lumbar joint had a compressive strength that exceeded loads imposed during heavy lifting. Miller, Schultz, Warwick, and Spencer (1986) examined lumbar spine motion segments and recorded stiffness values in response to shear forces and moments. They found that the segments could withstand shear loads of over 549N. They also found that the motion segments could twist up to 18° without failure and could translate up to 9mm under shear loads without failure.

Chaffin and Park (1973) discussed some implications of the cadaver data on low-back pain and injury risk. First, they pointed out that healthy discs do not rupture. Instead, the cartilage endplates which distribute compressive force loads to the vertebrae fail. Second, the large variation in compressive strengths shown by the cadaver studies could be caused by cumulative degeneration of the disc structure. The degeneration could be the result of many microfractures due to the strains associated with everyday life. Thus, the disc would become less resistant to heavy loading over time.

Based on a number of studies, including some of the cadaver research just mentioned, NIOSH (1981) recommended limits for spinal loading at the L5/S1 joint. Accordingly, most young healthy workers can tolerate a compressive force of 3400N on the L5/S1 disc. This level is referred to as the biomechanical Action Limit (AL). If predicted compressive forces for a task were less than this value, nominal risk would be present. NIOSH (1981) also stated that a compressive force of greater than 6400N could not be tolerated by most workers and labeled this the Maximum Permissible Limit (MPL). Tasks generating compressive values above this limit would be deemed unacceptable. Compressive force values between the AL and MPL would only be deemed acceptable if engineering or administrative controls were applied. These levels are widely accepted as safety limits for low-back compressive force and are used as criteria in biomechanical low-back studies.

2.3.3 Intraabdominal Pressure

Intraabdominal pressure (IAP) has been studied by biomechanics researchers as a possible source of force that the body generates to help relieve spinal loads. The theory is that when a flexion moment is developed about the spine by external forces, the posterior back muscles and pressure in the trunk cavities work to resist this moment. A good deal of research has been directed toward quantifying IAP and determining its significance to trunk loading. Chaffin and Andersson (1991) describe two methods for the measurement of IAP. In the first method, subjects swallow a radio pill whose frequency of transmission is altered by pressure. The pill signals are detected by an antenna placed close to the abdomen of the subject. The second method entails the introduction of a catheter-mounted pressure transducer orally or rectally into the trunk cavity. The transducer is often in the form of a silicone beam with resistors mounted on either side. The beam deflects under varying pressures which are recorded as a difference in electrical resistance. The catheter system

has been found to be more reliable than the pill, but is quite invasive. The radio pill is rather expensive and is also sensitive to temperature changes.

Many researchers have included IAP as an additional dependent variable in electromyographic studies of the trunk musculature leading to spinal loading predictions, but conflicting results have been obtained regarding the accuracy of IAP as a predictor of trunk loading. Marras, King, and Joynt included the measurement of IAP in a study of internal responses to dynamic trunk motion. This study is mentioned in the next section. Mairiaux and Malchaire (1988) found differences in IAP depending on whether the trunk was flexed or extended and also found that no significant relation between IAP variations and lumbar moments when lifting was carried out from a flexed trunk position. McGill and Norman (1987) reported that modeling IAP as a force vector producing an extension moment in the trunk was incorrect if the compressive effects of the abdominal muscles were not accounted for. They also suggested that IAP played a more complex role in spinal stabilization than previously assumed. Chaffin and Andersson (1991) noted that asymmetrical trunk loading creates large trunk stresses without the corresponding IAP response that occurs in symmetrical loading. Thus, the role of IAP in biomechanical low-back modeling and trunk loading is not yet fully understood and many contemporary low-back biomechanical models ignore IAP as a contributing variable to spinal loading.

2.3.4 Estimation of Internal Forces by Electromyographic Analysis

Electromyography is the measurement of muscle motor unit electrical potentials, or myoelectric activity. These electrical potentials have been shown to correlate well with static muscular force. EMG is one method other than biomechanical modeling by which lumbar muscle forces can be predicted. Also, EMG analysis is used to validate a low-back biomechanical model by comparing the model predictions of muscle force with EMG-based predictions of muscle force. This section covers significant research efforts

regarding EMG-based low-back modeling. Specifically, these models attempt to solve the indeterminate biomechanical problem by correlating EMG activity with lumbar muscle forces.

Ortengren, Andersson, and Nachemson (1981) conducted a study investigating the relationships of EMG, disc pressure, and intraabdominal pressure. Intradiscal pressure was measured by means of a miniature pressure transducer that was built into the tip of a needle and inserted into the third lumbar disc. Intraabdominal pressure was recorded with a pressure sensitive radio transducer swallowed as a pill. Twelve bipolar recessed surface electrodes picked up electromyographic activity. They were placed anteriorly at the eighth thoracic, first, third, and fifth lumbar vertebrae levels, on the rectus abdominus muscles, and on the oblique abdominal muscles. The participants included three females and one male on whom all three dependent measures were taken and ten males on whom only EMG activity was recorded. The experimental tasks involved holding weights ranging from 0 to 150N while keeping the trunk flexed at various angles. Some positions involving twisting were also studied. A total of 18 tasks were studied, representing symmetric and asymmetric loading. The investigators found no significant differences in EMG amplitude between the group of ten subjects and the group of four subjects under similar loading conditions. Signals recorded in the identical regions of the back responded similarly to the varied loading conditions in both groups. Correlations of $r^2 = 0.95$ and $r^2 = 0.97$, respectively, were found between measured disc pressure and lumbar myoelectric back activity for the symmetric and asymmetric conditions.

The study of internal responses to dynamic activity is important because many occupational tasks suspected of causing low-back pain are dynamic in nature. One of the first studies to investigate internal responses to dynamic activity was performed by Marras, et al. (1984). The researchers evaluated both isometric and isokinetic sagittal plane exertions about the lumbosacral joint. The electromyographic activity of ten trunk muscles

was recorded using intramuscular electrodes. Intraabdominal pressure was also recorded by means of a catheter transducer placed in the stomach. Subjects exerted a maximum extension force at maximum velocity while secured to an isokinetic dynamometer. In addition to the maximum velocity condition, subjects performed isokinetic exertions at 33% and 66% of their maximum velocity and also performed a maximum isometric exertion. The study showed that external torque production decreased once velocity was initiated. Significant coactivation was noted during all trials and the level of coactivation increased as velocity increased. A significant lag occurred between the initiation of intraabdominal pressure and torque, which also increased at greater levels of velocity. The study also revealed that the trunk muscles did not react according to a set pattern, because under some conditions EMG activity was lower during dynamic exertions and under some conditions it was higher compared to the isometric condition.

Marras and Reilly (1988) examined the temporal relationships of trunk muscle activity during isokinetic exertions at varying velocities. The experimental setup was very similar to that in Marras et al. (1984) and 10 males participated as subjects. The experimental trials included exertions at 25%, 50%, 75% and 100% of the subjects' maximum velocity and an isometric exertion. The researchers associated key event times with the EMG signal of each muscle and the intraabdominal pressure signal. The event times were classified as the time at which the signal increased from resting level, the time at which the signal reached its maximum, and the time at which the signal returned to resting level. Some interesting results were observed with respect to the event time occurrences. The start times of the various muscles were found to be relatively homogeneous under static conditions. Variability of peak time occurrences was found to decrease as velocity increased. Intraabdominal pressure was always the first signal to terminate. The authors also developed event time networks to describe the sequence of events that occurred under each velocity condition.

Reilly and Marras (1988) also developed a biomechanical model that predicted spinal compressive force and stress based on the networks of trunk muscle activity. Marras (1988) also compared the results from an earlier study (Marras et al., 1984) to a biomechanical model of the low-back proposed by Schultz and Andersson (1981). The correlations between the measured EMG activity and model predicted muscle forces were shown to be quite poor.

Very little research has been conducted in the area of three-dimensional dynamic low-back modeling but a recent effort (Marras and Sommerich, 1991a, 1991b) has made progress toward the development of such a model. While this model is not truly three-dimensional because motion was restricted to extension in a single plane, it did address asymmetric loading under dynamic conditions. The model had as its inputs the general categories of subject characteristics, EMG signals, and trunk kinematics and kinetics. These data are used to predict muscle forces and spinal compressive force at points in time. The compressive force data are then averaged over time. The model was applied in a controlled experiment using apparatus similar to previous research (Marras et al., 1984). Velocity was controlled by an isokinetic dynamometer which was aligned to the L5/S1 junction of the back by means of an asymmetric reference frame. The experimental trials were isokinetic extensions at varying velocities. Three different trunk loading combinations were used: a sagittally symmetric extension generating 27.1 Nm of torque, a sagittally symmetric extension generating 54.2 Nm of torque, and an asymmetric extension of 27.1 Nm with the trunk twisted 30° from the frontal plane. Each loading combination was repeated at velocities of 10, 20, and 30 deg/s. Good correlation was found between measured and predicted trunk torque. In the symmetric conditions, increasing peak compressive force was associated with both increasing torque and increasing velocity. The asymmetric conditions did not exhibit a similar trend, as peak compressive force was relatively constant for all velocities. The predicted muscle forces under different loading

conditions are shown in Figure 2.3, with the erector spinae (ERS) and the internal obliques (INO) exhibiting the most marked change.

2.3.5 Optimization-based Biomechanical Models

The analysis of loads on the trunk entails the calculation of a net reaction at the spine due to externally applied forces and subsequent estimation of internal body forces to counteract this net reaction. Both of these concepts have already been introduced. The externally caused reaction is composed of three force and three moment equations for a given point. The muscular system chosen to oppose the reaction is usually composed of more unknown quantities (muscle contraction forces) than number of equilibrium equations. Therefore, an indeterminate system exists. Electromyographic analysis, as discussed in previous sections is one method of estimating the muscle contraction forces present during spinal loading. Optimization techniques can also be implemented to solve the indeterminate system.

The basic components of an optimization scheme are an objective function and a system of constraints. The objective function and constraints are functions involving some set of unknown variables. A solution algorithm is implemented to first find a set of feasible solutions that meet the constraints and then choose an optimal solution from that set. The objective function is typically one of minimization or maximization of some cost. This cost in the case of biomechanical applications is usually some sort of physiological measure. Electromyography is often used to evaluate the validity of an optimization model. In the sections that follow, specific optimization techniques in the literature will be discussed with a special emphasis on methods proposed by Crowninshield and Brand (1981) and Bean, Chaffin, and Schultz (1988).

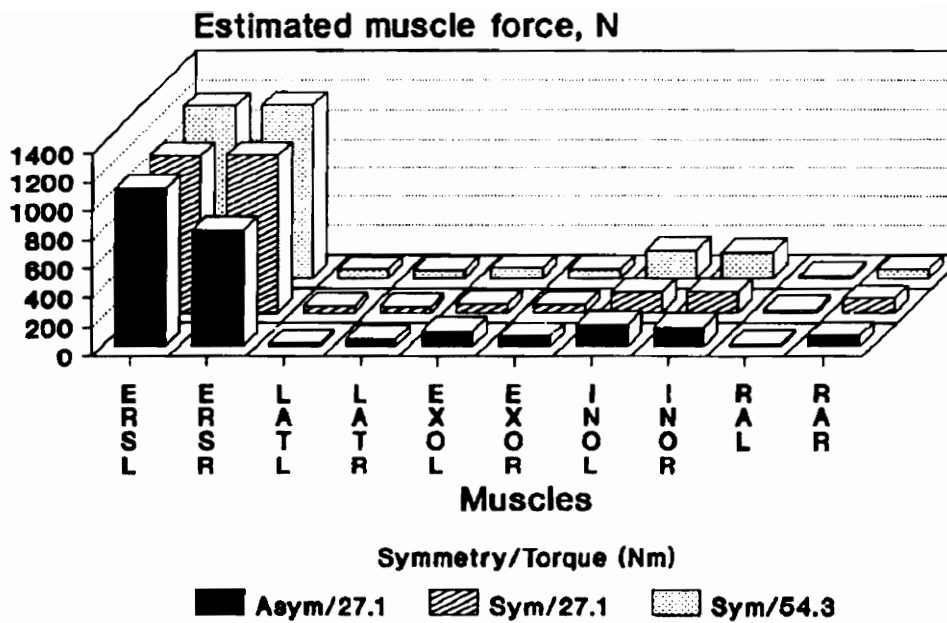


Figure 2.3 Average muscle force, over all subjects, of each of the ten muscles as a function of trunk symmetry and externally generated torque. Taken from Marras and Sommerich (1991).

2.3.5.1 Linear and Nonlinear Programming

In an early work, Nubar and Contini (1961) pointed out that individuals consciously or otherwise determine their motion or posture as to reduce total muscular effort to a minimum. Penrod, Davy, and Singh (1974) noted that the concept of minimum muscular effort could be related to reciprocal inhibition. They also stated that to minimize total effort, the number of active muscles would be no greater than the number of rotational degrees of freedom of a joint if the problem had a minimal effort objective function. The authors pointed out the fact that linear programming approaches predict orderly recruitment of muscles, while nonlinear methods encourage synergistic activity.

The prediction of antagonistic activity has been the focus of several alternate approaches to simple linear programming-based optimization modeling. Pederson, Brand, Cheng, and Arora (1987) proposed a scheme that included both linear and nonlinear techniques in an optimization algorithm for locomotion analysis. The unified method allowed for more synergistic and antagonistic muscle activity. They also pointed out that the nonlinear approaches yielded better concurrence with EMG measurements.

Dul, Townsend, Shiavi and Johnson (1984) evaluated the performance of linear and nonlinear approaches in the analysis of isometric knee flexion. They suggested that future methods should incorporate some constraints to address differences in fiber content among muscles. It is generally accepted that for endurance activities, slow twitch fibers have more force allocated to them and this is an important variable in determining load sharing among synergistic muscles. The same authors (Dul, Johnson, Shiavi, and Townsend, 1984) developed a physiological criterion for muscular load sharing based on maximizing muscular contraction endurance time and thereby minimizing fatigue. Endurance time for each muscle was expressed as a function of muscle force, maximum

muscle force, and percentage of slow twitch fibers. This optimization algorithm predicted synergistic muscle action, allocated more force to slow twitch dominant muscles, and allocated more force to larger muscles in a model for the knee joint. The authors also used the model to predict load sharing between two cat muscles during walking and standing and found good agreement between the predictions and actual published values.

Crowninshield (1978) applied an optimization scheme based on muscle intensity (muscle force per unit cross sectional area) to the analysis of a three muscle model of the elbow joint. The model had as its objective function the minimization of the sum of muscle intensities. The constraints included the moment and force equilibrium equations and a limit on the maximum allowable intensity of any muscle. The author expressed this intensity constraint as

$$0 \leq \frac{f_i(t)}{A_i} \leq \beta \quad (2.5)$$

where $f_i(t)$ represented the force of muscle i , A_i represented the cross sectional area of muscle i , and β represented the maximum allowable stress in the muscle. Another intensity value, $\beta(t)$, was defined as the smallest value of β for which a solution existed to the problem.

The optimization scheme was implemented using three different values for β . The first value of β was β much larger than $\beta(t)$ which represented the elbow muscles as having unlimited strength. The second value was $\beta = 60\text{N}$, the estimated maximum physiologically achievable muscle stress. The third approach was to set $\beta = 1.2\beta(t)$, which resulted in continuous synergistic activity of all three muscles modeled. The predicted muscle forces from this third approach agreed very closely with EMG activity of the three muscles. This relationship is illustrated in Figure 2.4.

An, Kwak, Chao, and Morrey (1984) also performed an analysis of the elbow joint and formed a linear program that had as its objective function the minimization of maximum

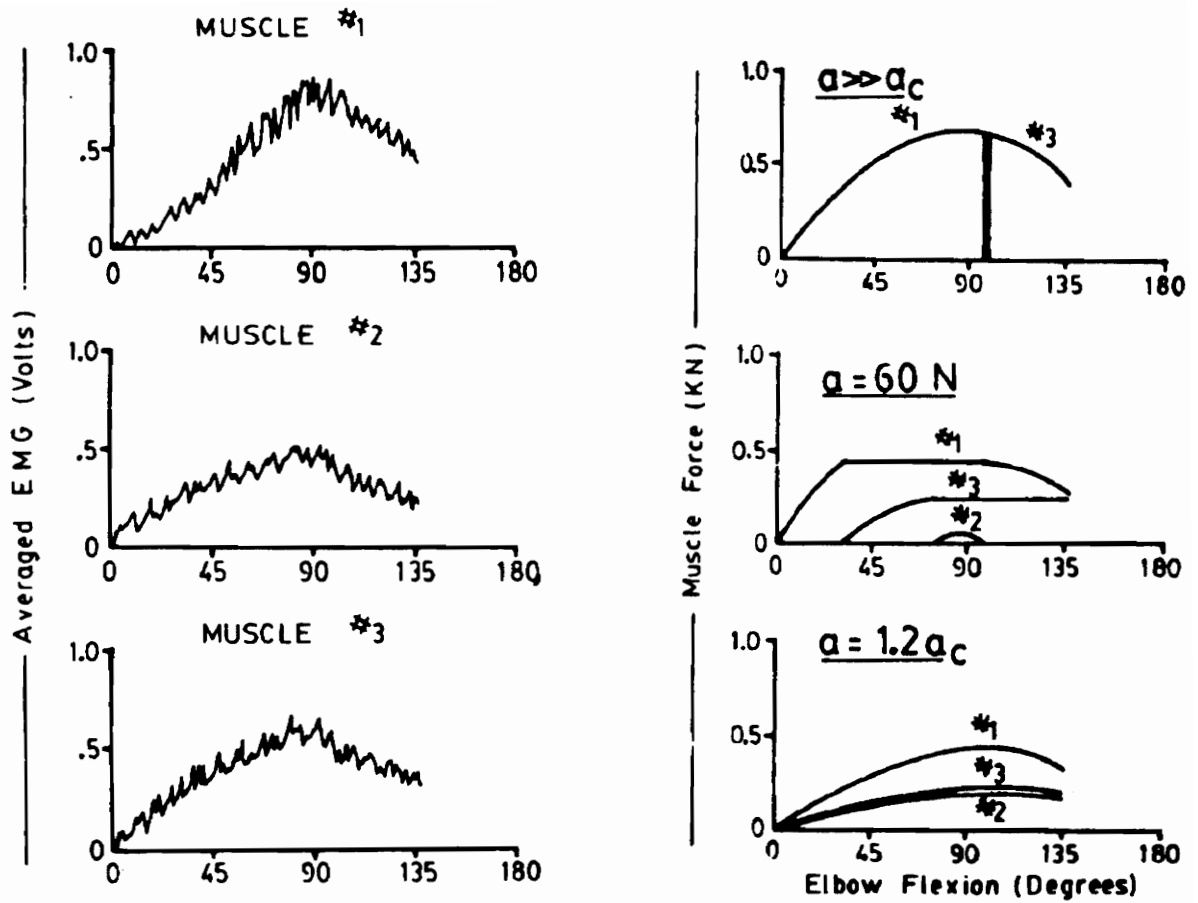


Figure 2.4 Average muscle EMG for three elbow muscles and predicted muscle forces under three optimization constraint conditions. Taken from Crowninshield (1978).

muscle intensity and moment equilibrium equations as constraints. The muscle forces predicted with this approach were in agreement with previously published EMG data.

Crowninshield and Brand (1981) proposed an optimization model based on muscular endurance but formulated it differently and much more simply than Dul et al. (1984). The authors stated that a maximum endurance function would occur when the equations of equilibrium about a joint are satisfied such that the Euclidean norm

$$u_n = \sqrt[n]{\sum_{i=1}^m \left(\frac{f_i}{A_i} \right)^n} \quad (2.6)$$

is minimized, where f_i represents the force of muscle i and A_i represents the physiologic cross sectional area of muscle i . This expression was based on the relation of individual muscle force generation capability to muscle cross sectional area. This norm is minimized when the relation

$$u = \sum_{i=1}^m \left(\frac{f_i}{A_i} \right)^n \quad (2.7)$$

is minimized, and this serves as the objective function for the optimization problem. The authors contended that a reasonable value for the power n is 3, which results in a typical muscle endurance time curve similar to Figure 2.5. When n is equal to 1, total muscle stress is minimized by high forces occurring in few muscles with large moment arms. In this case, the problem is identical to a linear programming formulation. Values of n equal to 2 or greater result in the prediction of lower individual muscle stresses and a higher number of active muscles.

2.3.5.2 Minimization of Disc Compressive Force

Schultz and Andersson (1981) postulated that when external loads are applied to the trunk, the muscles of the low-back region act to resist the external forces while at the same time minimizing compressive force on the spine. The authors used minimization of spinal

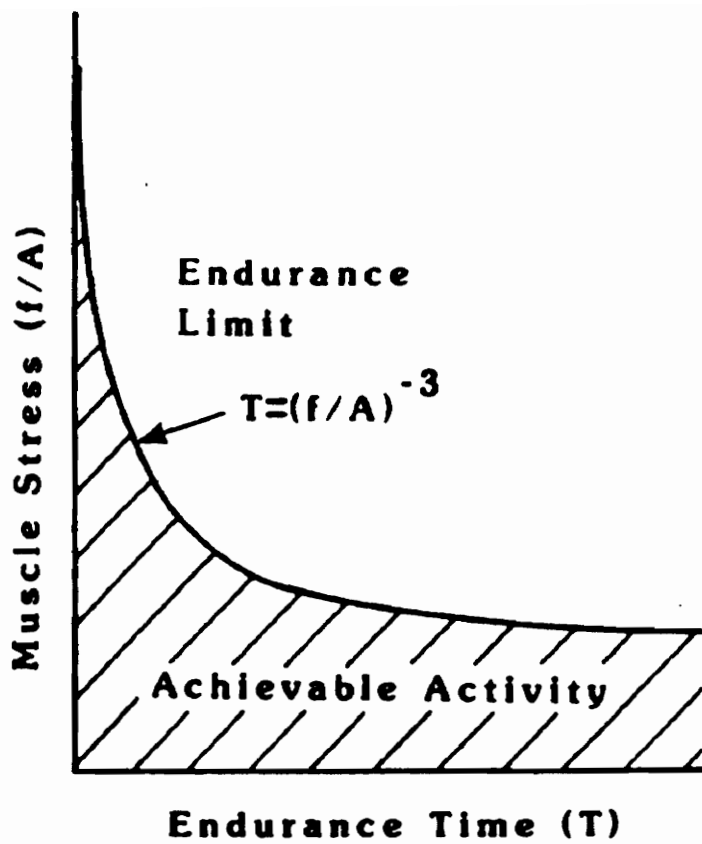


Figure 2.5 Typical muscular endurance function. Taken from Crowninshield and Brand (1981).

compressive force as the objective function of the linear program used to estimate lumbar muscle forces. The constraints in the problem were composed of the three equations of equilibrium stating that the sum of moments about the spinal disc of interest equal zero. The known parameters in the system included muscle moment arm lengths and the net reaction due to external forces. Linear programming was used to solve for the unknown muscle forces and subsequent disc compressive force. In effect, this approach is based on optimizing muscular effort because the lumbar muscles must contract in an optimal fashion in order to keep disc compressive force to a minimum. This method has been tested rather extensively using EMG and has also been tested using *in vivo* measurements of disc pressure. These studies are further discussed in Section 2.3.6.

2.3.5.3 Double Linear Programming

An optimization technique involving a double linear programming approach to the prediction of trunk muscle forces during spinal loading has been proposed by Bean et al. (1988). This method was developed in an attempt to refine the minimization of disc compressive force algorithms of Schultz and Andersson (1981) and Schultz et al. (1983). The double linear programming technique solves a two-objective problem with two successive linear programs. The procedure minimizes the maximum muscle intensity as reported in An et al. (1984) using the relations:

$$\begin{aligned}
 & \text{minimize } I && (2.8), \\
 \text{subject to:} & \quad \sum f_j d_{ij} = M_i, \\
 & \quad f_j / A_j \leq I, \\
 & \quad f_j \geq 0.
 \end{aligned}$$

The first constraints represent satisfaction of the conditions of equilibrium where f_j represents the unknown force in muscle j , d_{ij} is the moment arm for muscle j about axis i ,

and M_i is the externally caused moment about axis i . In the intensity constraint, A_j represents the cross-sectional area of muscle j and the last constraint is self-explanatory. The value of I obtained can be called I^* and is the lowest intensity value that will allow feasible solutions. This value is then included as a constraint in the second linear program, similar to that of Schultz et al. (1983), which seeks to minimize the sum of muscle forces or spinal compressive force using the relations:

$$\begin{aligned} & \text{minimize } \sum f_j && (2.9), \\ \text{subject to: } & \sum f_j d_{ij} = M_i, \\ & f_j / A_j \leq I^*, \\ & f_j \geq 0 \end{aligned}$$

with the variables having the same meaning as in the first linear program. The authors pointed out that the model has advantages of low cost, stable solutions, and relatively simple implementation on a microcomputer.

2.3.6 Validation of Optimization-Based Low-Back Models

Schultz, Andersson, Ortengren, Haderspeck, and Nachemson (1982a) reported a study which examined the relationship between biomechanical predictions of internal trunk activity, measured myoelectric activity, measured intradiscal pressure, and measured intraabdominal pressure. EMG, intradiscal pressure, and IAP were recorded using the same methods described above for Ortengren et al. (1981). The subjects studied were three females and one male. The participants were asked to perform 25 different static exertions while sitting or standing. These tasks involved resisting weights applied horizontally and vertically, which resulted in asymmetric and symmetric loads on the spine. The biomechanical model algorithms were based on a linear programming procedure that

minimized spinal disc compressive force. In a second set of algorithms, the effect of intraabdominal pressure was added.

The investigators found that the disc compressive force predicted by the biomechanical model correlated well with the measured intradiscal pressure under the conditions studied. This relationship is illustrated in Figure 2.6. Another interesting discovery was that internal forces contributed more to disc compressive force than large externally applied loads. Despite the fact that high correlations between model predictions and measured pressures were found, the biomechanical model relied on the assumption that antagonistic muscle activity was absent. This assumption could result in prediction of lower disc compressive forces than actually occurred. The failure to predict antagonistic activity is a common drawback of linear programming optimization models.

Schultz, Andersson, Haderspeck, Ortengren, Nordin and Björk (1982b) conducted a similar study in which one objective was to compare two optimization-based muscle force prediction algorithms with EMG activity. The participants, 10 male students, performed a series of 20 weight resisting tasks that imposed loads on the trunk. The tasks involved resisting weights in an upright standing posture with the trunk in flexion or extension, right lateral bending, and twisting. Myoelectric activity was recorded with twelve pairs of electrodes placed posteriorly at the C4, T8, and L3 levels, over the rectus abdominus muscles, and over the oblique abdominals. The first optimization model led to the minimization of compressive force on the L3 intervertebral disc. The second model led to the minimization of the largest muscle contraction intensity. The investigators found that tasks involving twisting or lateral bending did not load the spine significantly more than comparable sagittally symmetric tasks. The largest calculated spine loads occurred when the trunk was flexed 30°, even when no weights were held. Correlations between EMG activity and predicted muscle force for the minimum compressive force assumption ranged from 0.34 to 0.92. The minimum contraction intensity objective produced more consistent

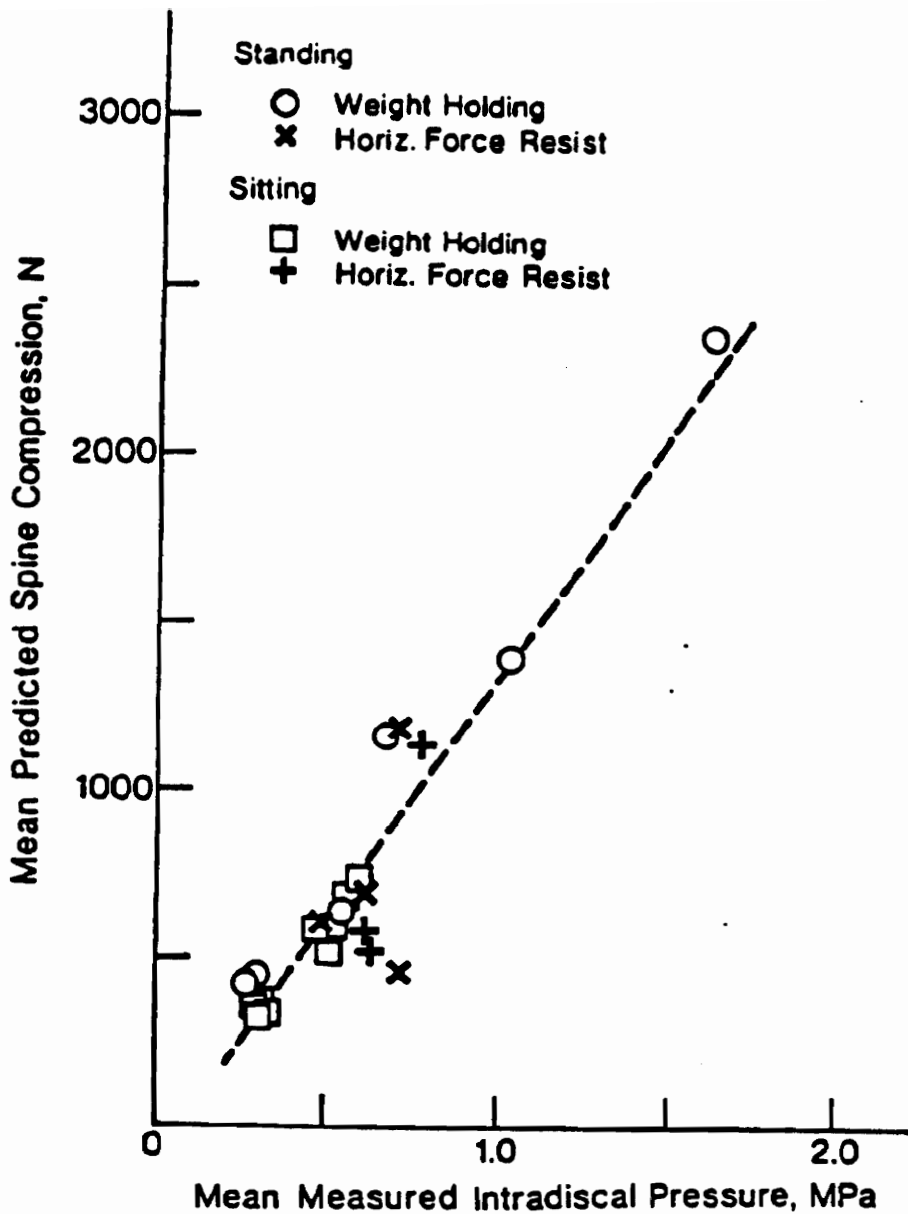


Figure 2.6 Predicted compression forces on the spine as a function of intradiscal pressure. The correlation coefficient for the point pairs is 0.94. Taken from Schultz et. al (1982a).

correlations of 0.67 to 0.88 between EMG and predicted muscle force. The finding that twisting and bending did not produce higher spinal loads contradicts the belief that these types of activities result in increased loading of the spine.

Schultz, Haderspeck, Warwick, and Portillo (1983) included nonlinear programming-based muscle force prediction techniques in a study on low-back biomechanical models. The effect of including more trunk muscles in the models was also investigated. The methods and experimental tasks were almost identical to those of Schultz, et al. (1982b). Four optimization schemes were used to compute the internal forces. The first minimized the maximum muscle contraction intensity, the second minimized compressive force on the spine, and the last two were nonlinear optimization schemes. The two nonlinear approaches predicted muscle forces based on minimizing the sum of the squares and minimizing the sum of the cubes of muscle contraction intensities. Also, the algorithms incorporated 10, 14 or 22 muscle equivalents. The investigators found that predictions of disc compressive force did not significantly differ among the 10, 14 and 22 muscle schemes. They also found, as did Schultz, et al. (1982b), that the minimization of muscle intensity algorithm showed the best correlation with measured EMG activity.

Other studies more recently reported have further investigated the validity of the muscle force prediction models and examined the EMG activity of the trunk musculature. Pope, Andersson, Broman, Svensson, and Zetterberg (1986) examined EMG activity during the development of axial torques. They found that considerable antagonistic muscular activity was present in the tasks studied, which as previously mentioned is not predicted by some linear programming techniques. The researchers also found that intraabdominal pressure had little effect on reducing the activity of the anterior trunk muscles. A third and most interesting discovery was that in the tasks studied, axial

twisting contributed significantly to large loads on the spine, contrary to the findings of Schultz et al. (1982b).

With regards to antagonistic activity, Zetterberg, Andersson and Schultz (1987) reported substantial myoelectric activity of the abdominal muscles during attempted trunk extension in addition to maximum activity of the erector spinae. They also pointed out the importance of accounting for antagonism in low-back biomechanical modeling. Schultz, Cromwell, Warwick, and Andersson (1987) investigated the performance of the maximum muscle intensity minimization model in cases of heavy exertion. They found that the model gave well correlated predictions of muscle activity with EMG under light and moderate loads, but was inadequate in the heavy loading conditions. They also observed antagonistic activity in some loading conditions. Hughes (1991) conducted an extensive electromyographic evaluation of optimization-based lumbar muscle prediction models. He found that in general, models which minimize compressive force on the spine are not valid in many conditions. He also found that models which predict muscle force based on the minimization of the sum of cubed muscle intensity hold up better in varied loading situations.

Hughes (1991) used the technique of Crowninshield and Brand (1981) to predict the forces of ten trunk muscles in a low-back biomechanical model based at the L3/L4 joint. The value of n in the objective function was set to 3, resulting in a model that minimized the sum of the cubed muscle contraction intensities (SCI). Trunk muscle EMG data were recorded during isometric trunk flexion, extension, and torsional loading of eight male subjects. The results indicated that the SCI model predicted some muscle activity in accordance with EMG measurements, but failed to predict the activity of the extensor musculature well. Hughes (1991) also reported good correlation between predicted values of the SCI model and measured torso EMG for major trunk muscle groups. He also noted that the SCI model showed favorable response during combined extension and lateral

bending movements. In these cases, the model predicted differential activity of the erector spinae muscles which was also evident in the EMG readings.

Hughes (1991) also evaluated the Bean et al. (1988) double linear programming model in a series of electromyographic studies. The DLP model failed to predict differential levels of erector spinae force during lateral bending motion. The model also does not predict antagonistic activity as do many linear programming models. The agreement between SCI model predictions of spinal compressive force and EMG-based spinal compressive force predictions was quite good, showing a correlation coefficient of 0.98. In torsion and flexion loadings, Hughes reported that the DLP model predicted higher compressive force loads than the SCI model of Crowninshield and Brand (1981). He also found that the DLP model could predict some extensor activity that the SCI model could not during combined torsion and flexion loading.

A reoccurring theme in these investigations is that while the optimization models offer reasonable predictions of muscle activity and spinal loading, many models fail to properly account for antagonistic activity. However, this fault must be weighed against the inherent disadvantages of EMG-based low-back models. The EMG models require substantial instrumentation and are quite intrusive, limiting the extent to which they can be applied in a practical setting. The optimization models may be more easily applied to real world settings, such as the evaluation of potentially stressful manual tasks in industry.

Even in light of Hughes' research there is no one optimization-based lumbar muscle force prediction model that works well in all situations of trunk loading. The double linear programming method of Bean et al. (1988) and the SCI model of Crowninshield and Brand (1981) appear to be the best non-invasive techniques available for the estimation of low-back compressive force. The DLP model will be used in this research to estimate loads on the spine during a simulated railroad hand brake setting task.

3. MODEL FORMULATION

This chapter describes the development of the biomechanical low-back model that was used to predict spinal loading in the experiment. Details of the experimental tasks are contained in the next chapter. This chapter is presented in three main sections. The first section describes the operation of the model that estimates the externally caused moment about the L3/L4 joint. This moment is initially expressed in a coordinate system orthogonal to the walls and floor of the laboratory. The second section outlines the procedures used to transform the moments and forces computed in the room reference frame to the reference frame defined by the body. The third section describes the application of the Bean et al. (1988) double linear programming method for estimating trunk muscle forces and consequently compressive force on the L3/L4 joint. The model is similar to a version developed by Hughes (1991).

3.1 External Force Model Formulation

The external moment resulting at the L3/L4 level is estimated by performing a static free body analysis on the links of the body above L3/L4. Recall that a static biomechanical system is governed by the equations of static equilibrium and in this case, can be expressed as:

$$\begin{aligned}\sum \mathbf{F}_{\text{external}} + \sum \mathbf{F}_{\text{internal}} &= 0 \\ \sum \mathbf{M}_{\text{external}} + \sum \mathbf{M}_{\text{internal}} &= 0\end{aligned}\tag{3.1},$$

where \mathbf{F} and \mathbf{M} are three-dimensional vectors representing the internal and external forces and moments acting on the body.

Data needed for the analysis are hand force vectors, posture coordinates, and link centers-of-mass and weights. The posture coordinates represent the positions of joint end points and centers-of-rotation in a three-dimensional coordinate system whose origin is located at the L3/L4 joint. The coordinate system is orthogonal to the walls and floor of the

laboratory and is shown in Figure 3.1. The force vectors and position coordinates are both measured in this reference frame. This reference frame is referred to in the text as the *room reference frame*. The variables used in the free body analysis are listed in Table 3.1. Center-of-mass locations for the limbs are calculated based on a percentage of link length reported by Webb Associates (1978). The torso center-of-mass formula is taken from Clauser, McConville, and Young (1969). Individual segment weights are computed based on percentages of total body weight as described in Webb Associates (1978) and in Clauser, McConville, and Young (1969).

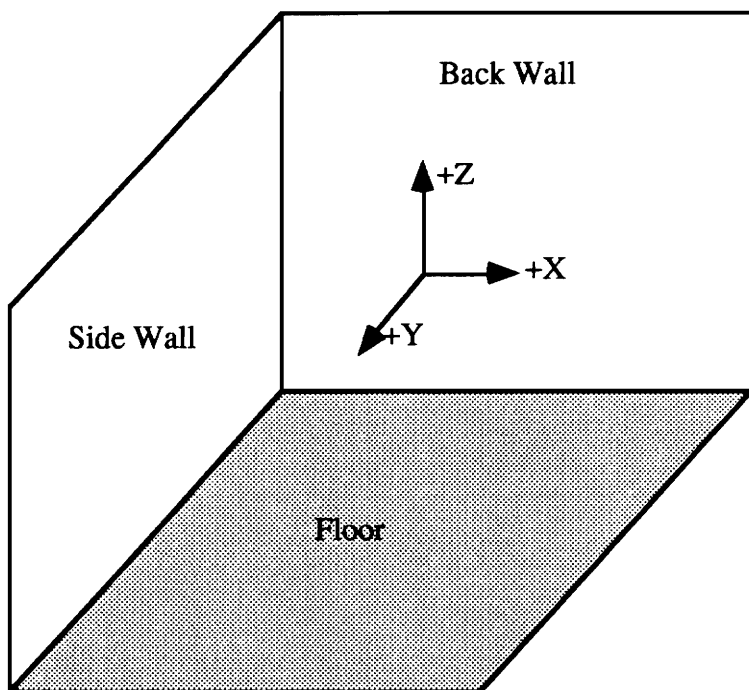


Figure 3.1 Orientation of the room coordinate system.

Table 3.1 Variables used in external force model. Moment arms r^j (cm) and forces F (N).

Variable	Description	Calculation
r^j_{LA}	lower arm center-of-rotation (elbow) to handgrip location for side j	measured during experiment
r^j_{LA-COM}	lower arm center-of-rotation to lower arm center-of-mass for side j	$0.43(r^j_{LA})$
r^j_{UA}	upper arm center-of-rotation (shoulder) to lower arm center-of-rotation for side j	measured during experiment
r^j_{UA-COM}	upper arm center-of-rotation (shoulder) to upper arm center-of-mass for side j	$0.436(r^j_{UA})$
r^j_{Torso}	torso center-of-rotation (L3/L4) to upper arm center-of-rotation for side j	measured during experiment
$r_{Torso-COM}$	torso center-of-rotation to torso center-of-mass	(head to trunk length) - (.491*bicrestal breadth + .408* head to trunk length + 1.313) ¹
F^j_{Hand}	external reaction force acting on hand for side j	measured during experiment
$F_{LA\ Wt}$	force due to weight of lower arm (same for both sides)	$0.023(\text{total body weight})^2$
$F_{UA\ Wt}$	force due to weight of upper arm (same for both sides)	$0.028(\text{total body weight})^2$
$F_{Torso\ Wt}$	force due to weight of torso (includes head and neck)	$0.508(\text{total body weight})$

¹ Refer to Clauser, McConville, and Young (1969) for explanation of terms.

² The weight of the total arm is divided into upper arm and lower arm (forearm and hands) segments according to the percentages reported in Webb Associates (1978).

The determination of the externally caused moment about L3/L4 is then a process of moment addition. The model first calculates the three-dimensional vector moment at the elbow for each side of the body, which is expressed as:

$$M^j_{elbow} = M^j_{ext\ force} + M^j_{seg\ wt} \quad (3.2),$$

where $M_{\text{ext force}}^j$ is the moment about the elbow due to the hand force acting at the hand grip location for side j . The component $M_{\text{seg wt}}^j$ is the moment due to the weight of the lower arm rotating about the elbow for side j . In expanded form, the equation can be expressed as:

$$M_{\text{elbow}}^j = (r_{\text{LA}}^j \times F_{\text{Hand}}^j) + (r_{\text{LA-COM}}^j \times F_{\text{LA wt}}) \quad (3.3).$$

The model next calculates the moment about each shoulder, which is expressed as:

$$M_{\text{shoulder}}^j = M_{\text{ext force}}^j + M_{\text{seg wt}}^j + M_{\text{elbow}}^j \quad (3.4),$$

where $M_{\text{ext force}}^j$ is now the sum of the hand force and lower arm weight acting at the elbow (end of the upper arm link) for side j . The vector $M_{\text{seg wt}}^j$ now represents the moment due to the weight of the upper arm rotating about the shoulder for side j . The quantity M_{elbow}^j is the same quantity from Equation 3.3. In expanded form, the moment about each shoulder is:

$$M_{\text{shoulder}}^j = \left[r_{\text{UA}}^j \times (F_{\text{Hand}}^j + F_{\text{LA wt}}) \right] + (r_{\text{UA-COM}}^j \times F_{\text{UA wt}}) + M_{\text{elbow}}^j \quad (3.5).$$

The model finally calculates the moment about the L3/L4 joint, expressed as:

$$M_{\text{L3/L4}} = \sum_{j=1}^2 M_{\text{ext force}}^j + M_{\text{seg wt}} + \sum_{j=1}^2 M_{\text{shoulder}}^j \quad (3.6),$$

where $M_{\text{ext force}}^j$ represents the moment due to hand force, lower arm weight, and upper arm weight acting the shoulder rotating about the L3/L4 joint. The vector $M_{\text{seg wt}}$ depicts the moment due to the weight of the torso (including head and neck) rotating about the L3/L4 joint. The moments due to external forces and the moments about the shoulder must be summed across sides because the L3/L4 moment is that of a singular joint. In expanded form, the moment about L3/L4 is:

$$\begin{aligned} \mathbf{M}_{L3/L4} = & \sum_{j=1}^2 \left[\mathbf{r}_{\text{Torso}}^j \times (\mathbf{F}_{\text{Hand}}^j + \mathbf{F}_{\text{LA Wt}}^j + \mathbf{F}_{\text{UA Wt}}^j) \right] \\ & + (\mathbf{r}_{\text{Torso-COM}} \times \mathbf{F}_{\text{Torso Wt}}) + \sum_{j=1}^2 \mathbf{M}_{\text{shoulder}}^j \end{aligned} \quad (3.7),$$

The model also resolves the external forces acting on the body, as these must be added when spinal disc compressive force is calculated. The external forces acting at L3/L4 are expressed as:

$$\mathbf{F}_{L3/L4} = \mathbf{F}_{\text{ext force}} + \mathbf{F}_{\text{seg wt}} \quad (3.8),$$

where $\mathbf{F}_{\text{ext force}}$ represents the forces due to external loads and $\mathbf{F}_{\text{seg wt}}$ represents the total force due to gravity acting upon individual body segments above L3/L4. The equation in expanded form is:

$$\mathbf{F}_{L3/L4} = \sum_{j=1}^2 \mathbf{F}_{\text{Hand}}^j + 2\mathbf{F}_{\text{LA Wt}} + 2\mathbf{F}_{\text{UA Wt}} + \mathbf{F}_{\text{Torso Wt}} \quad (3.9),$$

To this point, all positions and moments have been expressed relative to the room reference frame. The forces and moments now must be transformed and expressed in the reference frame of the body.

3.2 Transformation to Body Reference Frame

The implementation of the optimization-based model of low-back internal forces requires that the resultant forces and moments acting at the L3/L4 joint be expressed relative to a specific coordinate system of the body. The body reference frame is different from the axis system used in the previous section for resolution of the external forces. This body coordinate system is defined by a cutting plane orthogonal to the torsional axis of the L3/L4 vertebral section. Figure 3.2 shows the orientation of this coordinate system. Therefore, the resultant forces and moments must be transformed to

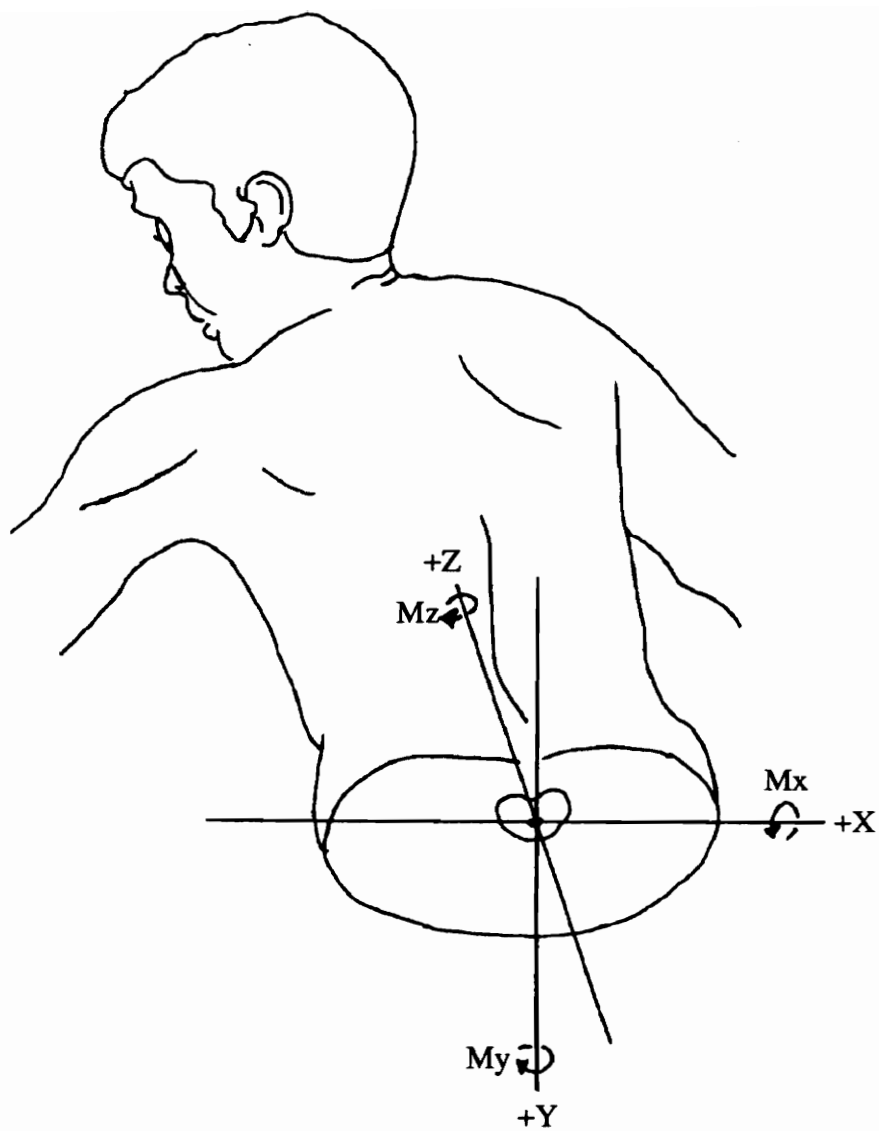


Figure 3.2 Three-dimensional coordinate system used in the model. Adapted from Hughes (1991).

the new cutting plane axis system. A description of the transformation process used in the biomechanical model follows.

The model first assumes that the Z - axis of the body is represented by a vector from L3/L4 to the midpoint of the two shoulders. This vector approximates the alignment of the spine and therefore also approximates the orientation of the torsional axis of the L3/L4 joint. This vector is still expressed in terms of the original coordinate system.

The next stage in the transformation process is to define a plane orthogonal to the Z - axis of the body. The *Gram-Schmidt orthogonalization process* is used to define this plane. A good discussion of the procedure can be found in Bradley (1975). Two vectors, γ_2 and γ_3 , which are both orthogonal to the Z - axis, are computed as:

$$\gamma_2 = \alpha_2 - \left[\frac{(\alpha_2 | \gamma_1)}{(\gamma_1 | \gamma_1)} \right] \gamma_1 \quad (3.10),$$

$$\gamma_3 = \alpha_3 - \left[\frac{(\alpha_3 | \gamma_1)}{(\gamma_1 | \gamma_1)} \right] \gamma_1 - \left[\frac{(\alpha_3 | \gamma_2)}{(\gamma_2 | \gamma_2)} \right] \gamma_2 \quad (3.11),$$

where γ_1 represents the Z axis expressed as a vector. The variables α_2 and α_3 are defined as any two vectors that are not scalar multiples of γ_1 , γ_2 , or γ_3 .

As part of the experimental measurements, a vector was established from the L3/L4 joint to a point located approximately 11 cm lateral of L3/L4. This vector was measured to establish to what degree the torso cutting plane had rotated about L3/L4. This point is not necessarily orthogonal to the Z - axis just defined. The X - axis is defined by projecting the vector just described onto the plane defined by γ_2 and γ_3 . The X - axis can then be expressed as

$$\beta = \left[\frac{(\alpha | \gamma_2)}{(\gamma_2 | \gamma_2)} \right] \gamma_2 + \left[\frac{(\alpha | \gamma_3)}{(\gamma_3 | \gamma_3)} \right] \gamma_3 \quad (3.12),$$

where α represents the L3/L4 lateral vector and γ_2 and γ_3 are as before.

The last body reference frame axis to be defined is the Y - axis which can be represented by a vector orthogonal to both γ_1 (the Z - axis) and β (the X - axis). The Y-axis can be expressed as

$$\delta = \gamma_1 \times \beta \quad (3.13),$$

or the cross product of γ_1 and β . Figure 3.3 illustrates the different axes defined in the equations just discussed.

Now that the axes that compose the body reference frame have been defined, it is necessary to create a transformation matrix that will be used to express vectors measured in the room reference frame in terms of the body reference frame. A good discussion of this process can be found in Craig (1989). The body reference frame axis vectors must be converted into unit vectors and then broken into their individual components. If x , y , and z are defined as the unit vectors of β , δ , and γ_1 respectively, then the individual components of these unit vectors can be expressed as:

$$\begin{aligned} x &= (a_1, a_2, a_3), \\ y &= (b_1, b_2, b_3), \\ z &= (c_1, c_2, c_3), \end{aligned} \quad (3.14),$$

and a 3 x 3 transformation matrix, ${}^{\text{room}}_{\text{body}}\mathbf{Trans}$, is constructed from these individual unit vector components as follows:

$${}^{\text{room}}_{\text{body}}\mathbf{Trans} = \begin{vmatrix} a_1 & a_2 & a_3 \\ b_1 & b_2 & b_3 \\ c_1 & c_2 & c_3 \end{vmatrix} \quad (3.15).$$

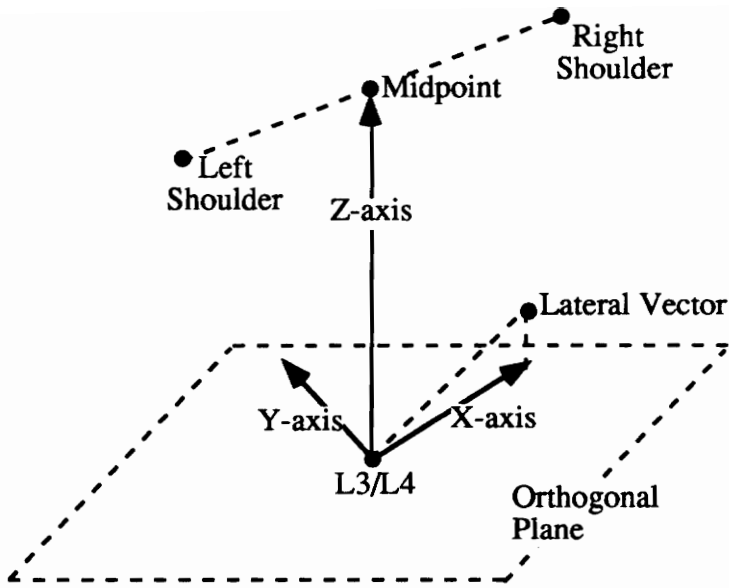


Figure 3.3 The axes of the body coordinate system as defined by the vectors β , δ , and γ_1 (X, Y, and Z - axes respectively). ;.

Any vector expressed in terms of the room reference frame can now be transformed to the body reference frame by simply multiplying by the transformation matrix as follows:

$${}^{\text{body}}\mathbf{V} = {}^{\text{room}}\mathbf{T}_{\text{body}} \text{Trans } {}^{\text{room}}\mathbf{V} \quad (3.16),$$

where ${}^{\text{body}}\mathbf{V}$ is the vector expressed in the body reference frame and ${}^{\text{room}}\mathbf{V}$ is the vector expressed in the room reference frame.

Thus, an algorithm has been described that estimates the net reaction of moments and forces acting at the L3/L4 joint due to external forces. A transformation matrix is used to convert the resultant moment and force vectors (Equations 3.7 and 3.9) to the body reference frame. These moments are then used as inputs to the optimization algorithms which estimate lumbar muscle forces that the body generates to resist the external forces and moments. The external force model and vector transformation process have been implemented as Pascal programs on an IBM PC. This software inputs force and posture data generated by other equipment for use in the model calculations. The force and posture measurement apparatuses are described in greater detail in the next chapter.

3.3 Optimization Model Formulation

The double linear programming (DLP) method of Bean et al. (1988) was used to estimate muscle forces and compressive force at the L3/L4 joint. The L3/L4 joint has been chosen instead of the L5/S1 joint because it is not well known how the orientation of the L5/S1 joint changes with three-dimensional body posture variations. The L3/L4 joint in this case is assumed to stay aligned with the torso.

The approach of a static free body analysis is used to implement the muscle force optimization scheme. The analysis is performed at an imaginary cutting plane at the L3/L4 level, which is equivalent to the orthogonal plane described in the previous section. Figure 3.4 shows the 5 muscle pairs to be included in the model: erector spinae (LES, RES),

latissimus dorsi (LLD, RLD) rectus abdominus (LRA, RRA), external obliques (LEO, REO), and internal obliques (LIO, RIO).

Muscle moment arms and muscle lines of action are the two pieces of anatomical information used to describe the muscle forces. Muscle cross sectional areas are included in the constraint equations for the optimization scheme. The muscle moment arms of Tracy et al. (1989) and the muscle lines of action of Dumas et al. (1988) were used in the model and are shown in Table 3.2. The cross sectional areas of Tracy et al. (1989) are multiplied by the z component of the unit force vector as described in McGill, Patt, and Norman (1988).

Table 3.2 Data used in optimization model: Moment arms r_x , r_y , r_z (cm), unit muscle force components t_x , t_y , t_z , and anatomical cross sectional areas A_i (cm²). Adapted from Hughes (1991).

Muscle	r_x^i	r_y^i	r_z^i	t_x^i	t_y^i	t_z^i	A_i
L. Erector Spinae	-3.82	-5.76	0.0	0.281	-0.052	-0.958	24.9
R. Erector Spinae	3.82	-5.76	0.0	-0.281	-0.052	-0.958	24.9
L. Rectus Abdominus	-3.38	7.95	0.0	-0.028	0.016	-0.9995	6.6
R. Rectus Abdominus	3.38	7.95	0.0	0.028	0.016	-0.9995	6.6
L. Internal Oblique	-11.39	0.96	0.0	-0.134	-0.574	-0.808	14.2
R. Internal Oblique	11.39	0.96	0.0	0.134	-0.574	-0.808	14.2
L. External Oblique	-12.62	1.09	0.0	0.376	0.322	-0.870	15.3
R. External Oblique	12.62	1.09	0.0	-0.376	0.322	-0.870	15.3
L. Latissimus Dorsi	-7.19	-5.42	0.0	0.340	-0.284	-0.897	3.9
R. Latissimus Dorsi	7.19	-5.42	0.0	-0.340	-0.284	-0.897	3.9

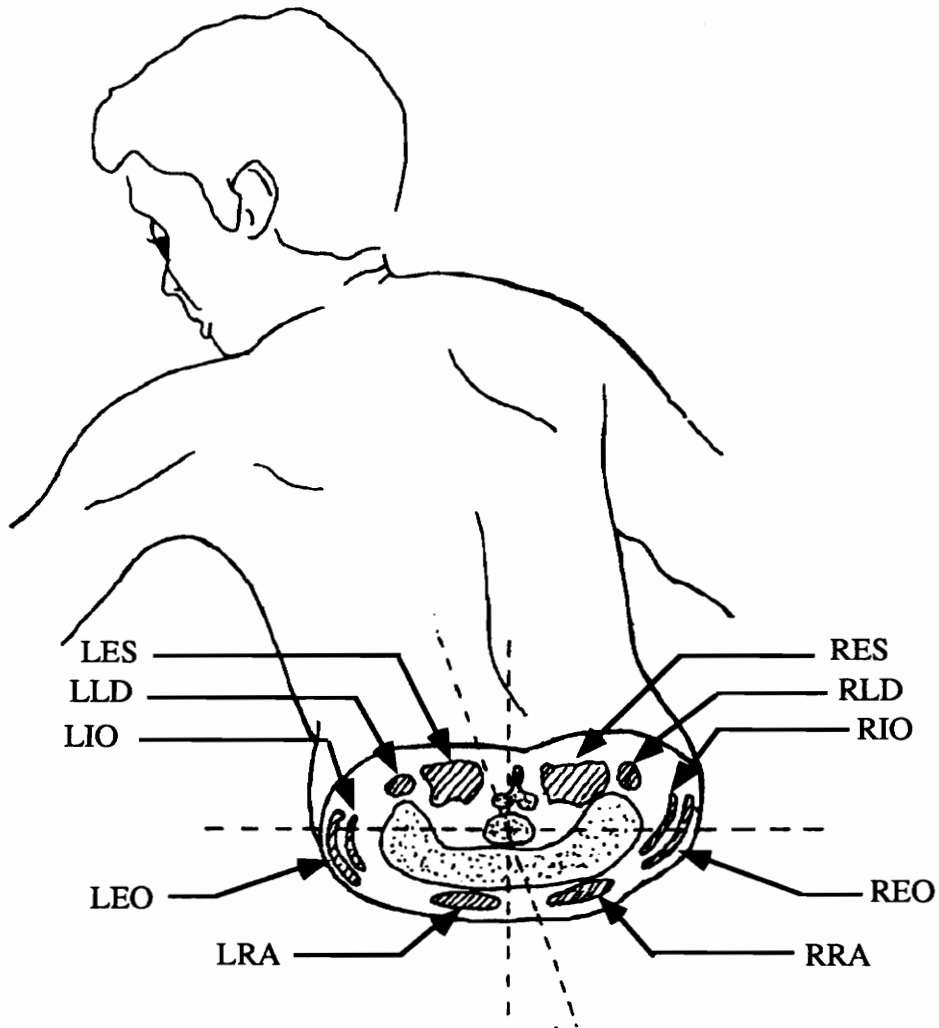


Figure 3.4 The 5 lumbar muscle pairs used in the model: Erector Spinae (LES, RES), Latissimus Dorsi (LLD, RLD), Internal Obliques (LIO, RIO), External Obliques (LEO, REO), and Rectus Abdominus (LRA, RRA). Adapted from Hughes (1991).

The requirement that the moments due to internal forces must balance the moments due to externally applied forces can be expressed as:

$$\sum_{i=1}^n \|\mathbf{f}_i\| (\mathbf{r}_i \times \mathbf{t}_i) + \mathbf{M}_{\text{ext}} = 0 \quad (3.17),$$

where \mathbf{M}_{ext} is the three-dimensional moment due to externally applied forces and \mathbf{f}_i is the three-dimensional force vector for muscle i . The variable n represents the number of muscles included in the analysis ($n=10$ in this case).

The Bean et al. (1988) DLP algorithm can be applied to the L3/L4 joint. The first step is to minimize the maximum muscle contraction intensity

$$\text{minimize } I \quad (3.18),$$

$$\text{subject to: } \sum_{i=1}^n \|\mathbf{f}_i\| (\mathbf{r}_i \times \mathbf{t}_i) = -\mathbf{M}_{\text{ext}}$$

$$\frac{\|\mathbf{f}_i\|}{A_i} \leq I,$$

$$\|\mathbf{f}_i\| \geq 0,$$

where \mathbf{f} represents the force in muscle i and \mathbf{r} and \mathbf{t} are three-component vectors representing the x , y , and z directions of moment arm and unit force, respectively. The variable \mathbf{M}_{ext} represents the three-component moment caused by the externally applied forces. The second step is to minimize the contribution of muscle force to spinal compressive force:

$$\text{minimize } \sum_{i=1}^n \|\mathbf{f}_i\| t_z^i \quad (3.19),$$

$$\text{subject to: } \sum_{i=1}^n \|\mathbf{f}_i\| (\mathbf{r}_i \times \mathbf{t}_i) = -\mathbf{M}_{\text{ext}}$$

$$\frac{\|\mathbf{f}_i\|}{A_i} \leq I^*,$$

$$\|f_i\| \geq 0,$$

where I^* represents the maximum intensity found as a result of the first optimization step.

Finally, compressive force at the L3/L4 disc is computed for the optimal solution by adding all lumbar muscle forces in the z direction (perpendicular to the cutting plane) and the resultant force due to external forces as follows:

$$F_{\text{Compression}} = \sum_{i=1}^n \|f_i\| t_z^i + F_{L3/L4z} \quad (3.21).$$

In this formula, $F_{L3/L4z}$ represents the z component of the external force acting on L3/L4 in equation 3.8.

4. METHOD

This chapter describes an experiment conducted to evaluate low-back stress resulting from the performance of a simulated wheel turning task. The experimental task mimics the method used by railroad yardmen to set railcar brakes. Subjects performed a series of isometric exertions on a mockup of the railcar hand brake arrangement during which posture and reactive forces at the hands were recorded. The modeling techniques developed in the previous chapter were used to predict spinal compressive force at the L3/L4 joint under the varying experimental conditions. Subjects also completed a series of standard whole-body strength tests.

4.1 Subjects

Sixteen college students served as participants in the research. They were recruited from the student body at Virginia Tech by means of advertisement. The subjects were divided into four groups of four subjects each, based on gender and anthropometry. This grouping is discussed in detail in Section 4.3. All participants were in good health and had no history of any low-back pain or musculoskeletal disorders. Each person was asked to complete a physical fitness questionnaire prior to participation. Each subject also filled out an informed consent form prior to the study. Subjects were reimbursed \$5 per hour for their time.

4.2 Apparatus

The equipment developed for the experiment includes force measurement instrumentation, a posture recording system, and a custom built rig that emulates the typical layout of the rear of a railcar. Whole-body static strength was assessed using a load cell and handle arrangement. Posture was measured by means of a three-dimensional motion analysis system. Load cells interfaced through amplifiers and analog-to-digital converters to a microcomputer were used to measure forces.

4.2.1 Whole-body Static Strength Measuring System

A single dimensional load cell system was used to assess static lifting strength. The system consisted of two handle sets, chain tether, floor anchor, load cell, and variable gain amplifier. The chain tether allowed the handle height above the floor to be adjusted. The load cell used was an Interface model SM-500. The variable gain amplifier was interfaced through the 16 channel Metrabyte Model STA-16 A/D board to an IBM Model 50 Personal Computer. The principal components of the static strength measuring system are shown in Figure 4.1.

4.2.2 Hand Brake Mockup

A steel rig structure was constructed to simulate the spacing and configuration of the ladder and hand brake area of a typical railroad boxcar. The dimensions of this rig closely match those of actual cars in use. A schematic of the rig, with important dimensions and components labeled, is shown in Figure 4.2. The ladder occupied the left side of the rig. The rungs were spaced at 19 inch intervals. A stamped steel brake wheel, 22 inches in diameter, was affixed to the right of the ladder. The wheel was mounted to a biomechanics force platform, which was in turn bolted to the rig framework. The force platform measured forces exerted on the brake wheel in three dimensions. A three-dimensional isometric load cell was mounted in one of the top two rung positions to measure forces exerted by the hand gripping the rung. The platform and load cell are covered in detail in the next section.

4.2.3 Force Measurement Apparatus

The force measurement apparatus was made up of the force platform, isometric load cell, amplifiers, and an analog-to-digital converter interfaced to a microcomputer. The AMTI Model OR6-5-1 Biomechanics Force Platform was used to simultaneously measure three force components along the X, Y, and Z - axes and three moments about

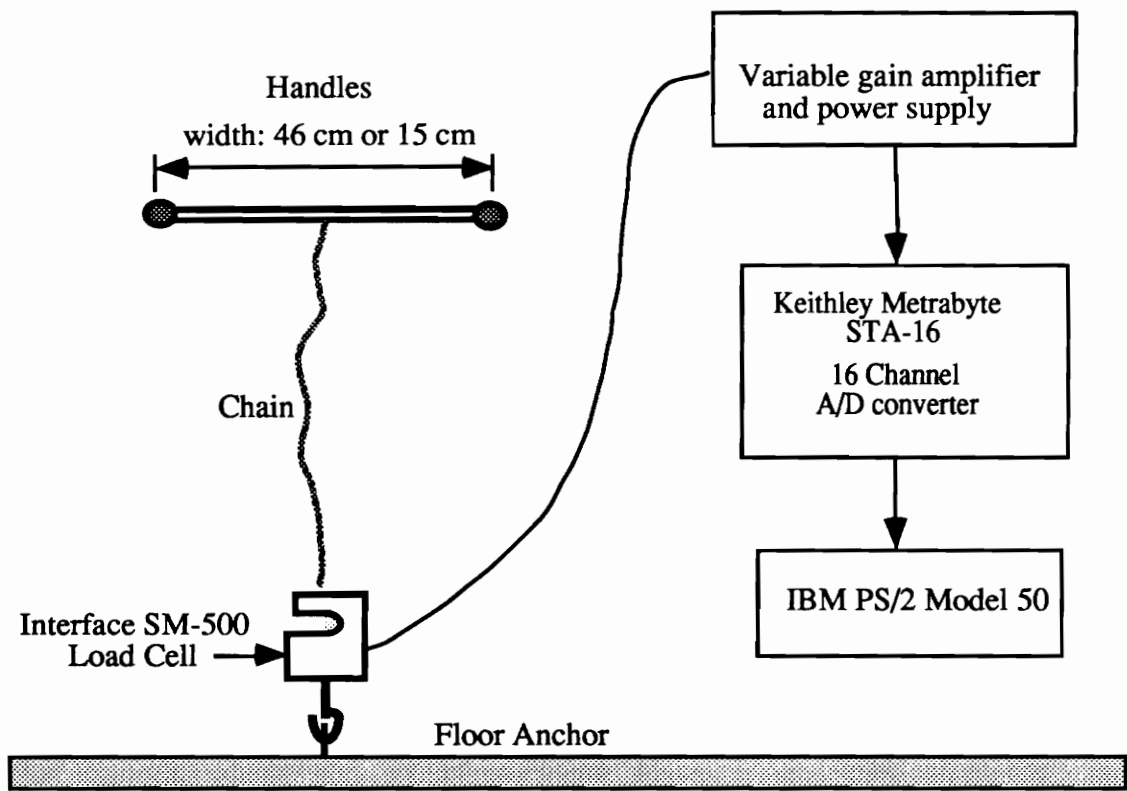


Figure 4.1 Schematic of whole-body static strength measurement system.

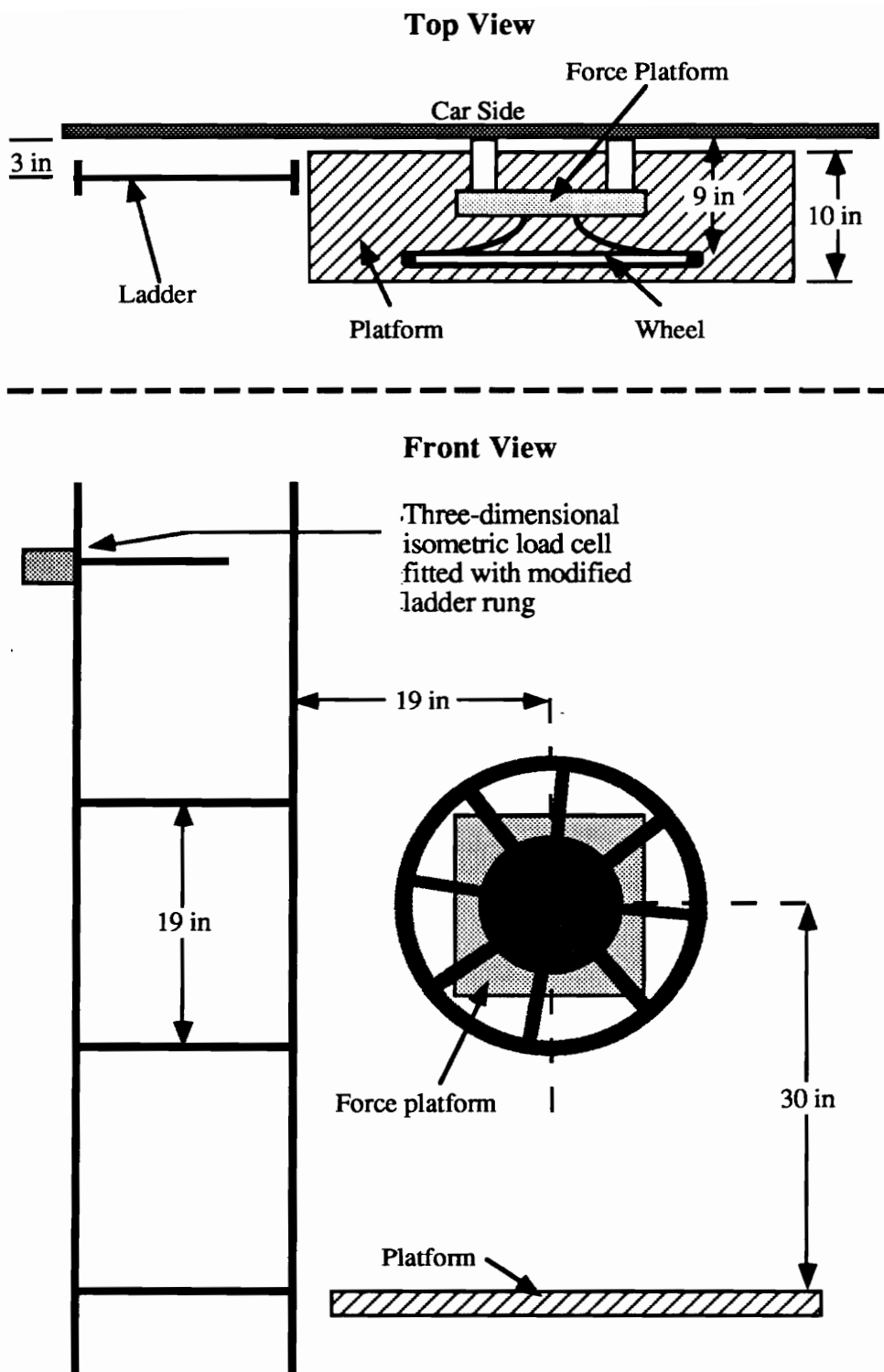


Figure 4.2 Schematic of custom rig built for the handbrake study.

each axis. The platform was connected to an AMTI Model SGA6-4 Strain Gage Amplifier system. The amplifier has six four-arm Wheatstone Bridge inputs, selectable bridge excitation of 2.5, 5.0, or 10.0 volts and adjustable gain of 1000, 2000, or 4000. The amplifier was configured with excitation set at 10.0 volts and gain at 1000 for the experiment. The force platform system was used to gather right hand force data.

The left hand force data was measured with a Lebow Products Model 6431 three-dimensional isometric load cell. The load cell is rated at 400 lbs capacity in each direction and was fitted with a modified ladder rung. The load cell was connected to a custom made six-channel bridge amplifier that incorporated variable gain of 1, 10, 100, and 1000 and excitation of 10 volts. The gain was set at 1000 for the experiment.

Signals from both the force platform and load cell amplifiers were fed to the 16-channel Keithely Metrabyte Model STA-16 analog-to-digital converter board. The A/D board was installed in an IBM Model 50 PS/2 Computer. Figure 4.3 is a schematic diagram illustrating the configuration of the force measurement apparatus. A computer program, written in Pascal was developed to enable the simultaneous collection of force data from all of the force inputs and to display feedback to subjects.

4.2.4 Posture Measurement System

A Northern Digital WATSMART three-dimensional motion analysis system was used to record subject posture data during the experimental trials. The system components included infrared emitting diodes, three infrared cameras, calibration frame, and the system unit which was interfaced to an IBM Model AT Personal Computer. The WATSMART system tracks the infrared diodes when attached to body targets. The three cameras were mounted above and outside the work envelope. Each camera was mounted to a stainless steel pole that was anchored in a small circular concrete base. The cameras were secured at a height of 2.45 m above the laboratory floor. The WATSMART

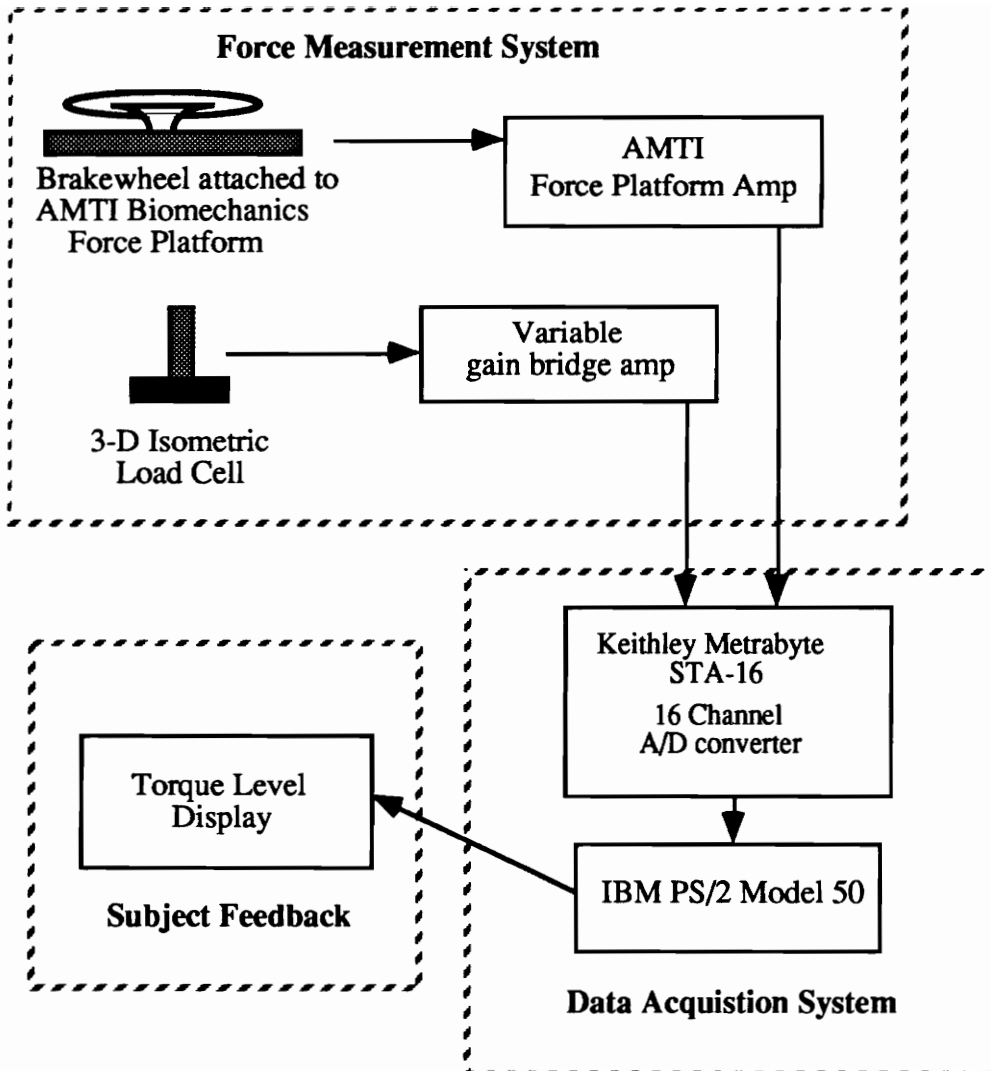


Figure 4.3 Force measurement apparatus configuration.

cameras are extremely sensitive to reflections and therefore the experimental area was bordered by black non-reflecting foam material hung as drapes on three sides and on the ceiling. Sheets of plywood that were painted flat black were placed on the floor to reduce reflections as well. Figure 4.4 depicts the overall layout of the experimental apparatuses and the specific locations of the three infrared cameras.

The WATSMART software employs a Direct Linear Transformation technique to reconstruct three-dimensional coordinates from the two-dimensional readings of at least two cameras. The system can track up to 32 points simultaneously at a maximum sampling rate of 4200 Hz. In the experimental trials, the infrared diodes were attached to joint endpoints and centers-of-rotation for the arms and trunk corresponding to the biomechanical model variables defined in Chapter 3. Therefore, the positions of the joints could be determined and used as input to the low-back biomechanical model to estimate disc compressive force. The data collection frequency was set at 20 Hz for the experiment. This frequency was used because the data files created for each trial became extremely large at higher collection rates.

For each experimental trial, position data was collected for each of eight points. These points defined the upper body linkage system of moment arms previously described in Table 3.1. Position markers were placed at each hand, elbow, and shoulder. Additionally, two markers were affixed in the low-back region, one located at the approximate level of the L3/L4 joint along the spinal column and the other located at the same level, but placed 11 cm laterally of the spinal column. The placement of the markers is illustrated in Figure 4.5.

4.2.5 Calibration Procedures

Calibrations were performed on each piece of equipment before each experimental session. The calibration procedure for the force measurement system

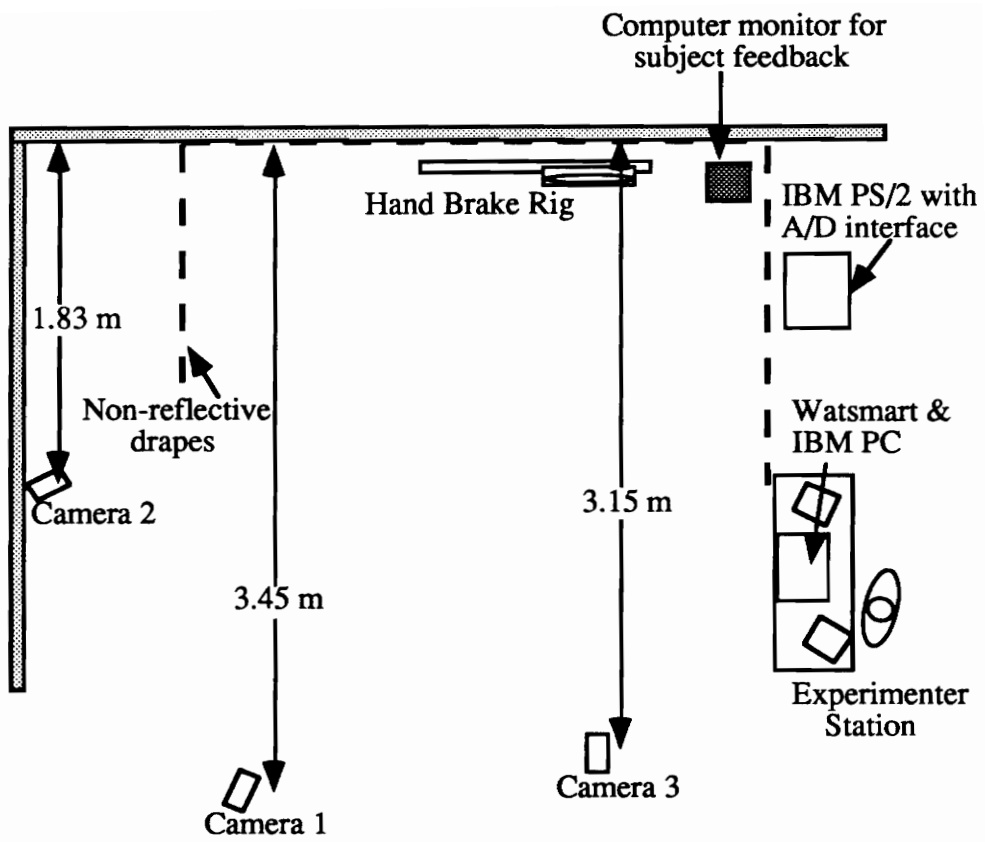


Figure 4.4 Top view of arrangement of experimental apparatus.

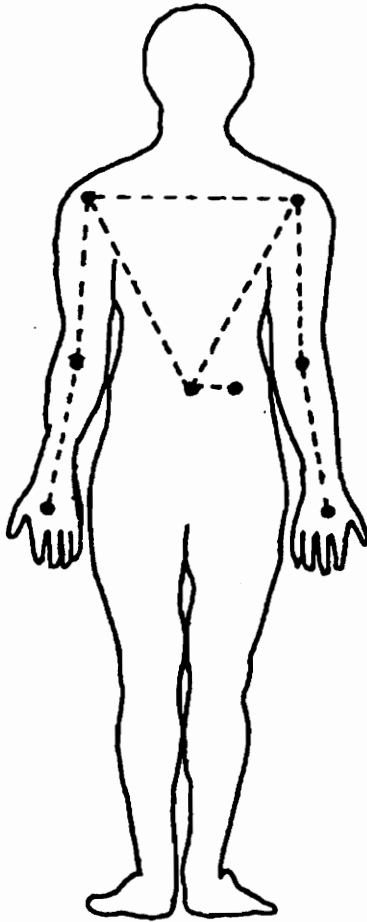


Figure 4.5 Posterior view of placement of WATSMART position markers on subject.

consisted of collecting A/D data with the load cell unloaded and then with the load cell loaded with a known force of 249N. A linear calibration equation was then defined by these two points and was used to compute loads from the A/D data gathered in the whole-body lifting trials.

The three-dimensional ladder rung load cell was calibrated using a similar procedure. In this case, data were collected with a known load of 162N applied in each of the three directions. This was accomplished by using a steel billet connected by cable through a pulley mount for the X and Y directions and by hanging the billet directly on the rung for the Z direction. The point of application of the load was kept constant by means of a notch in the ladder rung in which the billet hook could rest. Unloaded data were also collected in each direction. This calibration procedure was performed before and after each experimental session to ensure that minimal drift occurred in the load cell.

The force plate was calibrated to precision in the factory and therefore no calibration was needed during the experimental sessions. However, the force plate was checked prior to the experiment with known forces applied to the brake wheel and proved to be accurate. As a precautionary measure, unloaded data were collected before and after the experimental sessions to check for drift. Calibration of the WATSMART system was performed according to the manufacturer's guidelines.

4.3 Experimental Design

The experimental design was a mixed factors design with one between-subjects factor and three within-subjects factors. The design for the handbrake trials was a repeated measures design involving two trials per subject for each treatment combination totaling 32 trials per subject. The dependent measures included right hand force, left hand force, and three-dimensional body posture.

4.3.1 Independent Variables

Anthropometry (AN), between-subjects, 4 levels: Subjects belonged to one of four groups, defined by height and weight percentiles. Subjects fell into both of the height and weight percentile boundaries for the appropriate group. The percentiles were calculated from the anthropometry of 150 male college students and 150 female college students that participated in an earlier strength testing study (Virginia Tech Industrial Ergonomics Lab, 1992). The four groups are shown below in Table 4.1.

Table 4.1 Four levels of the independent variable *Anthropometry*;, based on data reported by The Virginia Tech Industrial Ergonomics Lab (1992).

Title	Definition	Stature Range (cm)	Weight Range (kg)
'Small Female'	Weight between 5th and 15th percentiles and height between 5th and 15th percentiles	151.3 - 158.6	40.8 - 52.1
'Average Female'	Weight between 45th and 55th percentiles and height between 45th and 55th percentiles	163.9 - 166.6	60.2 - 64.3
'Average Male'	Weight between 45th and 55th percentiles and height between 45th and 55th percentiles	170.4 - 174.2	67.1 - 72.4
'Large Male'	Weight between 85th and 95th percentiles and height between 85th and 95th percentiles	181.5 - 191.7	82.8 - 97.2

Torque Level (T), within-subjects, 4 levels: Subjects performed two maximum safe exertions on the hand brake, pulling with the most force they could safely exert. Subjects also performed two exertions at each of three submaximal torque levels: 75%, 50%, and 25% of the average torque level generated in the two maximum safe exertion trials.

Ladder Rung (R), within-subjects, 2 levels: Subjects gripped with their left hand at each of the top two ladder rung positions on the railcar rig mockup. The three-dimensional load cell was placed at the corresponding grip level for each set of trials.

Posture (P), within-subjects, 2 levels: Subjects assumed two different general body postures during the experiment. In one posture, the subjects were instructed to keep their shoulders and hips aligned as parallel to the back wall and railcar ladder as possible. This posture was referred to as 'facing the wall'. In the second posture, subjects were instructed to turn their shoulders and hips away from the wall and ladder and face toward the wheel. This posture was referred to as 'facing the wheel.' Figures 4.6 through 4.9 illustrate the four combinations of the experimental variables *Ladder Rung* and *Posture*.

4.3.2 Counterbalancing of Independent Variables

The variables *Ladder Rung* and *Posture* were counterbalanced by means of a random Latin Square presentation order. The specific coding of the treatment combination of the two variables is shown in Table 4.2. This coding scheme was maintained throughout the course of the experiment.

Table 4.2 Treatment combinations of the independent variables *Ladder Rung* and *Posture*.

Treatment code	<i>Ladder Rung</i>	<i>Posture</i>
1	Upper rung	Facing wall
2	Upper rung	Facing wheel
3	Lower rung	Facing wall
4	Lower rung	Facing wheel

A total of four random 4 x 4 Latin Squares were developed for the treatment ordering, one Latin Square for each level of the between-subjects variable *Anthropometry*. The four random Latin Squares generated for the actual experiment are shown in Table 4.3.

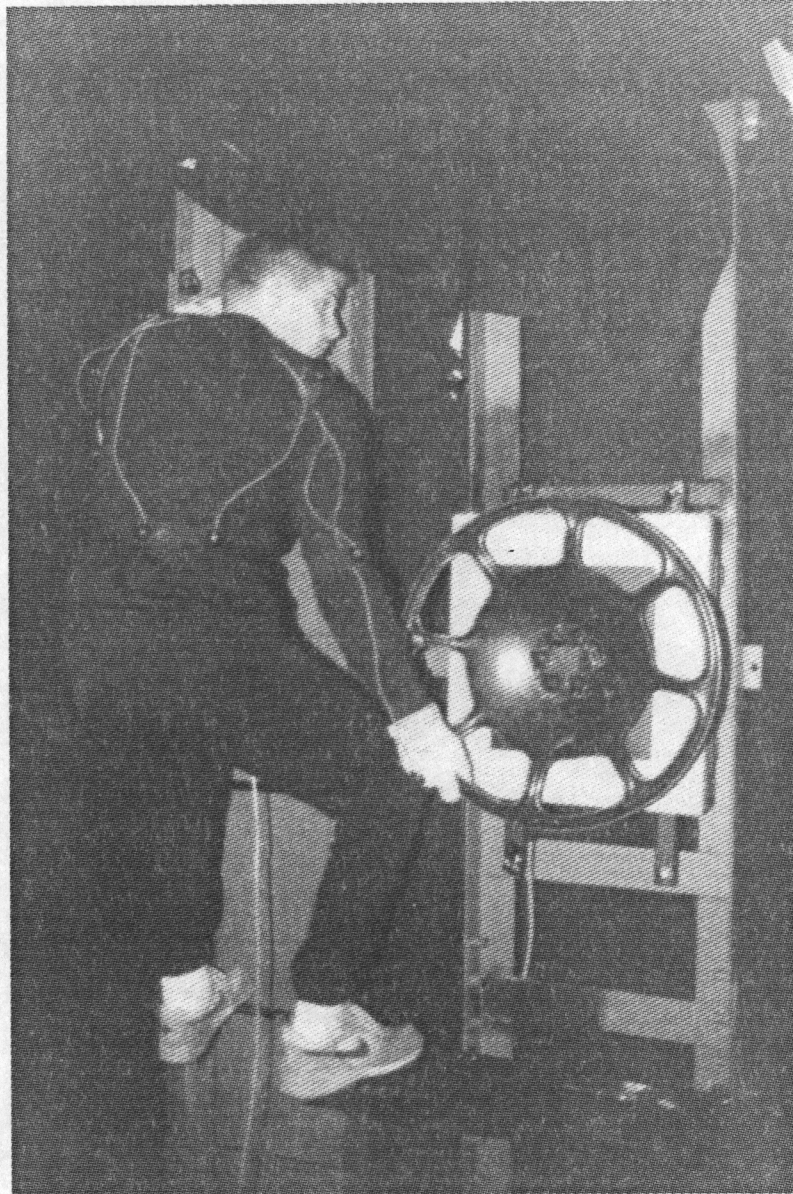


Figure 4.6 'Face the wall' posture with upper rung grip.

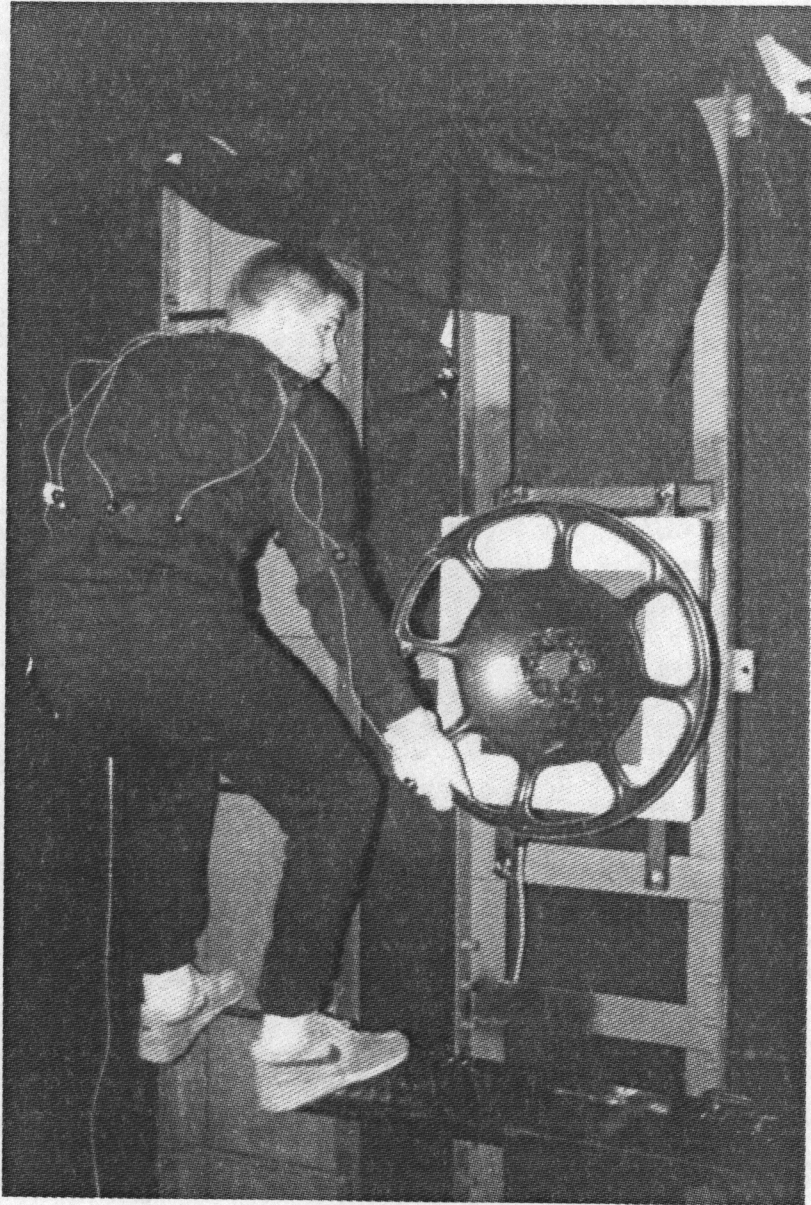


Figure 4.7 'Face the wall' posture with lower rung grip.

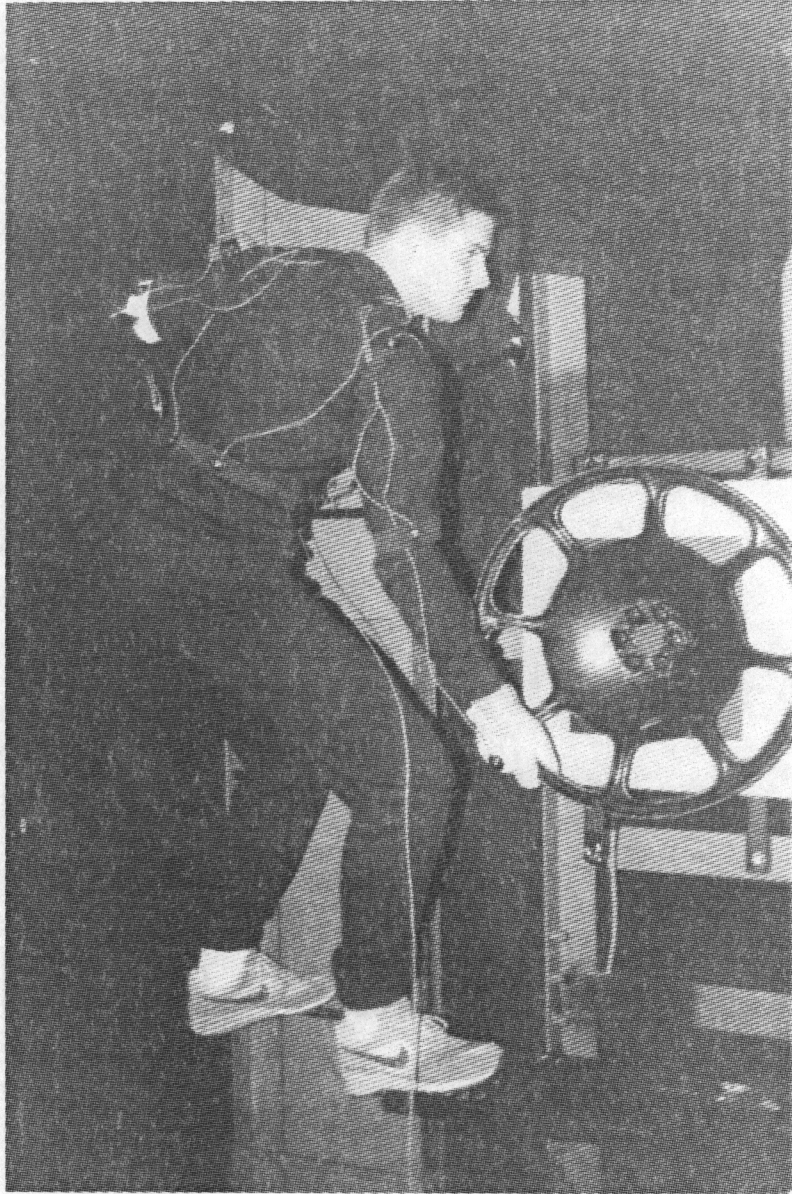


Figure 4.8 'Face the wheel' posture with upper rung grip.

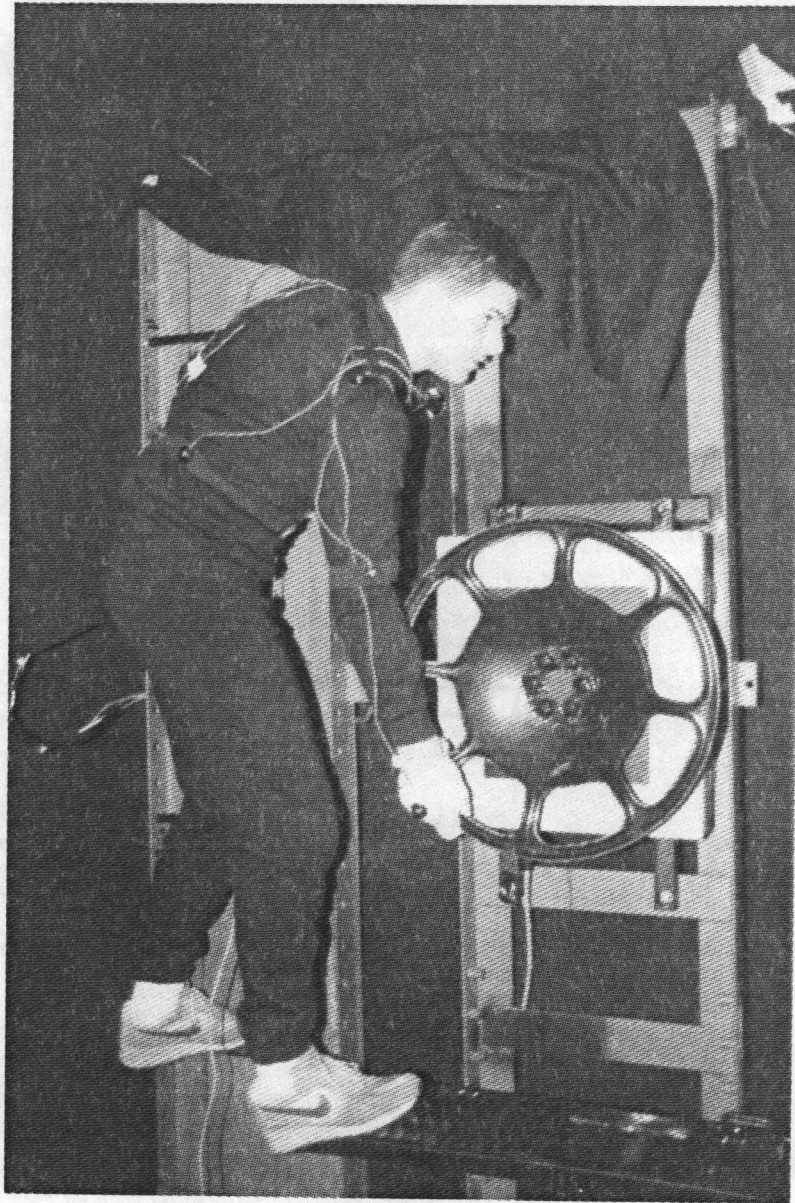


Figure 4.9 'Face the wheel' posture with lower rung grip.

Table 4.3 Random Latin Squares generated for the experiment.

<i>Anthropometry</i>															
<u>'Small female'</u>				<u>'Average female'</u>				<u>'Average male'</u>				<u>'Large male'</u>			
4	3	1	2	3	1	2	4	2	4	1	3	4	3	2	1
2	1	3	4	2	4	3	1	1	3	4	2	3	4	1	2
3	2	4	1	4	3	1	2	4	2	3	1	2	1	3	4
1	4	2	3	1	2	4	3	3	1	2	4	1	2	4	3

Each column of the corresponding Latin Square represented the treatment order of *Ladder Rung* and *Posture* combinations for a given subject. For example, for the last subject in the 'Large' male category, the order was treatment codes 1, 2, 4, and 3.

Within each *Ladder Rung* and *Posture* treatment combination, subjects undertook a total of eight hand brake strength trials, two at each of the four levels of *Torque Level*. The maximal trials always occurred first, so that the submaximal percentages could be calculated. The submaximal trials then proceeded in paired random order, that is, subjects always performed two consecutive trials at identical *Torque Level* levels. Table 4.4 shows an example of a possible trial order within a *Ladder Rung* and *Posture* treatment cell.

Table 4.4 Example treatment order of the independent variable *Torque Level*.

Order	<i>Torque Level</i>
1	Maximal
2	Maximal
3	50% of average maximum torque
4	50% of average maximum torque
5	25% of average maximum torque
6	25% of average maximum torque
7	75% of average maximum torque
8	75% of average maximum torque

4.3.3 Dependent Variables

The dependent measures in the study were the following:

Three-dimensional body posture: Three-dimensional body posture was recorded with the WATSMART system described in Section 4.2.4 for each individual trial. Posture was expressed as a set of three-dimensional coordinates (m) expressed in terms of the room reference frame that corresponded to the eight joint endpoints needed as inputs to the biomechanical model.

Left hand force: The three-dimensional force (N) that subjects exerted with their left hand was recorded for each trial.

Right hand force: The three-dimensional force (N) that subjects exerted with their right hand while performing each exertion was recorded for each trial.

The three dependent variables were all expressed in the room coordinate system. The variables just mentioned served as inputs for the calculation of compressive force present at the L3/L4 joint using the modeling procedures discussed in Chapter 3.

4.4 Experimental Task

The experimental task consisted of a maximal or submaximal graded isometric exertion on the hand brake. Subjects performed each exertion in a manner that simulated an attempt to turn the brake wheel. In some cases, subjects pulled with their "maximum safe effort", exerting the most force possible without placing themselves at risk of injury. In other cases, participants performed submaximal exertions on the wheel, holding the torque at 25%, 50%, or 75% of their maximum. All trials were 6 second static exertions, where the subject ramped up force to the desired level during the first 2 seconds and then held the force steady at the specified level for the remaining 4 seconds.

Subjects were given feedback during the submaximal trials by means of a computer monitor that duplicated the display that the experimenter watched. The feedback monitor was placed on the right hand side of the steel rig and was raised approximately 2.2 m above the floor. The placement of the feedback monitor is shown in Figure 4.10. The feedback display consisted of a graphical representation of the wheel torque the subject was generating. Subjects were instructed to hold their force within the bounds identified on the display. The bounds corresponded to levels of 5% above and 5% below the specified torque level. For example, in the 50% of maximum torque trials, the bounds were displayed at 45% and 55% of maximum torque for that condition. Figure 4.11 shows an example feedback display for this trial scenario.

4.5 Experimental Protocol

The experimental sessions took a total of 2.5 to 3 hours for each subject. The experiment was conducted in two sessions. In the first session, subjects completed informed consent forms, were given instructions and completed the whole-body strength testing. In the second session, the hand brake trials were conducted.

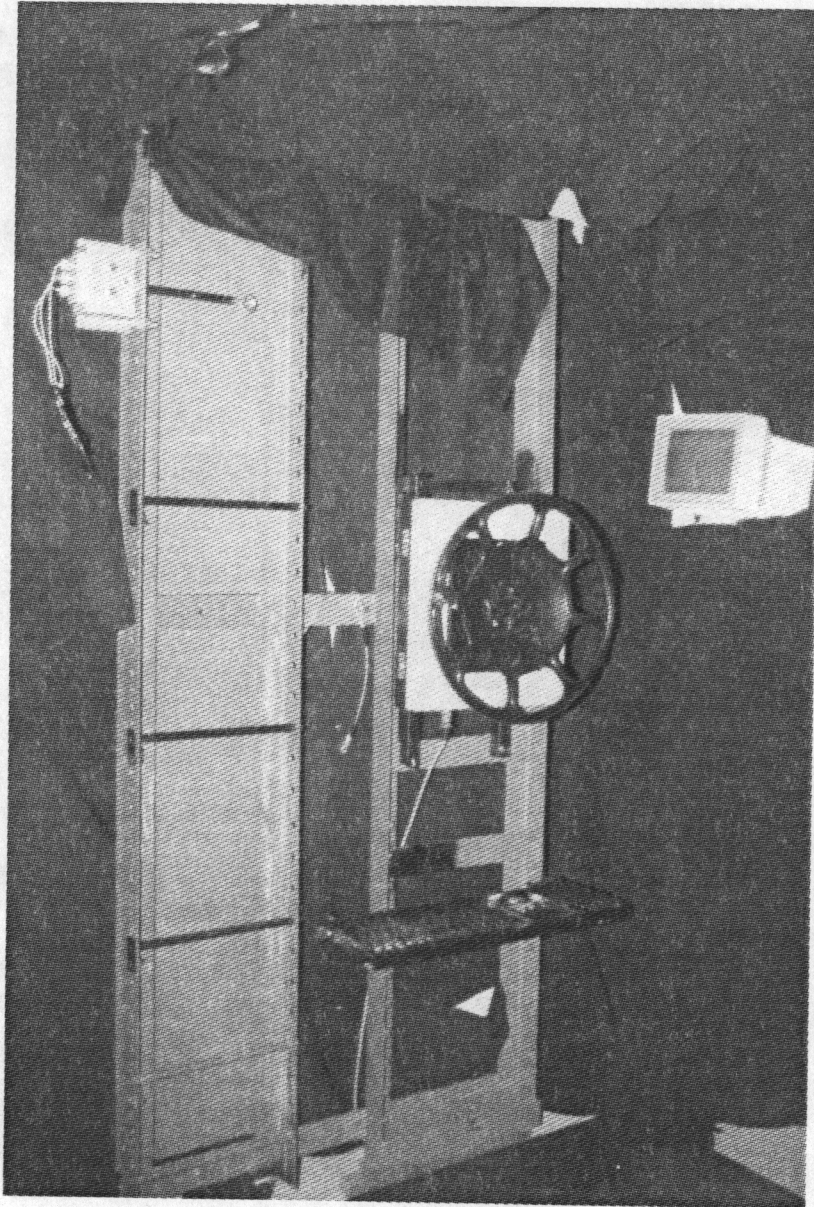


Figure 4.10 Photograph of handbrake rig showing feedback monitor.

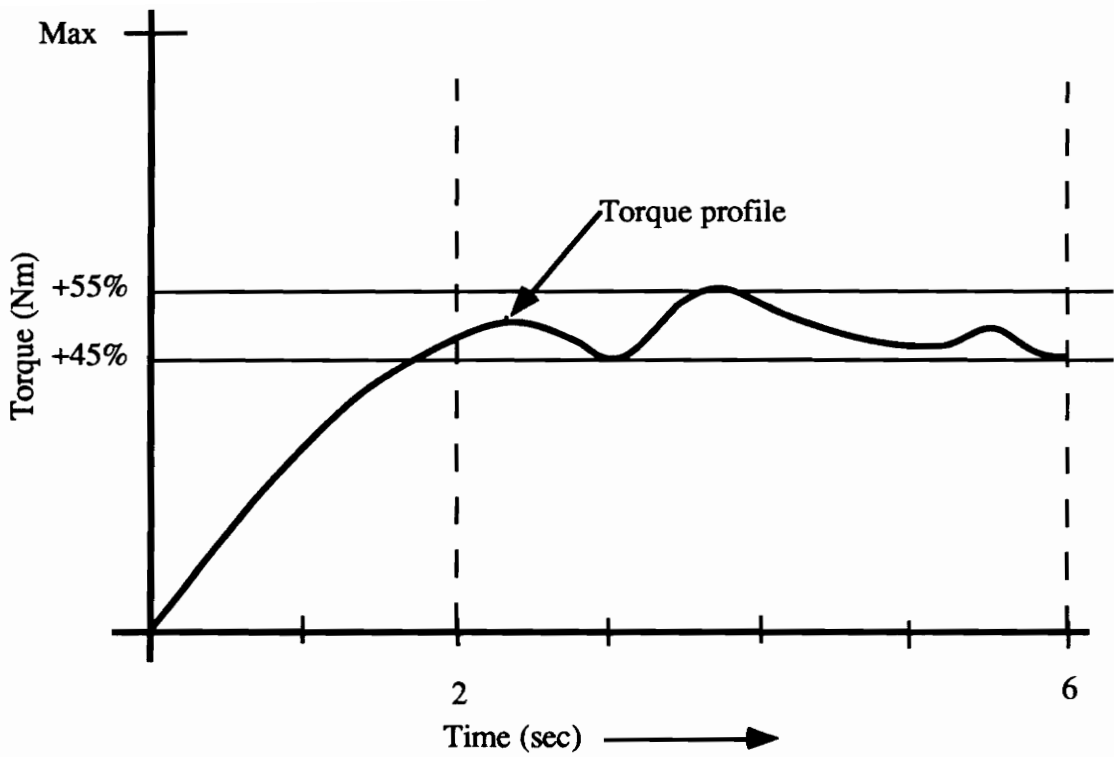


Figure 4.11 Example of visual feedback to subject during submaximal trial.

4.5.1 Session One

When the participant first arrived, he or she filled out an informed consent form and physical fitness questionnaire. The informed consent form can be found in Appendix A and the physical fitness questionnaire is located in Appendix B. When the documents were completed, several anthropometric measurements were recorded. The names and descriptions of each of the measurements can be found in Table 5.1.

Table 4.5 Anthropometric measurements taken during Session One.

Measurement (units)	Description
Weight (kg)	
Stature (cm)	Vertical distance from floor to top of head, with shoes off and arms relaxed at the sides looking straight ahead.
Bicrestal breadth (cm)	The horizontal distance between the right and left ilia measured with a body caliper exerting sufficient pressure to compress the tissue overlying the bone. ¹
Trochanteric height (cm)	The vertical distance from the floor to the uppermost point on the trochanter of the femur. ¹
Right hand grip strength (kg)	Maximum isometric exertion at a grip span of 6 cm.
Left hand grip strength (kg)	Maximum isometric exertion at a grip span of 6 cm.

¹ As defined in Clauser, McConville, and Young (1969).

Before continuing, the experimenter checked the stature and weight of each subject to make sure both measurements fell within the previously defined limits for the appropriate subject group. A summary of subject anthropometry is presented in Table 4.6. Individual subject anthropometric measurements are located in Appendix C.

Table 4.6 Summary anthropometric measurements of subject population.

Measure	Subject Group			
	Small Female	Average Female	Average Male	Large Male
Stature (cm)				
Mean	154.1	165.6	172.0	181.4
SD	2.5	1.6	0.8	1.4
Weight (kg)				
Mean	48.6	61.6	71.4	86.3
SD	1.0	1.9	1.3	2.1

Three isometric lifting tasks served as whole-body static strength evaluations. The whole-body trials were conducted to allow comparison to population strength norms if desired. The tests simulated leg lift, arm lift, and back lift situations. The postures used are shown in Figure 4.12. These postures were used by Chaffin, Herrin, and Keyserling (1978) in a study of isometric lifting strength of 108 female and 443 male industrial workers. Subjects were given instructions for the whole-body strength tests. The experimenter demonstrated the correct postures for each lift and described the strength testing protocol.

Subjects assumed the correct posture for each type of lift and performed a 6 second maximum voluntary exertion. The exertion consisted of building up force for the first 2 seconds and then holding at maximum exertion for 4 seconds. This procedure is similar to the standard static strength testing protocols of Caldwell, Chaffin, Dukes-Dobos, Kroemer, Laubach, Snook, and Wasserman (1974) and Chaffin (1975). The procedure was repeated for each of the three lift postures.

Participants performed one maximum safe whole-body exertion in each of the three specified postures. Rest breaks of at least 2 minutes were provided between each

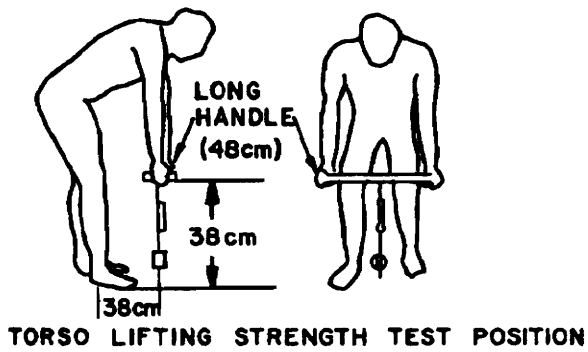
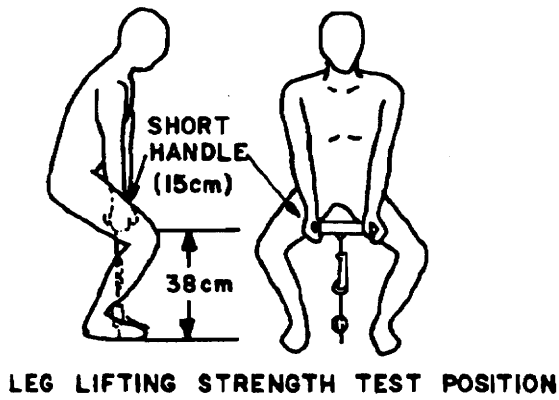
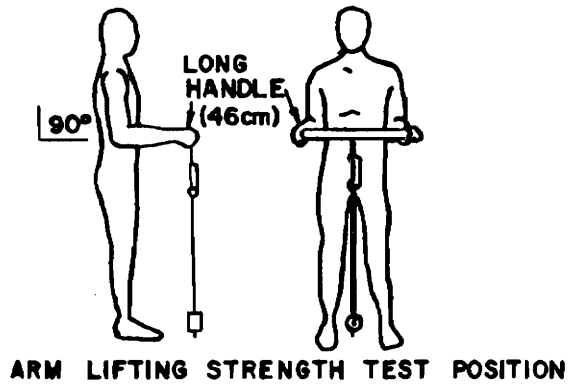


Figure 4.12 Three postures used for whole-body static strength testing. Adapted from Chaffin and Andersson (1991).

trial. Whole-body lift strength means for each subject group can be found in Table 4.7. The whole-body data are not further discussed in the Results section. After completion of the whole-body trials, subjects were given instructions on the hand brake trial procedures to be used in Session Two. The subjects were shown the different grips and postures, and were also told to keep their posture as consistent as possible within each treatment combination. To ensure that the force data collected for the left hand on the ladder rung was accurate, subjects were instructed to grip the rung with their middle finger over the notch in the rung used for calibration. It was also assumed that subjects did not induce a significant bending moment on the ladder rung.

Table 4.7 Summary mean whole-body lift strengths (N) for each subject group.

Lift	Subject Group			
	Small Female	Average Female	Average Male	Large Male
Leg				
Mean	433.5	579.0	956.3	1206.8
SD	116.1	154.5	268.3	329.4
Arm				
Mean	181.0	225.5	296.8	445.3
SD	46.5	44.7	58.3	120.7
Back				
Mean	214.75	382.8	413.8	692.8
SD	56.8	77.5	50.4	272.7

4.5.2 Session Two

During the second session, the subject was first reminded of the experimental procedures. The subject then donned the black clothing, which was worn to reduce reflections. The experimenter then attached the infrared diodes of the WATSMART system to critical joint locations. One diode was attached at the approximate grip center of each

hand. Diodes were placed at each elbow. Diodes were attached at the left and right acromion. One diode was attached to the posterior lumbar region at the L3/L4 level. This location was found by palpation of the vertebrae, starting from the L5/S1 joint. A final marker was placed at the same vertical level as the L3/L4 joint but spaced medially 11 cm. These locations approximated the joint locations needed as input to the biomechanical model. The vertical distance from the top of the subject's head to the midpoint between the two shoulder diodes was measured. This metric served as another input to the biomechanical model.

The subject was then asked to mount the railcar rig and initiate the experimental trials. Rest allowances of at least 2 minutes were provided between each trial. The experimenter made clear at all times that the subject could rest for longer if desired, and watched for signs of fatigue or reduced motivation. The experimenter also ensured that the subject kept a consistent posture and grip within each treatment combination. When the trials were completed, the experimenter removed the diodes and debriefed the subject. The subject was finally paid and thanked for his or her time.

5. RESULTS

5.1 Data Reduction

In order to arrive at predictions of spinal loading at L3/L4 given the position and hand force data collected during the experiment, several intermediate analyses were required. The major software routines that were used in the analysis are described in Appendix D.

The position and hand force data were both initially recorded in raw form and were then averaged over a specific time period and filtered for outliers and missing samples. These data were then used as inputs to the biomechanical model described in Sections 3.1 and 3.2 which computed the net reaction force and moment at the L3/L4 joint due to external forces. The net reaction force and moment about L3/L4 for each subject and experimental trial were finally input to an optimization package that was used to implement the Bean et al. (1988) DLP torso muscle modeling algorithm. This algorithm provided an estimate of the forces generated by the five lumbar muscle pairs to resist the externally generated moment and force at L3/L4. The final output from this algorithm was predicted compressive force at L3/L4. A schematic of the data reduction process can be found in Figure 5.1.

In the course of converting the raw experimental data to estimates of compressive force at L3/L4, several steps were taken to filter the data and ensure its validity. The hand force data collected from the three-dimensional load cell and force plate proved to be highly reliable. As a check to ensure minimal drift of the load cells, calibration parameters were recorded before and after the experimental session for each subject. No excessive drift was noticed in any of the experimental session data.

The position measurements obtained with the WATSMART system were less reliable than the force measurements. Position coordinates for each joint endpoint were

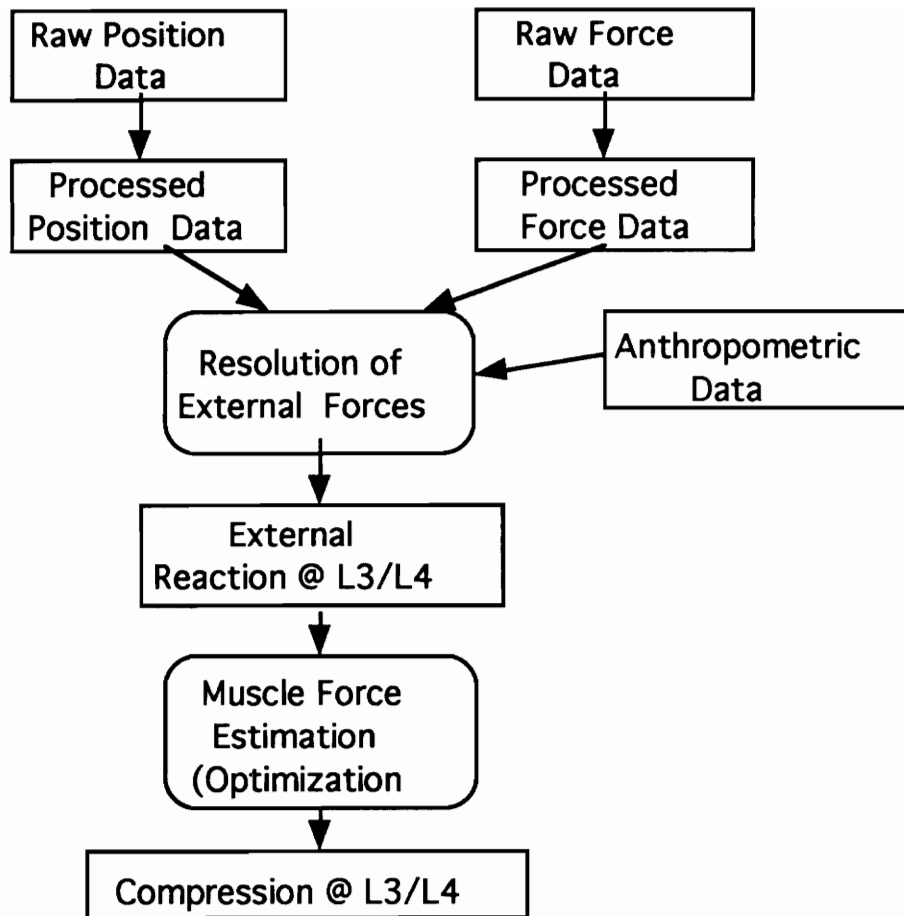


Figure 5.1 Flow diagram showing steps in data reduction.

recorded as the average between the second and fifth second of each experimental trial. This mean was based on the 60 data points recorded during the three-second specified interval. Some of the data samples exhibited high variability, indicated by a large standard deviation during the sample period. Samples with high variance ($>0.05m$) were replaced by the average of the valid joint coordinate values within a treatment combination. Position means based on sample sizes of less than 60 were accepted if high variance was not evident in the data. If no valid data points existed in the original sampling interval, a mean position was computed based on observations outside of the 60 sample range. If no reliable position data could be obtained outside the original range or the entire data set was missing, the coordinate was replaced by the average of the valid joint coordinate values within the same treatment combination of *Ladder Rung* and *Posture*. This filtering process resulted in the replacement of less than 2 percent of the original data points.

5.2 Predicted Compressive Force at L3/L4

The compressive force estimates at the L3/L4 joint were subjected to a repeated measures analysis of variance (ANOVA). Recall that the experimental variables were the following: *Anthropometry (AN)*, *Torque Level (T)*, *Ladder Rung (R)*, and *Posture (P)*. The ANOVA revealed that all main effects, two two-way interactions, and one three-way interaction were significant at $p < .05$. Table 5.1 is the ANOVA summary table for the analysis. The main effect of *Anthropometry* was subjected to the Newman-Kuels Sequential Range Test to identify significant differences among the four treatment means. The analysis showed that the 'Small Female' group compressive force mean and the 'Average Female' group compressive force mean were both significantly different from the 'Large Male' group compressive force mean at $p < 0.01$. This trend is illustrated in Figure 5.2.

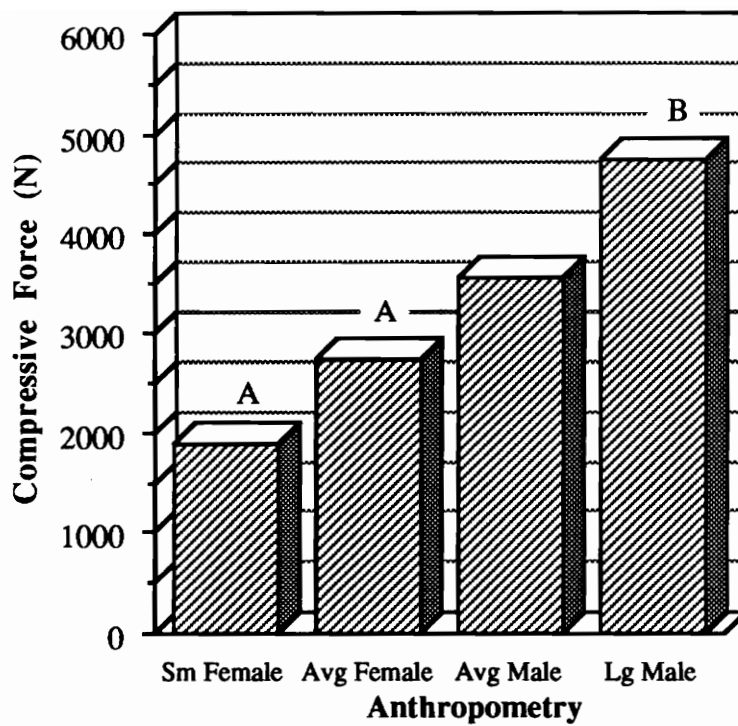


Figure 5.2 Main effect of *Anthropometry* plotted against predicted compressive force at L3/L4. Columns labeled A were found to be significantly different from B ($p < 0.05$) in post hoc testing.

The significant main effect of *Ladder Rung* ($p < 0.001$), as shown in Figure 5.3, revealed that less predicted compressive force occurred when using the upper rung grip. Orthogonal polynomial contrasts were run on the main effect of *Torque Level* ($p < 0.001$) to test for any linear or quadratic trends. The analysis revealed a strong effect of a linear function for the data as can be seen in Figure 5.4. Table 5.2 shows the results from the Orthogonal Polynomial Contrast analysis.

The *Posture* main effect ($p < 0.05$) indicated that the 'face the wall' position resulted in less predicted compressive force than the 'face the wheel' stance. Figure 5.5 illustrates the effect. The 'large male' subject group experienced a much greater increase in compressive force at the maximum level of Torque than the other subject groups, evidenced by the significant ($p < 0.001$) *Torque Level* x *Anthropometry* interaction which is plotted in Figure 5.6. The *Posture* x *Ladder Rung* interaction ($p < 0.01$) revealed that the gripping the lower rung and facing the wheel resulted in greater compressive force than the other combinations, as seen in Figure 5.7. Two other interactions, *Torque Level* x *Ladder Rung* and *Posture* x *Ladder Rung* x *Anthropometry* were significant at $p < 0.05$ and are graphed in Figures 5.8 and 5.9 respectively.

Table 5.1 ANOVA summary table for predicted compressive force at the L3/L4 joint.

Source	df	SS	MS	F	p	G-G
Between-Subjects						
AN	3	2.85765 E8	9.52551 E7	7.47	0.0044	
S/AN	12	1.52961 E8	1.27468 E7			
Within-Subjects						
R	1	1.71389 E7	1.73819 E7	24.63	0.0003	0.0003
R x AN	3	2.51811 E6	8.39371 E5	1.19	0.3551	0.3551
R x S/AN	12	8.46754 E6	7.05628 E5			
T	3	1.75872 E8	5.86239 E7	109.91	0.0001	0.0001
T x AN	9	8.1906 E7	9.10067 E6	17.06	0.0001	0.0001
T x S/AN	36	1.92018 E7	5.33385 E5			
P	1	1.1 E7	1.1 E7	7.72	0.0167	0.0167
P x AN	3	3.53748 E6	1.17916 E6	0.83	0.5039	0.5039
P x S/AN	12	1.71049 E7	1.42541 E6			
P x R	1	2.86716 E6	2.86718 E6	9.61	0.0092	0.0092
P x R x AN	3	4.0199 E6	1.334 E6	4.47	0.0251	0.0251
P x R x S/AN	12	3.58074 E6	2.98395 E5			
P x T	3	55130.44	18376.81	0.10	0.9610	0.9206
P x T x AN	9	1.25336 E6	1.39262 E5	0.74	0.6725	0.6341
P x T x S/AN	36	6.8002 E6	1.88894 E5			
P x T x R	3	4.36802 E5	1.45600 E5	1.80	0.1632	0.1790
P x T x R x AN	9	9.57608 E5	1.06400 E5	1.32	0.2605	0.2783
P x T x R x S/AN	36	2.89934 E6	80537.3			
T x R	3	1.61245 E6	5.37484 E5	3.87	0.0170	0.0335
AN x T x R	9	1.74202 E6	1.93557 E5	1.39	0.2278	0.2561
T x R x S/AN	36	5.00407 E6	1.39002 E5			

Table 5.2 Orthogonal Polynomial Contrast analysis on main effect *Torque Level*.

Fit	df	SS	MS	F	p
Linear	1	1.726043 E8	1.726043 E8	323.60	0.0001
Quadratic	1	2.916128 E6	2.916128 E6	5.46	0.0250

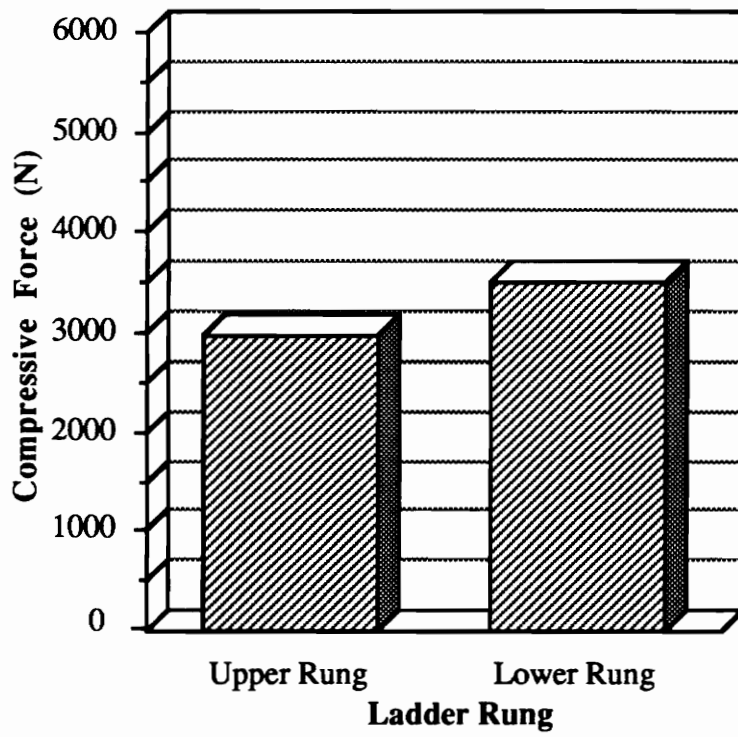


Figure 5.3 *Ladder Rung* main effect plotted against predicted compressive force at L3/L4.

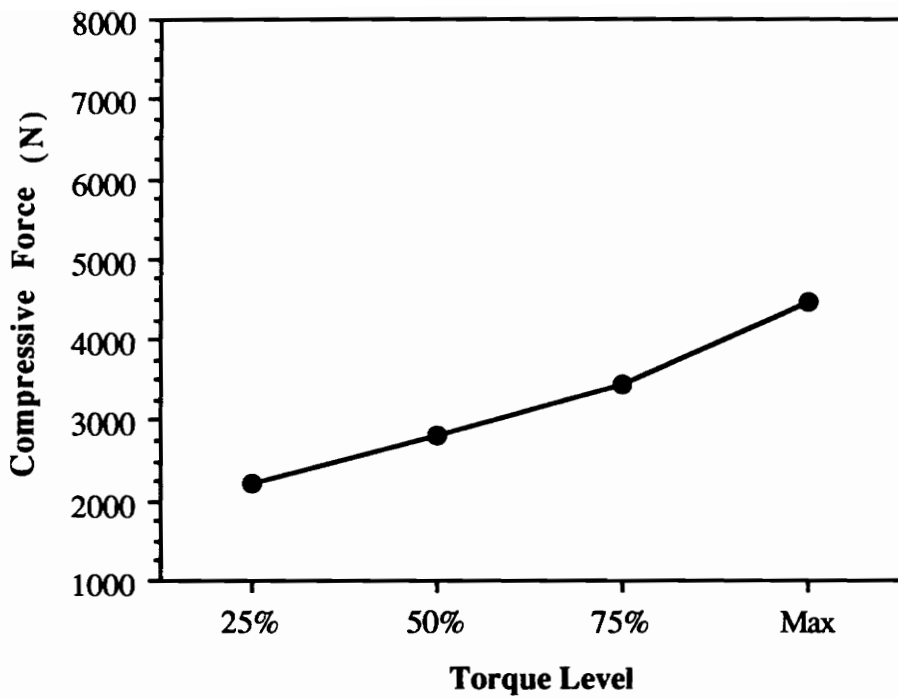


Figure 5.4 *Torque Level* main effect plotted against predicted compressive force at L3/L4

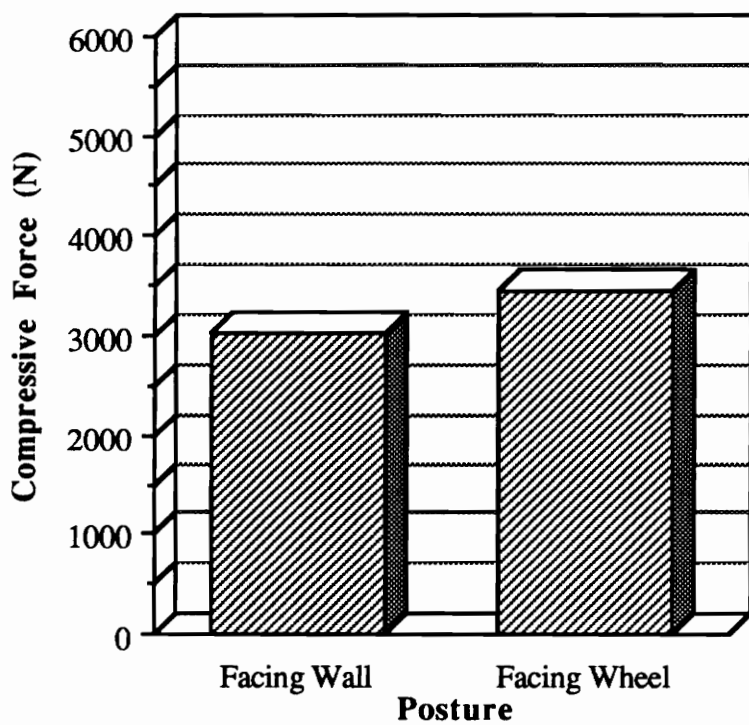


Figure 5.5 *Posture* main effect plotted against predicted compressive force at L3/L4.

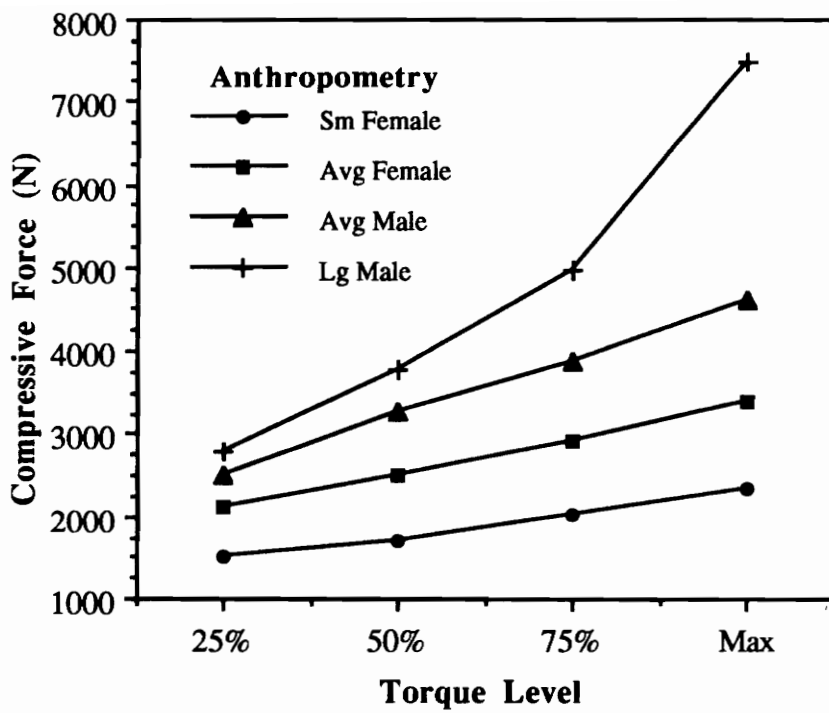


Figure 5.6 *Torque Level x Anthropometry* interaction plot against predicted compressive force at L3/L4.

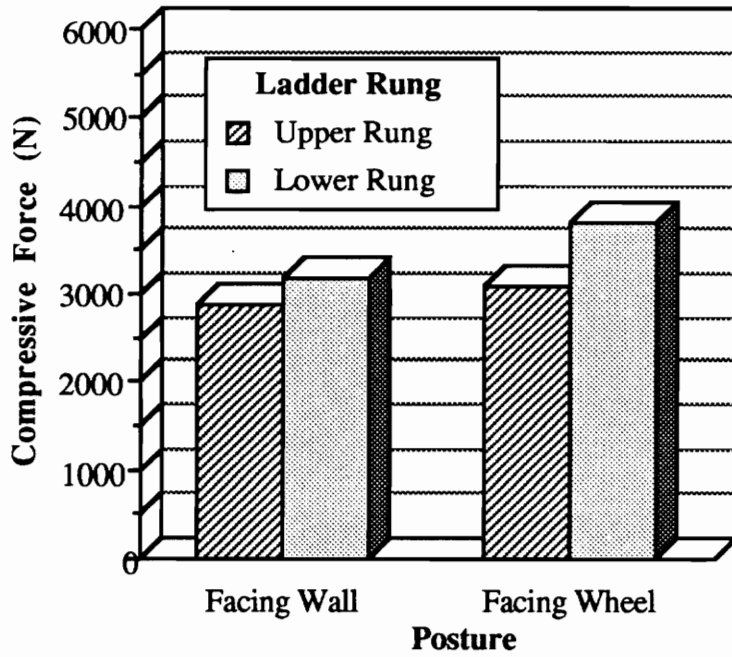


Figure 5.7 *Posture x Ladder Rung* interaction plotted against predicted compressive force at L3/L4.

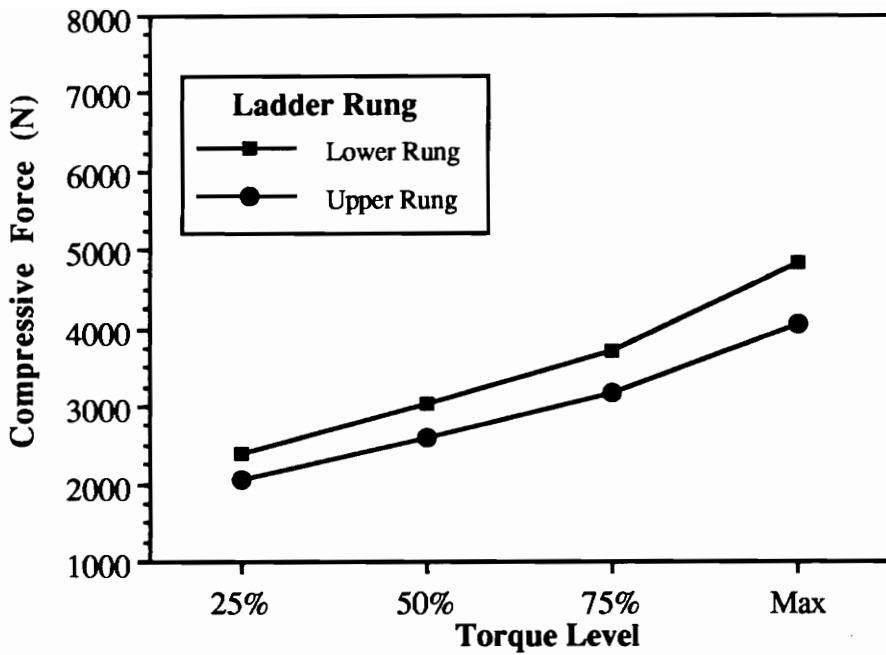


Figure 5.8 *Torque Level x Ladder Rung* interaction plotted against predicted compressive force at L3/L4.

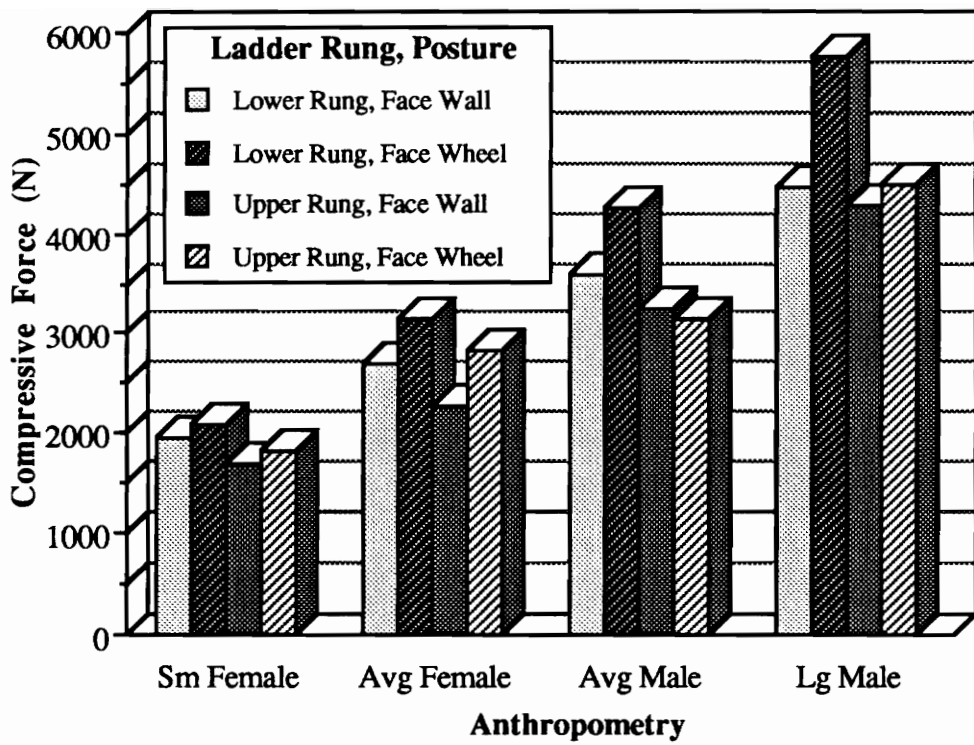


Figure 5.9 *Posture x Ladder Rung x Anthropometry* interaction plotted against predicted compressive force at L3/L4.

5.3 Analysis of Maximum Torque Levels

An additional set of analyses was undertaken to investigate the effects of the experimental variables on the maximum torque that subjects could generate with the hand brake. An ANOVA was run on the torque levels generated at the maximum level of the variable *Torque Level*. Table 5.3 contains the summary for this ANOVA. The two significant effects ($p < .02$) of *Anthropometry* and *Ladder Rung* are plotted in Figures 5.10 and 5.11 respectively.

Another ANOVA was run on the predicted compressive force values at L3/L4 for the same dataset. The analysis is summarized in Table 5.4. The three main effects of *Anthropometry*, *Ladder Rung* and *Posture* in this analysis were significant at $p < .05$ and are illustrated in Figures 5.12 through 5.14. Finally, for means of comparison, the mean torque levels at maximum level of *Torque Level* and corresponding predicted compressive force values are presented in Table 5.5.

Table 5.3 ANOVA summary table for maximum torque about the hand brake wheel.

Source	df	SS	MS	<i>F</i>	<i>p</i>	G-G
Between-Subjects						
AN	3	46524.39	15508.13	4.96	0.0182	
S/AN	12	37499.19	3124.93			
Within-Subjects						
R	1	506.90	506.90	7.59	0.0174	0.0174
R x AN	3	462.73	154.24	2.31	0.1280	0.1280
R x S/AN	12	800.69	66.72			
P	1	41.93	41.93	1.51	0.2423	0.2423
P x AN	3	83.63	27.87	1.01	0.4240	0.4240
P x S/AN	12	332.69	27.72			
R x P	1	293.29	293.29	3.60	0.0822	0.0822
R x P x AN	3	11.34	3.78	0.05	0.9861	0.9861
R x P x S/AN	12	978.06	81.51			

Table 5.4 ANOVA summary table for predicted compressive force at L3/L4 at maximum hand brake torque.

Source	df	SS	MS	<i>F</i>	<i>p</i>	G-G
Between-Subjects						
AN	3	2.37408 E8	7.91361 E7	17.56	0.0001	
S/AN	12	5.40711 E7	4.50593 E6			
Within-Subjects						
R	1	9.56015 E6	9.56015 E6	26.99	0.0002	0.0002
R x AN	3	2.94863 E6	9.8288 E5	2.77	0.0871	0.0871
R x S/AN	12	4.2506 E6	3.54216 E5			
P	1	3.416 E6	3.416 E6	4.91	0.0468	0.0468
P x AN	3	3.31121 E6	1.10374 E6	1.59	0.2442	0.2442
P x S/AN	12	8.35021 E6	6.95851 E5			
R x P	1	1.66167 E6	1.66167 E6	7.55	0.0177	0.0177
R x P x AN	3	1.87705 E6	6.25668 E5	2.84	0.0824	0.0824
R x P x S/AN	12	2.64104 E6	2.20086 E5			

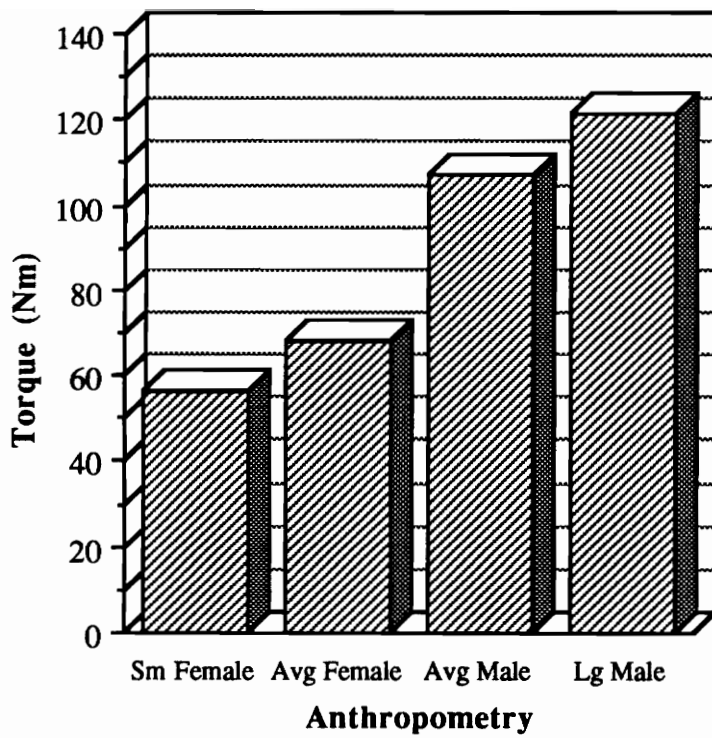


Figure 5.10 *Anthropometry* main effect at maximum torque plotted against torque.

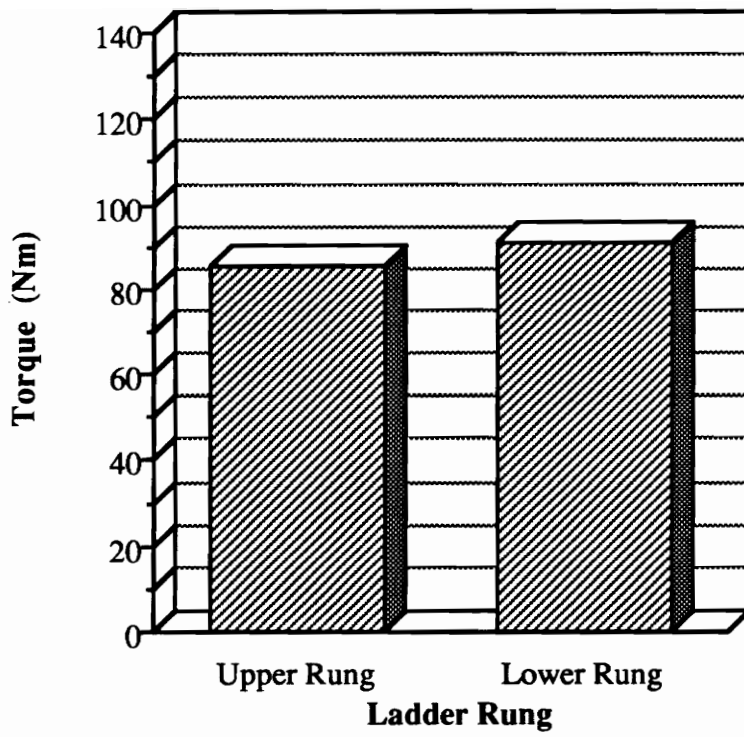


Figure 5.11 *Ladder Rung* main effect at maximum torque plotted against torque.

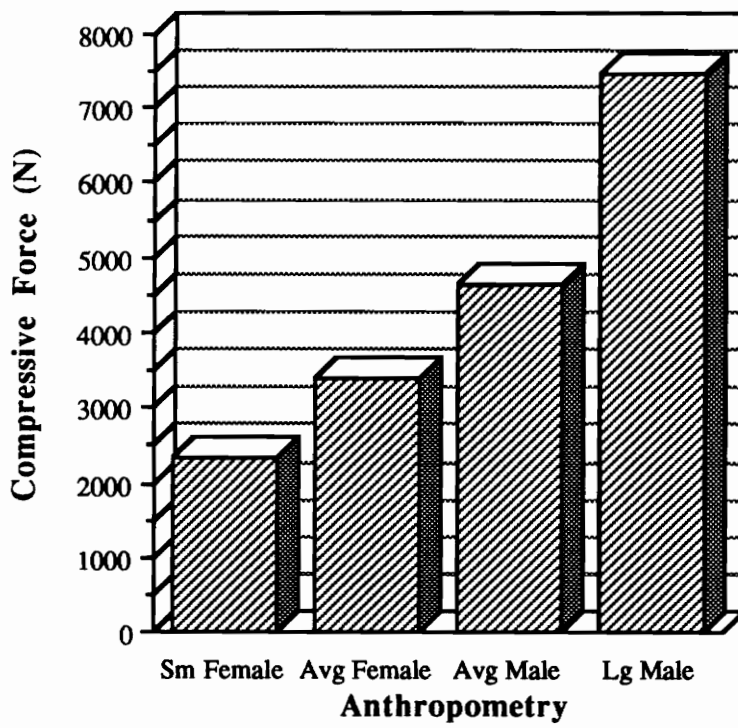


Figure 5.12 *Anthropometry* main effect at maximum torque plotted against predicted compressive force at L3/L4.

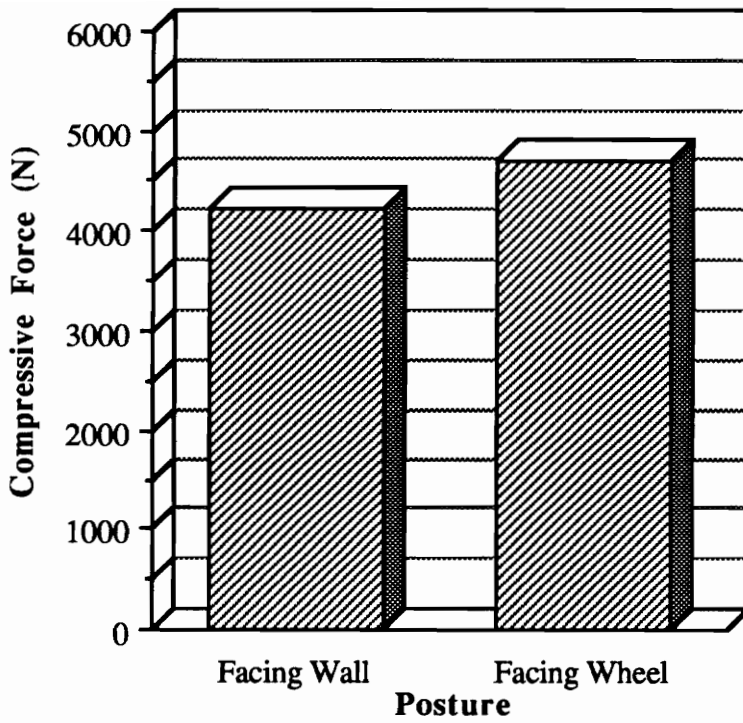


Figure 5.13 *Posture* main effect at maximum torque plotted against predicted compressive force at L3/L4.

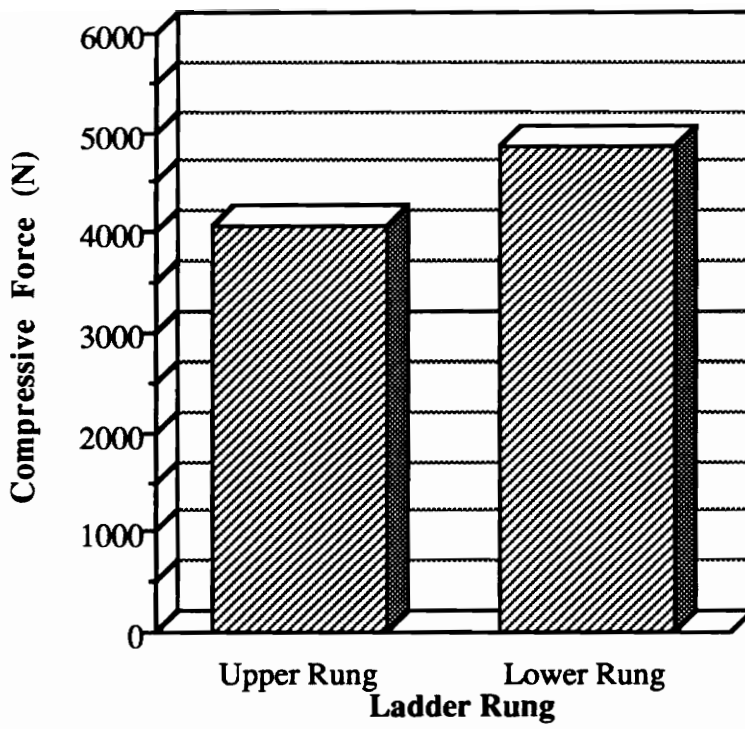


Figure 5.14 *Ladder Rung* main effect at maximum torque plotted against predicted compressive force at L3/L4.

Table 5.5 Mean torque at maximum level of *Torque Level* and corresponding predicted compressive force at L3/L4 for each level of *Anthropometry, Ladder Rung, and Posture*.

<i>Anthropometry</i>	<i>Ladder Rung</i>	<i>Posture</i>	Torque		Predicted Compressive force (N)
			Nm	ft-lbs.	
Sm Female	Lower Rung	Face Wall	55.6	(41.0)	2516
		Face Wheel	56.4	(41.6)	2424
	Upper Rung	Face Wall	59.0	(43.5)	2304
		Face Wheel	53.8	(39.7)	2091
Avg Female	Lower Rung	Face Wall	63.3	(46.7)	3291
		Face Wheel	70.4	(51.9)	3923
	Upper Rung	Face Wall	71.0	(52.4)	2877
		Face Wheel	68.2	(50.3)	3487
Avg Male	Lower Rung	Face Wall	103.4	(76.3)	4874
		Face Wheel	106.2	(78.3)	5508
	Upper Rung	Face Wall	113.3	(83.6)	4077
		Face Wheel	106.0	(78.2)	4021
Lg Male	Lower Rung	Face Wall	114.5	(84.5)	7130
		Face Wheel	114.4	(84.4)	9094
	Upper Rung	Face Wall	133.2	(98.2)	6751
		Face Wheel	124.9	(92.1)	6969

5.4 Torque levels at the NIOSH AL and MPL

Recall that one of the objectives of this research was to predict the amount of brake torque that would cause low-back compressive force to reach potentially hazardous levels. As was mentioned in Chapter 2, the NIOSH (1981) recommended Action Limit (AL) and Maximum Permissible Limits (MPL) for low-back compressive force were 3400N and 6400N respectively. Although the limits recommended by NIOSH were based on compressive force at the L5/S1 joint and assumed symmetric loading of the trunk, it was

felt that these values are the most widely accepted and therefore most reasonable limits to use for the L3/L4 joint.

To predict hand torque levels that would be required to produce these amounts of compressive force at L3/L4, linear regression analysis was used. This approach was justified by the fact that the orthogonal polynomial contrast analysis used in Section 5.2 showed a highly significant linear trend in the *Torque Level* vs. compressive force plot. One regression equation was computed for each treatment cell for each subject. In other words, each regression was based on a sample of eight data points corresponding to the eight trials that a subject performed under each treatment combination of the experimental variables *Posture* and *Ladder Rung*. Each equation took the form:

$$\hat{y} = \beta_0 + \beta_1 x \quad (5.1),$$

where \hat{y} is the prediction of compressive force at L3/L4 and x represents hand brake torque in Nm. The variables β_0 and β_1 are the intercept and slope of the regression equation. Appendix E contains a summary of the slope, intercept, and R^2 values for each of the 64 regression equations that were calculated. Most of the equations exhibited excellent linear fits, as evidenced by R^2 values of 0.8 and greater. However, two of the equations computed for subject one and two equations for subject two were deemed unacceptable for further analysis. The compressive force data in these cases were scattered and did not increase with increasing levels of *Torque Level*.

The resulting regression equations for each subject and treatment condition were then used to solve for brake torque levels that produced compressive force equal to 3400N and 6400N. An ANOVA was performed on each of the two data sets and the results are summarized in Table 5.6 and Table 5.7. The data from subjects one and four were eliminated from the analyses because of the poor regression fit previously mentioned. The mean torque levels at the AL and MPL for each treatment combination are summarized in

Table 5.8. These means also are based on the reduced data set used in the ANOVA's. The ANOVA on the AL torque revealed a significant main effect of *Ladder Rung* ($p < 0.01$) and a significant interaction of *Posture x Ladder Rung x Anthropometry* ($p < 0.05$). The ANOVA on the MPL torque also showed the main effect of *Ladder Rung* to be significant ($p < 0.01$) and the effect of *Anthropometry* was significant as well ($p < 0.05$). The significant effects for the ANOVA on the AL torque are plotted in Figure 5.15 and Figure 5.16. The significant effects for the ANOVA on the MPL torque are plotted in Figure 5.17 and Figure 5.18.

Table 5.6 ANOVA summary table for analysis of predicted hand brake torque at the NIOSH Action Limit for low-back compressive force.

Source	df	SS	MS	F	p	G-G
Between-Subjects						
AN	3	6708.63	2236.21	0.73	0.5567	
S/AN	10	30593.77	3059.38			
Within-Subjects						
R	1	5951.63	5951.63	17.49	0.0019	0.0019
R x AN	3	700.70	233.57	0.69	0.5806	0.5806
R x S/AN	10	3403.09	340.31			
P	1	517.47	517.47	0.70	0.4226	0.4226
P x AN	3	1848.33	616.11	0.83	0.5060	0.5060
P x S/AN	10	7402.09	740.21			
R x P	1	65.75	65.75	0.25	0.6281	0.6281
R x P x AN	3	3936.11	1312.04	4.98	0.0228	0.0228
R x P x S/AN	10	2633.50	263.35			

Table 5.7 ANOVA summary table for analysis of predicted hand brake torque at the NIOSH Maximum Permissible Limit for low-back compressive force.

Source	df	SS	MS	F	p	G-G
Between-Subjects						
AN	3	73250.54	24416.85	4.03	0.0405	
S/AN	10	60575.67	6057.57			
Within-Subjects						
R	1	27000.98	27000.98	17.63	0.0018	0.0018
R x AN	3	6730.35	2243.45	1.47	0.2826	0.2826
R x S/AN	10	15317.95	1531.80			
P	1	36.60	36.60	0.01	0.9407	0.9407
P x AN	3	9036.45	9036.45	0.48	0.7044	0.7044
P x S/AN	10	62958.95	9295.90			
R x P	1	171.09	171.09	0.08	0.7897	0.7897
R x P x AN	3	9472.63	3157.54	1.39	0.3035	0.3035
R x P x S/AN	10	22800.97	2280.10			

Table 5.8 Mean predicted hand brake torque levels (Nm) at the NIOSH AL and MPL compressive force limits. Values in parentheses are torque in ft.-lbs.

		Lower Rung Grip				Upper Rung Grip			
		Face Wall		Face Wheel		Face Wall		Face Wheel	
		Nm	ft.-lbs.	Nm	ft.-lbs.	Nm	ft.-lbs.	Nm	ft.-lbs.
Sm Female (n=2)	AL	57.3	(42.3)	71.7	(52.9)	81.2	(59.9)	82.4	(60.8)
	MPL	141.2	(104.1)	202.3	(149.2)	178.2	(131.4)	202.4	(149.3)
Avg Female (n=4)	AL	65.6	(48.4)	65.4	(48.2)	111.5	(82.2)	60.9	(44.9)
	MPL	174.4	(128.6)	174.3	(128.6)	264.9	(195.4)	194.8	(143.7)
Avg Male (n=4)	AL	61.0	(45.0)	40.6	(30.0)	76.22	(56.2)	91.2	(67.3)
	MPL	167.9	(123.8)	146.8	(108.3)	216.2	(159.5)	255.3	(188.3)
Lg Male (n=4)	AL	46.2	(34.1)	36.0	(26.6)	56.6	(41.8)	56.4	(41.6)
	MPL	110.6	(81.6)	92.0	(67.9)	133.0	(98.1)	132.1	(97.4)

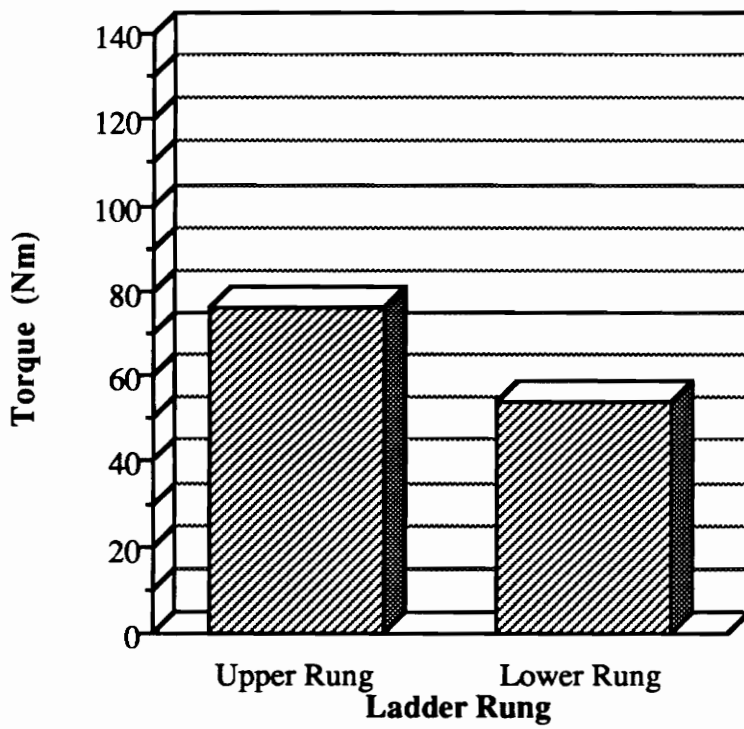


Figure 5.15 Main effect of *Ladder Rung* plotted against predicted torque at NIOSH Action Limit for compressive force.

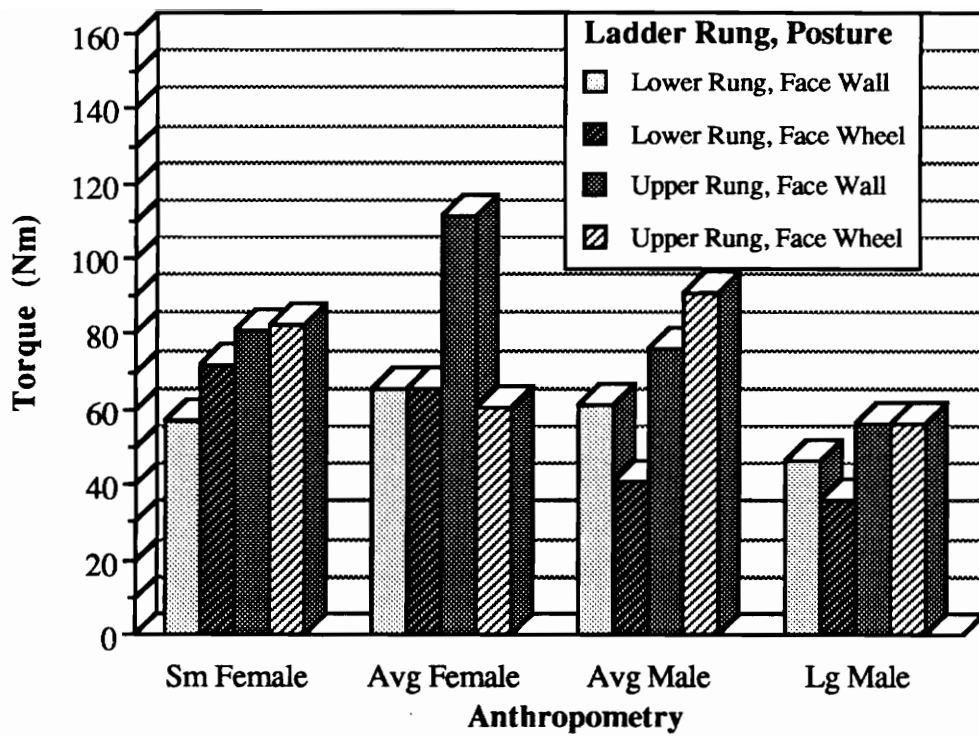


Figure 5.16 Interaction effect of *Posture x Ladder Rung x Anthropometry* plotted against predicted torque at NIOSH Action Limit for compressive force.

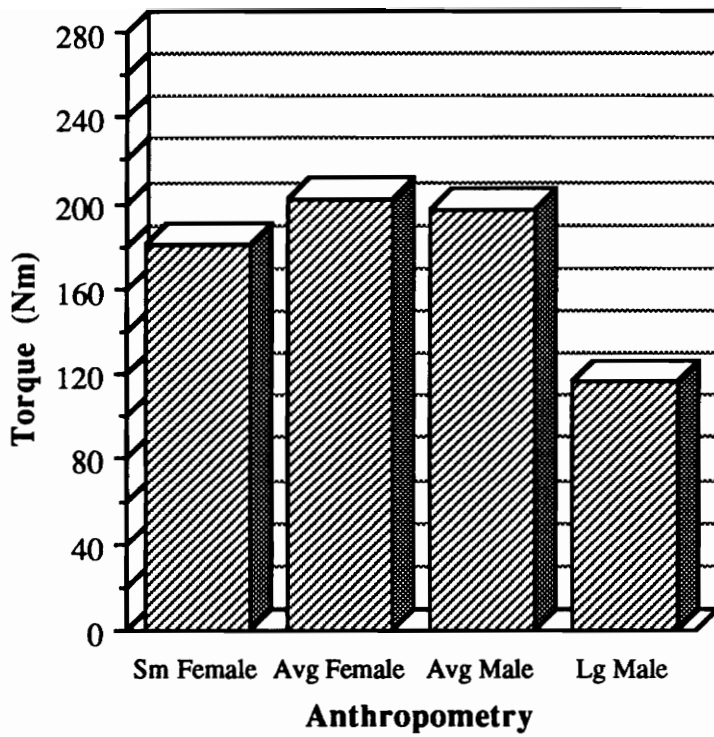


Figure 5.17 Main effect of *Anthropometry* plotted against predicted torque at NIOSH Maximum Permissible Limit for compressive force.

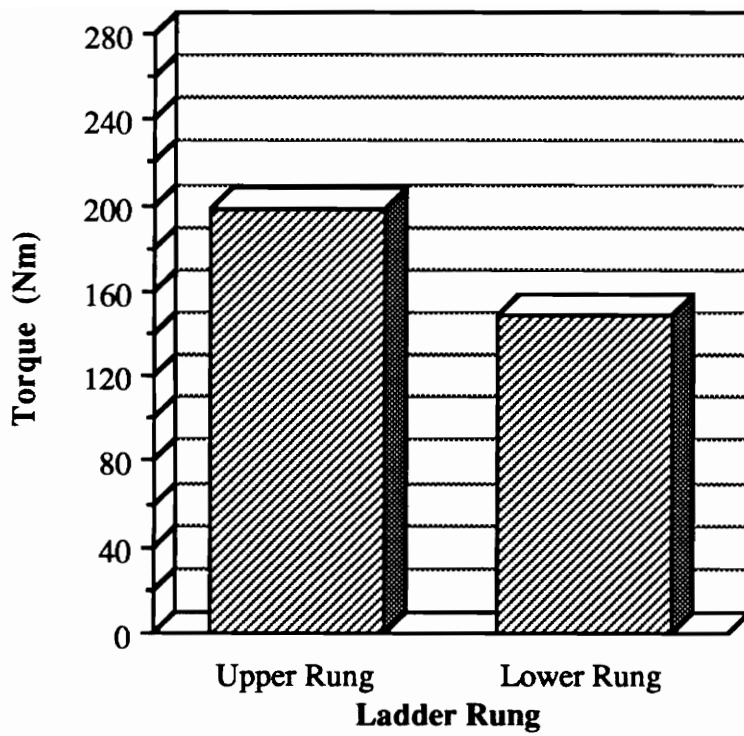


Figure 5.18 Main effect of *Ladder Rung* plotted against predicted torque at NIOSH Maximum Permissible Limit for compressive force.

6. DISCUSSION

6.1 Estimated Compressive Force at L3/L4

The results of the study suggest that estimated compressive force at L3/L4 was sensitive to manipulation of the experimental variables. The significance of the main effect *Anthropometry* demonstrated that under the conditions of this study, larger persons experienced higher levels of compressive force and males were subject to greater compressive force than females. Subjects with greater weights would produce higher compressive force levels simply due to the larger force at L3/L4 caused by the weight of the torso and arms. In addition, males generated larger forces at the hands, which would in turn produce higher levels of compressive force.

The main effect of *Torque Level* was expected, since higher hand forces are required to produce higher torques and thus should result in greater loading of the trunk. As expected, the variable showed a highly significant linear relationship with compressive force as evidenced by the significant first order effect in the orthogonal polynomial contrast analysis. The *Torque Level* x *Anthropometry* interaction is fairly intuitive, implying that larger subjects can generate higher torques and therefore experience greater trunk loading.

Perhaps the most interesting effects occurred among the effects of *Ladder Rung*, *Posture*, and the *Ladder Rung* x *Posture* interaction. Gripping at the lower rung resulted in higher compressive force than gripping on the upper rung. This effect can be explained by the fact that the body posture that subjects assumed when gripping at the lower rung was quite asymmetric. The asymmetric posture created larger moment arms for the external forces due to loads at the hands and body segment weights, and in turn resulted in a greater moment at L3/L4. The hand forces in this case were also higher, as evidenced by the significantly higher torques that could be generated about the wheel with the lower rung grip (see Figure 5.10). The main effect of *Posture* showed that less compressive force was

present when subjects faced the wall, which entailed attempting to keep the hips and shoulders as parallel to the wall as possible. Most subjects assumed a fairly upright posture in order to face the wall and therefore the moment arms for external forces were kept to a minimum. In addition, this posture discouraged the use of the trunk muscles to create a torsional moment about L3/L4, which was possible in the 'face the wheel' posture.

The interaction of *Ladder Rung* and *Posture* revealed that gripping at the lower rung and facing the wheel caused the greatest amount of compressive force, while the upper rung grip and 'face the wall' combination resulted in the lowest average compressive force. This trend can also be explained in terms of asymmetric loading. The upper rung grip and 'face the wall' posture combination forced subjects to assume an upright stance as opposed to the lower rung grip and 'face the wheel' posture where subjects felt comfortable assuming a crouched stance. The crouched position resulted in asymmetric loading and subjects could also generate a twisting or torsional force at the torso that would result in more torque about the wheel. The increased torso muscle activity due to the twisting and asymmetry would subsequently increase compressive force. The crouched position also resulted in the torso of the subject being distanced from the brake wheel allowing a larger moment arm from the hands to L3/L4. The crouching position also allowed subjects to use their body weight to increase torque on the wheel.

6.2 Maximum Torque and Resulting Compressive Force at L3/L4

The analysis at maximum torque levels revealed some of the same trends observed in the overall compressive force data. The average maximum torque generated by females was 54 percent of the average maximum torque generated by males. Correspondingly, the average compressive force at L3/L4 for maximum torque exertions for females was 47 percent of the average compressive force for males at maximum torque. Both maximum torque and compressive force at maximum torque were affected significantly by *Ladder*

Rung. This relationship points out an inherent tradeoff with this particular task. Certain stances or work postures may allow a person to generate a greater amount of force and therefore torque, but these positions also result in a higher level of predicted compressive force.

Posture affected compressive force at maximum torque, but not maximum torque itself. This result would indicate that when maximum exertions are involved, it may be safer to use the 'face the wall' posture because it causes less low-back compressive force and the same amount of torque can still be generated about the hand brake wheel.

6.3 Comparison of Predicted Compressive Force with Recommended Guidelines

As mentioned in the previous chapter, it was decided that the NIOSH (1981) AL of 3400N and the MPL of 6400N would serve as criteria against which to judge the levels of low-back compressive force predicted from the experiment. Recall from Chapter 2 that according to NIOSH, compressive force levels below the AL were pose nominal risk, levels between the AL and MPL require mediation with administrative or engineering controls, and that levels above the MPL were unacceptable. Estimated compressive force values from the experiment exhibited a wide range, especially when compared with the NIOSH limits.

Across all levels of *Anthropometry*, *Ladder Rung* and *Posture*, hand brake exertions at approximately 75 percent of maximum produced estimated L3/L4 compressive forces equal to the NIOSH Action Limit (see Figure 5.3). This finding suggests that maximal exertions in any posture should be avoided. However, when the data are broken down by *Anthropometry*, the greater risks to males and especially the Large Male group become obvious. Predicted compressive force for the Large Male group exceeded the AL at 50 percent of maximum torque and exceeded the MPL at maximum torque. The Average

Males exceeded the AL at 75 percent of maximum torque and did not exceed the MPL. These trends are illustrated in Figure 5.5.

Recall that subjects were instructed to pull on the hand brake with their maximum safe effort. Based on the compressive force predictions and the NIOSH limits, there appears to be a discrepancy between what subjects (especially males) perceive to be safe torque limits and what actually are safe torque limits. For example, the Large Male subject group experienced an average of over 9000N compressive force at L3/L4 for maximum safe effort trials in the 'face the wheel' *Posture* and lower rung *Ladder Rung* combination.

On the other hand, predicted compressive force at maximum torque for the Small Female group never exceeded the NIOSH Action Limit. The Average Female group exceeded the AL for compressive force when using the lower rung and facing the wheel and when using the upper rung and facing the wheel.

6.4 Prediction of Torque from Compressive Force Limits

The objective of this part of the analysis was to arrive at reasonable predictions of torque levels that resulted in L3/L4 compressive force levels equal to the NIOSH Action Limit and Maximum Permissible Limit. The ANOVA's that were performed on the data yielded inconsistent results. The effect of *Ladder Rung* was significant at $p < 0.002$ in both the AL and MPL analyses, but there were no other significant main effects or interactions common to both analyses. At the Action Limit, the *Ladder Rung* x *Posture* x *Anthropometry* interaction was significant at $p < 0.05$ and in the Maximum Permissible Limit analysis, the effect of *Anthropometry* was significant at $p < 0.05$.

Despite the conflicting ANOVA results, some general conclusions can be reached regarding reasonable torque limits. Based on the prediction equations, it appears that torque levels ranging from 40 to 80 Nm cause compressive forces at L3/L4 to reach the NIOSH Action Limit for all subject groups. The predictions also indicate that torques in

the 180 to 200 Nm range could cause Maximum Permissible Limit compressive forces in females and average males and that 120 Nm would have the same effect in large males. These predictions must be viewed with caution for a number of reasons. One important cause for concern is the fact that the predictions for compression at the MPL fell well outside the range of data from which the regression equations were created. This was true especially for the female subjects, whose predicted compressive force rarely exceeded even the Action Limit. It can be shown that the error associated with predictions outside of the range of the actual data becomes very large. The deviation among the slopes of the regression equations was also a sign of possible weakness in the predictions. Finally, fluctuations in posture within a treatment combination could have caused spurious results.

6.5 Weaknesses in Models, Methods, and Equipment

While many of the initial aims of this research were satisfied, a number of shortcomings associated with the project should be noted as they may have adversely affected the results. One of the most significant areas of concern was the accuracy with which the Bean et al. (1988) double linear programming method could predict lumbar muscle forces. The model does not take into account antagonistic co-contraction and therefore may have underestimated muscle forces. Hughes (1991) found through EMG analysis of lumbar muscle activity during spinal loading that co-contraction can add between 12% and 14% to spinal compressive force in asymmetric situations. The nature of the DLP optimization formulation could also lead to underestimation of muscle force. The fact that the method seeks to minimize maximum muscle intensity and then minimize compressive force implies that force will be allocated to large muscles and some muscles will not be predicted to be active, as opposed to nonlinear approaches which would more evenly distribute the load among the muscles.

The accuracy of the lumbar muscle moment arm and unit force data is also subject to question. The data were the most detailed available at the time, but was based on limited observations. It is also not known how the geometry of these muscles varies with changes in individual anthropometry, gender, or posture.

A fundamental shortcoming in low-back modeling to date is the misuse of the term *compression*. Researchers, including those at NIOSH, have ignored the fact that compression is a metric of force per unit area and not of force alone. Current low-back biomechanical models (including the one developed in this research) fail to account for the possible differences in spinal disc area for different anthropometries. The results from this research indicated that females experienced much lower levels of predicted *compressive force* at L3/L4 during the experimental exertions. This assumes that small females and large males have the same size intervertebral discs. However, it is likely that spinal disc area lessens with a corresponding decrease in body size. Therefore if compression was considered instead of compressive force, the effect of *Anthropometry* would likely be less salient.

As mentioned in Chapter 5, the position data obtained with the WATSMART motion analysis system could not be relied upon with complete confidence. The system was prone to errors caused by reflections from the environment and markers situated at awkward angles to the cameras. The placement of the position markers also varied somewhat during the experimental sessions and errors related to body segment anthropometry could have occurred. However, the postural data obtained were likely more reliable than data gathered with an indirect means of posture measurement.

Finally, the control of the experimental variable *Posture* was quite difficult. The aim of the study was to manipulate general body posture and this resulted in vague instructions to subjects. Body size also affected the ease and comfort with which subjects could assume the designated posture and grip combinations.

6.6 Future Research

As is the case with most areas of biomechanics, a great deal of research is still needed to better define and model the musculoskeletal system of the trunk. More specifically, future research should:

- Provide a more comprehensive body of data on lumbar muscle moment arms, unit muscle force components, and cross sectional areas. Research in this area should also account for the influence of gender and body size on the data.
- Gather data on spinal disc area and characterize changes in disc area due to anthropometry changes.
- Better define the inertial properties of the human torso, concentrating on the accurate measurement of center-of-mass locations relative to lumbar spinal joint locations.
- Quantify the changes that occur in trunk muscle geometry in twisted and flexed postures.
- Develop and validate models of lumbar muscle force activation that account for antagonistic co-contraction.
- Investigate the utility of occupational spinal disc loading limits that account for shear forces in addition to compressive forces.
- Develop a realistic model of the link system of the torso and upper extremities that accounts for true joint rotational and translational characteristics.

6.7 Summary and Conclusions

Overall, the results of this research can be summarized as follows:

- A model was developed to predict compressive forces at the L3/L4 joint based on inputs of body posture, anthropometry, and resultant forces at the limbs.

- The experiment revealed that predicted compressive force at L3/L4 was affected by changes in body posture, ladder rung grip, and wheel torque level.
- Exertions at voluntary maximum levels in some postures resulted in predicted compression that exceeded established safety guidelines.
- Researchers must be careful to consider the limitations inherent to low-back biomechanical models and use discretion in the interpretation of model predictions.

7. REFERENCES

- Adams, M.A., and Hutton, W.C. (1981). The effect of posture on the strength of the lumbar spine. *Engineering Medicine*, 10(4), 199-202.
- An, K.N., Kwak, B.M., Chao, E.Y., and Morrey, B.F. (1984). Determination of muscle and joint forces: a new technique to solve the indeterminate problem. *Journal of Biomechanical Engineering*, 106, 364-367.
- Bean, J.C., Chaffin, D.B., and Schultz, A.B. (1988). Biomechanical calculation of muscle contraction forces: A double linear programming method. *Journal of Biomechanics*, 21(1), 59-66.
- Bradley, G.L. (1975). *A primer of linear algebra*. Englewood Cliffs, NJ: Prentice Hall.
- Caldwell, L.S., Chaffin, D.B., Dukes-Dobos, F.N., Kroemer, K.H.E., Laubach, L.L., Snook, S.H. and Wasserman, D.E. (1974). A proposed standard procedure for static muscle strength testing. *American Industrial Hygiene Association Journal*, 35(4), 206-210.
- Chaffin, D.B. (1975). Ergonomics guide for the assessment of human static strength. *American Industrial Hygiene Association Journal*, 36, 505-511.
- Chaffin, D.B. (1988). Biomechanical modeling of the low-back during lifting. *Ergonomics*, 31(5), 685-697.
- Chaffin, D.B., and Andersson, G.B.J. (1991). *Occupational biomechanics*. New York: John Wiley and Sons.
- Chaffin, D.B., and Park, K.S. (1973). A longitudinal study of low-back pain as associated with occupational weight lifting factors. *American Industrial Hygiene Association Journal*, 34, 513-524.
- Clauser, C.W., McConville, J.T., and Young, J.W. (1969). Weight, volume, and centers of mass of segments of the human body. (Tech. report AMRL-TR-69-70). Ohio: Aerospace Medical Research Laboratories.
- Craig, J.J. (1989). *Introduction to robotics: mechanics and control*. New York: Addison-Wesley.
- Crowninshield, R.D. (1978). Use of optimization techniques to predict muscle forces. *Journal of Biomechanical Engineering*, 100, 88-92.
- Crowninshield, R.D. and Brand, R.A. (1981). A physiologically based criterion of muscle force prediction in locomotion. *Journal of Biomechanics*, 14(11), 793-801.
- Dempster, W.T. (1955). Space requirements of the seated operator. (Tech. Report WADC-TR-55-159). Ohio: Aerospace Medical Research Laboratories.

- Dul, J., Johnson, G.E., Shiavi, R., and Townsend, M.A. (1984). Muscular synergism II. A minimum fatigue criterion for load sharing between synergistic muscles. *Journal of Biomechanics*, 17(9), 675-684.
- Dul, J., Townsend, M.A., Shiavi, R., and Johnson, G.E. (1984). Muscular synergism I. On criteria for load sharing between synergistic muscles. *Journal of Biomechanics*, 17(9), 663-673.
- Dumas, G. A., Poulin, M.J., Roy, B., Gagnon, M., and Jovanovic, M. (1988). A 3-D digitization method to measure trunk muscle lines of action. *Spine*, 13, 532-541.
- Evans, F.G., and Lissner, H.R. (1959). Biomechanical studies on the lumbar spine and pelvis. *Journal of Bone and Joint Surgery*, 41-A(2), 278-290.
- Ginsberg, J.H. and Genin, J. (1984). *Statics and Dynamics*. New York: John Wiley and Sons.
- Hughes, R. E. (1991). *Empirical evaluation of optimization-based lumbar muscle force prediction models*. Unpublished doctoral dissertation, The University of Michigan, Ann Arbor, MI.
- Jäger, M. and Luttman, A. (1989). Biomechanical analysis and assessment of lumbar stress during load lifting using a dynamic 19-segment human model. *Ergonomics*, 32, 93-112.
- Mairiaux, P.H., and Malchaire, J. (1988). Relation between intra-abdominal pressure and lumbar stress: Effect of trunk posture. *Ergonomics*, 31(9), 1331-1342.
- Marras, W.S. (1988). Predictions of forces acting upon the lumbar spine under isometric and isokinetic conditions: A model - experiment comparison. *International Journal of Industrial Ergonomics*, 3, 19-27.
- Marras, W.S., and Sommerich, C.M. (1991a). A three-dimensional model of loads on the lumbar spine: I. Model structure. *Human Factors*, 33(2), 123-138.
- Marras, W.S., and Sommerich, C.M. (1991b). A three-dimensional model of loads on the lumbar spine: II. Model validation. *Human Factors*, 33(2), 139-150.
- Marras, W.S., King, A.I., and Joint, A.L. (1984). Measurement of loads on the lumbar spine under isometric and isokinetic conditions. *Spine*, 9, 176-178.
- Marras, W.S., Reilly, C.H. (1988). Networks of internal trunk-loading activities under controlled trunk-motion conditions. *Spine*, 13(6), 661-667.
- McGill, S.M., and Norman, R.W. (1987). Reassessment of the role of intra-abdominal pressure in spinal compression. *Ergonomics*, 30(11), 1665-1588.
- McGill, S.M., Patt, N., and Norman, R.W. (1988). Measurement of the trunk musculature of active muscles using CT scan radiography: Implications for force and moment generating capacity about the L4/L5 joint. *Journal of Biomechanics*, 21, 329-241.

- Miller, J. A. A., Schultz, A.B., Warwick, D.N., and Spencer, D.L. (1986). Mechanical properties of lumbar spine motion segments under large loads. *Journal of Biomechanics*, 19(1), 79-84.
- National Institute for Occupational Safety and Health (1981). *A work practices guide for manual lifting* (Tech. Report No. 81-122). Cincinnati, OH: U.S. Department of Health and Human Services.
- Nemeth, G., and Ohlsen, H. (1986). Moment arm lengths of trunk muscles to the lumbosacral joint obtained in vivo with computed topography. *Spine*, 2, 158-160.
- Nubar, Y., and Contini, R. (1961). A minimal principle in biomechanics. *Bulletin of Mathematical Biophysics*, 23, 377-391.
- Ortengren, R., Andersson, G.B.J., Nachemson, A. (1981). Studies of the relationship between lumbar disc pressure, myoelectric back muscle activity, and intraabdominal pressure. *Spine*, 6(1), 98-103.
- Pederson, D.R., Brand, R.A., Cheng, C. and Arora, J.S. (1987). Direct comparison of muscle force predictions using linear and nonlinear programming. *Journal of Biomechanical Engineering*, 109, 192-199.
- Penrod, D.D., Davy, D.T., and Singh, D.P. (1974). An optimization approach to tendon force analysis. *Journal of Biomechanics*, 7, 123-129.
- Pope, M.H., Andersson, G.B.J., Broman, H., Svensson, M., and Zetterberg, C. (1986). Electromyographic studies of the lumbar trunk musculature during the development of axial torques. *Journal of Orthopaedic Research*, 4(3), 288-297.
- Reid, J.G., and Costigan, P.A. (1985). Geometry of adult rectus abdominus and erector spinae muscles. *The Journal of Orthopaedic and Sports Physical Therapy*, 6(5), 278-280.
- Reilly, C.H. and Marras, W.S. (1988). SIMULIFT: A simulation model of human trunk motion. *Spine*, 14(1), 5-11.
- Roebuck, J.A., Kroemer, K.H.E., and Thomson, W.G. (1975). *Engineering anthropometry methods*. New York: Wiley-Interscience.
- Schultz, A.B., and Andersson, G.B.J. (1981). Analysis of loads on the lumbar spine. *Spine*, 6(1), 76-82.
- Schultz, A.B., Andersson, G.B.J., Haderspeck, K, Örtengren, R., Nordin, M., and Björk, R. (1982b). Analysis and measurement of lumbar trunk loads in tasks involving bends and twists. *Journal of Biomechanics*, 15, 669-675.
- Schultz, A.B., Andersson, G.B.J., Örtengren, R., Haderspeck, K, and Nachemson, A. (1982a) Loads on the lumbar spine: Validation of a biomechanical analysis by measurements of intradiscal pressures and myoelectric signals. *Journal of Bone and Joint Surgery*, 64A, 713-720.

- Schultz, A.B., Cromwell, R., Warwick, D., and Andersson, G.B.J. (1987). Lumbar trunk muscle use in standing heavy isometric exertions. *Journal of Orthopaedic Research*, 5, 320-329.
- Schultz, A.B., Haderspeck, K., Warwick, D., and Portillo, D. (1983). Use of lumbar trunk muscles in isometric performance of mechanically complex standing tasks. *Journal of Orthopaedic Research*, 1(1), 77-91.
- Tracy, M.F., Gibson, M.J., Szypryt, E.P., Rutherford, A., and Corlett, E.N. (1989). The geometry of the muscles of the lumbar spine determined by magnetic resonance imaging. *Spine*, 14, 186-193.
- Virginia Tech Industrial Ergonomics Laboratory (1992). [Association of American Railroads Hand Brake Study]. Unpublished summary data.
- Webb Associates (Eds.). (1978). *Anthropometric source book volume I: Anthropometry for designers*. NASA Reference Publication 1024. Washington, D.C.: National Aeronautics and Space Administration.
- Webster, B.S., and Snook, S.H. (1990). The cost of compensable low back pain. *Journal of Occupational Medicine*, 32(1), 13-15.
- Wilson, D.B., and Wilson, W.J. (1983). *Human anatomy*. New York: Oxford University Press.
- Zetterberg, C., Andersson, G.B.J., and Schultz, A.B. (1987). The activity of individual trunk muscles during heavy physical loading. *Spine*, 12, 1035-1040.

APPENDIX A: Informed Consent Form for Experiment

PARTICIPANT'S INFORMED CONSENT FORM

This form constitutes informed consent by you to participate in this study. Please read it in its entirety and then sign on the next sheet.

Thank you for participating in this research. This study is being conducted by the Industrial Ergonomics Laboratory of the Human Factors Engineering Center at Virginia Tech, in conjunction with the Association of American Railroads. It addresses the need to determine whether railroad yard workers can safely produce the forces necessary to "set" hand brakes under most operating conditions. If present guidelines are found to be inappropriate, the research will attempt to specify reasonable force levels which ensure operator safety.

If you choose to participate in this research you will be asked to exert your maximal strength in a number of simulated hand brake tasks and lift tasks. Some of the experimental tasks will involve *maximal safe exertions*. It is important when you complete these strength trials that you exert what you feel to be your **maximum safe effort**, that is the maximum force you can exert without risking injury. Only you can be the judge of what your maximum safe effort is, and you should not exceed that level, nor will anyone associated with this experiment ask you to do so.

The experiment will be conducted in three hours on one day. After completing and signing this consent form and background questionnaire, your height and weight will be measured. Then, you will be asked to complete a series of strength trials. The first strength trials are whole body maximum isometric exertions, which will be used for comparison to population norms. Then, you will be asked to complete a series of strength trials which simulate the setting of a hand brake on a railroad box car. You will be given a rest period after each trial. Your posture will be recorded by means of an infrared camera system during the hand brake trials. Infrared diodes will be attached to your hands, elbows, shoulders, and low-back. If at any time during the experiment you feel that you cannot participate further or that you need additional rest, please inform the experimenter.

Data collected during the study will be considered confidential and will be treated with anonymity to the extent possible.

There is a possibility that you might experience some discomfort during the experiment, or in the days immediately following the experiment. This discomfort could include one or more of the following:

- 1) Muscle fatigue in the arms, legs or low-back region.
- 2) Pain in the palms of the hands due to gripping the brake wheel.
- 3) Back pain.

Precautions will be taken to insure your safety throughout the duration of the experiment. They include:

- 1) Screening of your health history.
- 2) Close monitoring by the experimenter.
- 3) Ample rest breaks.

As a participant in the study, you are entitled to certain rights:

1) You may withdraw from the experiment at any time for any reason without forfeiting pay for time spent up until withdrawal.

2) Any of the research team members will answer any questions that you may have, and you should not sign this consent form until you understand fully all of the terms involved. The members of the research team are:

Christian A. Johnson, Graduate Student (ph. 953 - 0327)

Dr. Jeffrey C. Woldstad, Virginia Tech Faculty Member (ph. 231 - 4927)

Additional questions regarding your rights as a subject should be addressed to Dr. E.R. Stout, Chairman of the Institutional Review Board, 301 Burruss Hall (ph. 231-5281).

Your signature below indicates that you have read this document and the description of the experiment attached to it in its entirety, that your questions have been answered, and that you consent to participate in the study described.

Signature: _____ Date: _____

Printed name: _____

Address: _____

APPENDIX B: Subject Physical Fitness Questionnaire

**ERGONOMIC EVALUATION OF HANDBRAKE DESIGN
SUBJECT PHYSICAL FITNESS QUESTIONNAIRE**

Subject's Name: _____ SSN: _____

Address: _____

Telephone Number:(____) _____ Date of Birth: _____

Sex: _____ Height: _____ Weight: _____

Which hand do you write with (circle one): Right Left

Which best describes your present physical condition (circle one):

Poor Fair Good Excellent

Please describe any physical activities you presently participate in on a regular basis:

Sports (name):

_____ : _____ times per week

_____ : _____ times per week

Other (name):

_____ : _____ times per week

_____ : _____ times per week

Which hand do you write with? _____

Have you ever had a hernia (Yes or No)? _____

Have you ever had a back injury (Yes or No)? _____

Have you had any back pain during the last year (Yes or No)? _____

Have you ever had any back pain (Yes or No)? _____

Have you ever had any joint dislocations, broken bones or other physical injuries in the last year (Yes or No)

Are you presently taking any medication or drugs (Yes or No)? _____

Do you presently have any physical impairment or injury worth noting (Yes or No)? _____

Can you think of any injury, or illness you might have which could be aggravated by physical activity or participation in this experiment (Yes or No)? _____

If you answered yes to any of the above or have any other remarks you feel are pertinent to your participation, please elaborate on the back of the page:

Subject's Signature and Date

APPENDIX C: Individual Anthropometry of Subject Population

Table C.1 Summary table of subject anthropometry.

Subject	Measure			
	Stature (cm)	Weight (kg)	Age (yrs)	Handedness
Small Female				
1	151	48	22	L
2	153.5	49.5	19	R
3	157	49.5	21	R
4	155	47.5	19	R
Average Female				
5	167	63.5	21	R
6	166.5	59.5	18	R
7	163.5	60.5	22	R
8	165.5	63	20	R
Average Male				
9	172	72	19	R
10	172	69.5	27	R
11	173	72	20	R
12	171	72	21	R
Large Male				
13	180.5	84.5	21	R
14	180.5	87.5	20	R
15	181	84.5	21	L
16	183.5	88.5	21	R

APPENDIX D: Summary Table of Data Analysis Software



Table D.1 Names and uses of different data analysis programs.

Program	Use
COLLECT.EXE	Collected raw positional data with the WATSMART system in 2-D format and saved to disk along with calibration parameters.
CONVERT.EXE	Converted the 2-D data created by COLLECT.EXE to 3-D coordinates and saved to disk.
DISPLAY.EXE	Read the 3-D files created by CONVERT.EXE and wrote them in ASCII format to disk.
WATCALC.PAS	Input 3-D positional data created by DISPLAY.EXE, averaged positional data over the specified time frame, flagged missing data points and highly variable data. Final output was a 3-D coordinate location for each joint endpoint for each experimental trial.
LB.PAS	Enabled collection of raw force data from both the three-dimensional joystick and force plate. Wrote raw A/D data and calibration parameters to disk file.
LBANAL.PAS	Converted A/D unit measures of force to force in N for each hand. Wrote three-dimensional hand force values to disk for each experimental trial.
MOMMODEL.PAS	Input hand force values created by LBANAL.PAS and positional data created by WATCALC.PAS. Performed biomechanical modeling routines to compute moment and force vectors at L3/L4 joint due to external forces. Wrote force and moment vectors to disk for each trial.

Table D.1 (continued) Names and uses of different data analysis programs.

Program	Use
Comp.m and MICCJ.m procedures written for <i>MATLAB</i> on the Apple Macintosh.	Input force and moment vectors created by MOMMODEL.PAS. Performed double linear programming procedure (Bean et al., 1988) to estimate lumbar muscle force levels generated to resist external moment about the L3/L4 joint. Added muscle force vectors to external force vector to arrive at estimate of total force at L3/L4 due to external and internal forces. Estimated compression at L3/L4 was equal to the Z - component of this total force.

APPENDIX E

Summary of Regression Analyses of Wheel Torque on Compression at L3/L4

Table E.1 Coefficients, R^2 values , and model significance levels for linear regressions for each treatment cell and each subject. * indicates significance at $p < 0.01$, ** indicates significance at $p < 0.05$.

Subject	Treatment	β_0	β_1	R^2	Significance	Comments
1	1	912.95	17.03	0.926	*	
1	2	1826.9	-1.03	0.010		Thrown out for ANOVA
1	3	1232.43	13.79	0.503	**	
1	4	1499.08	4.62	0.122		Thrown out for ANOVA
2	1	1025.82	30.13	0.937	*	
2	2	1283.95	21.46	0.683	**	
2	3	1213.14	45.68	0.959	*	
2	4	1626.7	19.69	0.967	*	
3	1	748.88	31.73	0.974	*	
3	2	1412.38	29.99	0.948	*	
3	3	1438.2	29.4	0.952	*	
3	4	1926.72	27.58	0.827	*	
4	1	377.11	15.45	0.867	*	
4	2	751.40	2.23	0.319		Thrown out for ANOVA
4	3	634.78	11.24	0.729	*	
4	4	1292.97	3.20	0.099		Thrown out for ANOVA
5	1	1951.15	23.04	0.739	*	
5	2	2494.05	29.45	0.962	*	
5	3	2351.18	21.78	0.768	*	
5	4	1746.33	57.69	0.765	*	
6	1	2180.73	19.21	0.887	**	
6	2	2746.93	12.35	0.722	*	
6	3	2416.82	36.48	0.917	*	
6	4	2799.93	23.22	0.674	**	
7	1	417.9	12.89	0.919	*	
7	2	172.27	37.76	0.909	*	
7	3	383.78	25.15	0.946	*	
7	4	528.79	26.69	0.942	*	
8	1	608.85	31.66	0.912	*	
8	2	1386.23	26.99	0.728	*	
8	3	1290.39	31.26	0.725	*	
8	4	1289.05	21.17	0.349	**	

Table E.1 Continued

Subject	Treatment	β_0	β_1	R^2	Significance	Comments
9	1	2166.04	17.64	0.853	*	
9	2	1580.8	20.21	0.897	*	
9	3	2628.53	28.4	0.959	*	
9	4	2773.41	25.33	0.894	*	
10	1	953.85	21.3	0.941	*	
10	2	1285.24	18.71	0.871	*	
10	3	1503.72	19.27	0.931	*	
10	4	1798.71	29.87	0.956	*	
11	1	1132.07	30.71	0.839	*	
11	2	2126.76	11.21	0.825	*	
11	3	1482.69	36.31	0.928	*	
11	4	2155.65	21.39	0.881	*	
12	1	2483.49	19.81	0.837	*	
12	2	1587.13	37.61	0.929	*	
12	3	1038.4	35.95	0.828	*	
12	4	2215.7	45.67	0.858	*	
13	1	1322.02	38.02	0.841	*	
13	2	1130.04	34.18	0.772	*	
13	3	861.78	47.79	0.917	*	
13	4	657.92	53.91	0.941	*	
14	1	1322.02	38.02	0.841	*	
14	2	1130.04	34.18	0.772	*	
14	3	861.78	47.79	0.917	*	
14	4	657.92	53.91	0.941	*	
15	1	210.47	59.54	0.748	*	
15	2	540.15	71.87	0.885	*	
15	3	335.75	80.29	0.789	*	
15	4	41.9	121.41	0.934	*	
16	1	1442.8	30.83	0.972	*	
16	2	1548.36	35	0.956	*	
16	3	2384.64	31.71	0.978	*	
16	4	2930.2	34.02	0.945	*	

VITA

Christian A. Johnson was born in Poughkeepsie, New York on September 22, 1968. He spent the first 15 years of his life in New York and then moved to Raleigh, North Carolina in the summer of 1983. He graduated from Millbrook High School in 1986, and completed his B.S. degree in Industrial Engineering and Operations Research from Virginia Tech in 1990. He continued his studies immediately in the graduate Human Factors and Safety Engineering options in Industrial and Systems Engineering at Virginia Tech and received his M.S. degree in July of 1992. He is an active member of the Human Factors Society, the American Society of Safety Engineers, and the Institute of Industrial Engineers. He will finally enter the real world as an Associate Engineer in the Safety Engineering Department at IBM Corporation's ADSTAR Company in San Jose, California where he will initially manage manufacturing area ergonomics.



Christian A. Johnson